

Response to the referees

We appreciate the two anonymous reviewers and Dr. Erbland for reviewing our manuscript. Below, we give a point-by-point response to the comments and suggestions of the three reviewers (comments and suggestions in black; [response in blue](#)).

Reviewer #1

[We appreciate the reviewer's time in reviewing our manuscript and respect the need for clarification on several points.](#)

General comments

The manuscript by Shi et al. reports snow pit results of nitrate and its isotopic composition along a traverse from coastal East Antarctic to the interior of the plateau and evaluates the effects of post-depositional processing on snow nitrate. The dataset covers an extensive area and appears to be valuable. However, much of the work (mainly the interpretation) in this manuscript repeats, at a less comprehensive level, what have been done in previous publications (e.g., [Erbland et al., 2013; Frey et al., 2009]) in the same journal. The perhaps only new content compared with the previous work is that the snowpits in this study cover a greater depth. However, the interpretation/discussion on this part is flawed. In particular, the authors state in the abstract that "Predicting the impact of post-depositional loss, and therefore changes in the isotopes with depth, is highly sensitive to the depth interval over which an exponential decrease is assumed". This statement/conclusion comes from the practice that the authors break down the entire snowpit to several depth intervals, use the Rayleigh fractionation model to calculate the fractionation constant, and apply the approach in Erbland et al. [2013] (i.e., using an exponential regression to calculate the asymptotic values of nitrate concentration and isotopes at depth below the photic zone) to a greater depth than the photic zone (up to 300 cm deep). This practice is particularly problematic for several reasons:

[We disagree that our work is less comprehensive; in fact, we are providing a more extensive dataset than previously presented across the plateau \(esp. with depth\), newer data from the inland EAIS, and observations from coastal snowpits that resolve seasonality, which has not been included in previous work. Additionally, it is critically important that we see repeatability in the results that have been presented in Frey et al. \(2009\) and Erbland et al. \(2013\). In fact, it is suggested that Dr. Erbland agrees with this point based on his comments on this same manuscript. The extensive work that has been done, particularly at Dome C, has provided almost the entire insight we have into the post-depositional photolytic loss of nitrate from surface snow and we are applying this understanding to other sites to better our understanding overall.](#)

First, the Rayleigh Fractionation model calculates the "apparent fractionation constant" [Erbland et al., 2013], which is influenced by the degree of post-depositional processing. The degree of the post-depositional processing is in turn influenced by surface UV

intensity, snow accumulation rate and snow light-absorbing impurities (e.g., [Zatko *et al.*, 2013]). When use this model to calculate the fractionation constant at different depth intervals, e.g., 0-25 cm, 25 -100 cm, and 100 cm to bottom, difference is expected on the result, as well as the logarithmic relationships between the isotope values and concentrations (or mass fraction of nitrate called in this study). This is because that at 25-100 cm, UV intensity is less than in the shallower layer, therefore the degree of post-depositional processing is smaller, which leads to a smaller "apparent fractionation constant" and a weaker relationship between the isotope values and concentrations. This is similar to the observations on snowpits from sites with different snow accumulation rates, i.e., at site with a lower snow accumulation rate the apparent fractionation constant is greater [Erbland *et al.*, 2013] and the calculated logarithmic relationship is stronger (Table 2 of this manuscript) due to the higher degree of post-depositional processing.

The apparent fractionation can vary between sites, but should be constant at a given site over a period of time in which the boundary conditions have not changed. In the Rayleigh equation, the fractionation constant does not vary with the fraction of reactant lost (i.e. the degree of post-depositional loss by a single process (e.g. photolysis)). A simple analog is the evaporation of water – the fractionation constant does not vary with the *amount* of water lost to evaporation. Thus, for a single site in which loss is considered to be dominated by a single process (photolysis) the apparent fractionation constant should hypothetically reflect the true fractionation constant and would not change for the amount of nitrate lost by that process, under Rayleigh conditions. We agree with the referee that UV intensity would be greatest in the near surface snow, and that light is attenuated with depth. This leads to an expected decrease in the amount of loss of nitrate with depth, as the light is attenuated the chance for photolytic loss is also attenuated. However, the fractionation constant associated with photolysis should not change (there is a small caveat to this discussed below at the **). Take for example, nitrate right at the surface of the snow. If it were exposed for a short amount of time and 30% of the nitrate was photolyzed, the fractionation constant associated with photolysis would be $^{15}\epsilon_{\text{photo}}$. The same nitrate at the surface exposed for a longer amount of time, would lead to greater loss, e.g. 80%, but the fractionation due to photolysis ($^{15}\epsilon_{\text{photo}}$) does not change, only the amount of loss changes. In this example, the $\delta^{15}\text{N}$ of nitrate would be different for the shorter and longer exposure times, because of the amount of loss, but the $^{15}\epsilon_{\text{photo}}$ would remain the same in each case.

*(**Even if it is assumed that the irradiance spectrum does not remain constant with depth (i.e. the attenuation of shorter wavelength light is greater than for longer wavelengths and Zatko *et al.* (2013) calculated that the e-folding depth for 400 nm is 10 cm deeper than 305 nm), this increase in proportion of longer wavelengths would shift the fractionation constant to slightly more negative values with depth – but this change in the fractionation constant is again not directly related to the amount of loss but it is rather the shift in the spectral actinic flux that influences the “true” $^{15}\epsilon$. This is opposite of what is actually observed (e.g. the apparent $^{15}\epsilon$ shifts to more positive values deeper in fig. 4 of the original*

version).

Savarino et al.'s (2007) atmospheric measurements attribute a distinct seasonal cycle in the isotopes of nitrate to variable nitrate/NO_x sources. A similar seasonal cycle is found in the coastal snowpits presented here. At these sites any loss due to photolysis is convolved with the imprint of the seasonal changes in the isotopes. Thus, the derived apparent fractionation factor changes, not simply because there is a different amount of loss, but because it is obscured by the addition of other factors – in this case the imprint of a significant seasonal cycle, which is preserved in the coastal region (due to less loss by photolysis). At the other extreme is the inland EAIS (Dome A, Dome C, Vostok), where the photolysis of nitrate is so dominant that the isotopic expression of a single loss process is well explained by the fractionation constant associated with photolysis. Following from this, the changes in the apparent $^{15}\epsilon$ and strength in the calculated logarithmic relationship noted by the reviewer above for different accumulation regimes can be viewed as reflecting the degree to which other factors (source/oxidant seasonality) are overprinted by photolytic fractionation which, although obviously related to loss, is different than attributing these changes to fractionation progressively changing with loss.

Second, it does not make sense to use the Rayleigh model to calculate the fractionation constant at depth below the photic zone. The authors perform this at the depth intervals of 25-100 cm and 100-bottom (200 or 300 cm deep). The e-folding depth of UV radiation in the plateau is 10-20 cm based on observation [France et al., 2011], and 18-22 cm based on model [Zatko et al., 2013] which was recently suggested to be overestimated by ~20% [Libois et al., 2013]. But in any case, most (95%) of UV radiation disappears below the photic zone (in general 3 times of the e-folding depth, which is ~60 cm the maximum), where photolysis of snow nitrate is inhibited. Therefore, what is the point do use the Rayleigh model for the depth interval of 100-200(300) cm?

As the reviewer points out below “*Underneath the photic zone, nothing will change any more in theory.*” We are, in fact, working under this very assumption. The reviews and comments on the manuscript raise the need to better address and clarify this in the text, and we have re-calculated the apparent fractionation factors ($^{15}\epsilon$ and $^{18}\epsilon$) over the depth intervals of 0-20cm, 0-40cm, and 0-60cm (Table 2 in the revised version), to better represent our aim. We have also added several paragraphs of text to sections 4.2 and 4.3 to address the concerns raised by the reviewer. If indeed nothing changes under the photic zone (our working hypothesis), then the apparent fractionation constant that is derived over an interval below the photic zone, should reflect that for an interval near the surface. In other words, as the nitrate moves out of the photic zone the imprint of the photolysis (fractionation constant) should be “locked in.” So if that apparent fractionation constant changes with the depth interval over which it is calculated (even in the photic zone), why would this be? Our paper aims to consider this question and test our current understanding of how we explain the changes in the isotopes of nitrate with depth (e.g. is it a result of changing boundary conditions such as overhead ozone,

something in situ, or something else?). If the isotopic behavior is not constant with depth, then what is the appropriate interval *near the surface* over which to calculate an apparent fractionation factor or construct an asymptotic function? The extensive work by Erbland et al. (2013) on the EAIS suggested that we need only understand the top ~20 cm. We find that this is not sufficient and indeed the apparent fractionation factor changes with the depth interval considered. We are then exploring how to explain these changes with depth and how to build confidence in quantifying them near the surface.

Third, the authors apply the approach of the exponential regression to different depth intervals and to a depth well below the photic zone, and claim that the "asymptotic values and thus the prediction of nitrate concentration and isotopic values in ice cores depend on which depth interval the exponential regression is done". This also does not make sense. The exponential decrease is expected from the effect of post-depositional loss. Underneath the photic zone, nothing will change any more in theory. So what's the point to do this regression to a depth well below the photic zone? The basic idea of doing such a regression in Erbland et al. [2013] is, given the condition that the degree of post-depositional processing is constant during the period that a certain layer of snow stays in the photic zone, nitrate concentration and its isotopic composition in that layer will approach constant values and can be predicted (i.e., the asymptotic values in Erbland et al. [2013]) once that layer is buried below the photic zone. However, this is not saying that at every snow layer below the photic zone, nitrate concentration and its isotopic composition should be the same. Because the concentration and isotopic composition below the photic zone are also influenced by that in the originally deposited snow. In addition, the degree of post-depositional processing could also vary with time, given the possible changes in UV radiation, accumulation rate and snow impurities. This alone can lead to difference in nitrate concentration and its isotopic composition in different snow layers below the photic zone. For example, snow layer at 100 cm vs. that at 300 cm in Dome A, snow at the layer of 300 cm deep deposited probably ~ 40 to 50 years ago, while the layer at 100 cm deposited slightly over a decade ago. During this time period, the degree of post-depositional processing certainly varies (e.g., at least stratospheric ozone layer change a lot since the 1980s), thus even the originally deposited values were the same, their asymptotic values (after post-depositional processing) should be different. Therefore, the values of concentrations and isotopic below the photic zone differing from the predictions of exponential regression, as observed by the authors, doesn't mean necessary that other processes occur in deeper layers below the photic zone. This makes their major conclusion, which is "Predicting the impact of post-depositional loss, and therefore changes in the isotopes with depth, is highly sensitive to the depth interval over which an exponential decrease is assumed", flawed.

From the comments of the reviewer, we agree that there is a clear need to clarify our starting assumptions in the manuscript and what we are testing (see new text in sections 4.2 and 4.3 in particular). If we assume that nothing changes below the photic zone and that the apparent fractionation factor derived near the surface is explained by

photolytic processing of nitrate, why then does the apparent fractionation factor change depending on the depth interval over which you calculate it? The relationship that is captured by calculating the asymptotic values can be compared against what has actually happened since we have deep snowpits (see new Fig. 6). Comparing the calculated relationships against the observations can then allow for deriving how the isotopic composition has changed and by what processes other than photolytic loss near the surface – *for example*, changes associated with the originally deposited source signal, changes in chemistry prior to deposition, changes in ozone, changes in situ at depth outside of the photic zone or ? This effectively asks what observations in the snow do you use to calibrate the asymptotic function? How do we build confidence that we can distinguish photolytic loss from other changes in the isotopic composition of nitrate? How well can you reconstruct past nitrate signals at the surface – how much do you need to know about what happened in the surface snow and over what depth interval? We are exploring these questions in this manuscript.

In addition to the above, there are many other concerns as follows:

1. Section 2.2.: sample analysis: the authors claim that only 5 nmol nitrate in sample is required to do the isotopic analysis. I am concerned in practice, how the authors ensure that their samples in each run exactly contain the same amount of nitrate as the standards. In other words, how close is their sample peak area to the peak area of all standards? This is critical, because that it is known the influence of background/blank is larger at smaller quantity of sample nitrate, thus a decay of the measured isotope ratios along with sample nitrate quantity is observed [Costa *et al.*, 2011]. It is okay if the standards are exactly at the same size as the samples, as all the background is equally corrected. However, at such a small 5 nmol level, a slight size difference between the standards and the samples will lead to probably significant over-correction or under-correction. So if the data are going to be published, I suggest the authors add information on the sample peak area vs. standard peak area in a particular run to validate the quality of the data.

We agree with the reviewer, and the additional information on the nitrate amounts of samples and standards are now included in the revised manuscript and in the supporting information. At Brown University, it is a standard practice that nitrate concentrations in the samples and standards be very similar for each run of samples, i.e., the injected volumes of both samples and standards are similar (see tables below). In this case, any effects due to blanks/different volumes can be minimized. In addition to this point, we also run replicates and report the pooled standard deviation for paired replicates (or triplicates) along with the pooled standard deviations of the reference materials. Because our reference materials are run many times, the pooled standard deviations for these are necessarily smaller than that which we find for replicate sample analyses (that are only run a small fraction of the number of times the reference materials are run).

The maximum injection volumes are near 55 μ L for the method at Brown University

(see the figure below). The autosampler carousel is designed to fit either 20 mL vials or 60 mL vials – both vials have the same size septa caps (see the figures below), and the purging needle is designed such that the carrier gas and sample outflow into the rest of the system near the very top of the vial (such that a volume near 60 mL can be achieved). We have tested the addition of high volume samples extensively, and include additional information on this in the manuscript and in the supplemental material (Tables S1 and S2 in supporting information).

As requested by the referee, below is an example table of data obtained from a 5 nmol run. It is critically important when running very low concentrations to include standards/reference materials that are very close in concentration for correcting the data (i.e. there is a “volume” effect such that is accounted for when using samples and standards of the same volume), and we apologize for not including detailed information on this originally. Below is also two additional tables of data obtained on internal working standards (now included as Tables S1 and S2 in supporting information). The first is a mix of USGS 35+USGS 34, and the second is KNO_3 . Both are used as internal standards for quality control purposes (they are treated as samples and corrected to reference materials in each run). Each has been injected for different volumes in different runs and its isotope values corrected to reference materials in each run that are close in concentration (i.e. close in injection volume). As you can see this also shows excellent reproducibility over a variety of runs and range in (low) concentrations for $\Delta^{17}\text{O}$, $\delta^{15}\text{N}$, and $\delta^{18}\text{O}$.

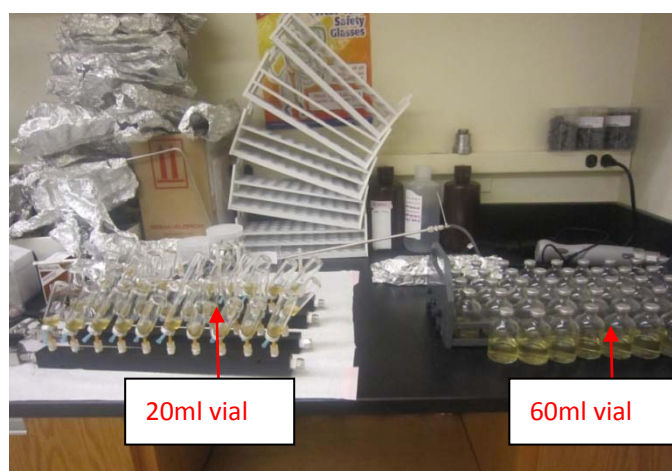


Figure: The two types of injection vials (e.g., 20ml and 60ml) used at Brown University.

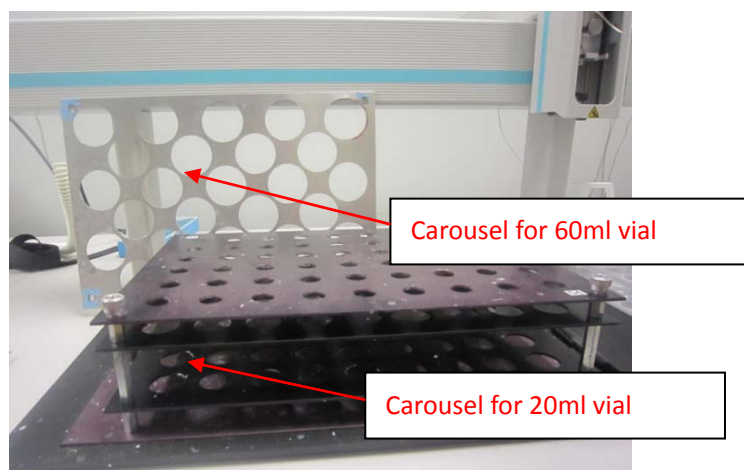


Figure: The autosampler carousel designed to fit either 20 mL vials or 60 mL vials

Table: Example raw data using 5nmol injections. Note that the “flush vial N₂O” is a vial filled with reference gas that serves as an additional quality check on the system prior to and after completing a sample run.

Sample/Standard	Injection volume, ml	Peak area, Vs	rd ¹⁵ N uncorrected	rd ¹⁸ O uncorrected
flush vial N ₂ O		22.1	-0.7	-0.2
flush vial N ₂ O		23.6	-0.9	-0.5
Blank		<0.2		
USGS 35	25.0	3.7	3.7	44.9
USGS 32	25.0	4.3	156.9	20.3
USGS 34	25.0	4.0	-3.5	-28.6
IAEA N3	25.0	4.2	3.7	17.7
Sample-2	24.5	3.8	271.6	40.2
Sample-4	24.5	4.4	299.1	35.8
Sample-7	25.1	4.5	323.3	35.2
Sample-8	22.1	4.3	299.0	36.5
Sample-9	23.6	4.2	290.3	37.2
IAEA N3	25.0	4.2	3.9	17.6
USGS 35	25.0	4.0	3.5	44.2
USGS 34	25.0	4.1	-3.0	-28.2
USGS 32	25.0	4.2	155.5	20.3
Sample-12	24.6	4.3	346.2	33.0
Sample-13	29.0	3.7	318.2	34.6
Sample-15	27.3	3.9	323.2	37.3
Sample-16	29.3	3.7	308.9	38.9
Sample-17	26.4	3.4	284.1	42.8
Sample-18	24.4	3.9	289.5	40.2
Sample-19	28.0	4.0	269.7	42.4
USGS 32	25.0	4.2	155.3	20.4
IAEA N3	25.0	4.4	3.9	17.4
USGS 35	25.0	3.9	3.4	44.7

USGS 34	25.0	4.0	-3.2	-28.8
flush vial N ₂ O		25.5	-1.1	-1.0

Table: Results of an internal quality control, KNO₃. The $\delta^{15}\text{N}(\text{NO}_3^-)$ mean is $58.37 \pm 0.62\text{‰}$, with the range of 57.52-59.59‰. The mean of $\delta^{18}\text{O}(\text{NO}_3^-)$ is $30.65 \pm 0.52\text{‰}$, with the range of 29.55-31.50‰.

$\delta^{15}\text{N}(\text{NO}_3^-)$	$\delta^{18}\text{O}(\text{NO}_3^-)$	Injected volume (mL)	Concentration (μM)
59.39	30.43	20.00	0.50
58.19	30.85	20.00	0.50
58.37	30.80	20.00	0.50
57.52	31.13	16.67	0.60
58.77	30.62	16.67	0.60
58.12	30.59	13.33	0.75
57.66	31.50	13.33	0.75
58.73	30.16	13.33	0.75
58.39	31.31	10.31	0.97
57.71	31.00	10.00	1.00
58.26	31.01	10.00	1.00
58.48	30.82	10.00	1.00
57.70	30.45	10.00	1.00
57.57	31.04	10.00	1.00
58.96	29.93	10.00	1.00
59.59	29.77	10.00	1.00
59.31	30.16	10.00	1.00
58.70	30.88	10.00	1.00
58.27	29.55	10.00	1.00
57.76	31.01	6.67	1.50

Table: Results of $\Delta^{17}\text{O}$ for USGS35/34 mixture, an internal quality control. The mean $\Delta^{17}\text{O}(\text{NO}_3^-)$ of $11.45 \pm 0.44\text{‰}$ and the range of 10.88-12.21‰.

$\Delta^{17}\text{O}(\text{NO}_3^-)$	NO ₃ ⁻ amount (nmol)	Concentration (μM)	Injected volume (mL)
11.26	50.00	5.00	10.00
10.89	50.00	5.00	10.00
10.88	50.00	3.00	16.67
11.06	50.00	3.00	16.67
11.78	50.00	2.00	25.00
10.94	50.00	2.00	25.00
11.62	50.00	1.50	33.33
11.71	50.00	1.00	50.00
12.21	50.00	1.00	50.00
11.83	50.00	1.00	50.00
11.59	45.00	3.00	15.00
11.37	45.00	2.00	22.50
11.23	40.00	1.00	40.00
11.20	40.00	1.00	40.00

2. Section 4.1.2.: in this part, the authors completely ignore the what likely occurs in the gas phase. Re-oxidation in the overlying air (i.e., the equilibrium in the air snow interface [Erbland *et al.*, 2013; Frey *et al.*, 2009]) and in the interstitial air of snowpack also occurs. Although the re-oxidation in the condensed phase is likely dominated, the authors should at least discuss other processes.

We appreciate the reviewer's point here. The title of the section has been changed to "Aqueous phase "secondary" NO₃⁻ formation" since the focus of the section is on the condensed phase alone. Other parts of the manuscript consider the gas phase re-oxidation.

3. Section 4.1.3.: Why "the importance of this process (volatilization) is unclear"? Hasn't the relative importance of this physical release to photolysis been evaluated extensively in [Erbland *et al.*, 2013; Frey *et al.*, 2009] and concluded clearly that photolysis dominates in the post-depositional processing? These two references are cited in this same section and the authors pretty much rely on the results of these two previous publications here to make the discussion.

In addition, the field experiments in [Erbland *et al.*, 2013]) suggested a fractionation constant with respect to the physical release of close to or below zero. Doesn't this imply that the assumption and model result on the isotopic effects of physical release in [Frey *et al.*, 2009] are less reliable?

Our purpose here was to review the state of the science and consider both the theoretical and the experimental results in terms of our observations. The text 4.1.3 has been clarified. There are several inconsistencies between the theoretical and experimental results in the two publications, and we are noting the disagreements and the lack of experimental values for ¹⁸ε. The experiments are far from perfect, but do indeed give a sense that the theoretical cases considered by Frey *et al.* (2009) may not be applicable in the field or to conditions at Dome C. (And note here that Dr. Erbland's comments on our manuscript suggest, as we have, using the field experiment results with caution).

4. Section 4.2.: This is by far the part with the largest issue. Much of them have been discussed above in the general comments, but there are additional concerns. In page 31959, the last paragraph, the authors suggest the d18O continued to change below the photic zone is due to re-formation of nitrate in the gas phase through O₃ oxidation. There are several problems with this. First, d18O increases from the depth of ~10 cm continued to a depth of 200 cm. At depth below the photic zone (i.e., < 60 cm), how NO_x is produced and how much oxidants (O₃) are available in the interstitial air?

We suggested the in situ processing as a hypothesis, but there is a clear need to clarify

this, consider several hypotheses, and to better construct our arguments as to whether this in situ change is even likely/possible. We have extensively modified sections 4.2 and 4.3 to better consider different hypotheses and clarify our arguments. Based on the reviewer's concerns, we have removed the specific discussion regarding in situ (i.e. in snow) gas phase re-oxidation.

Second, why this phenomenon is not observed in Pit 6? which should be expected if the authors are correct.

It is not clear why each pit must behave the same in order to justify or negate the hypothesis. Three of the four pits in the interior of the EAIS show increases in $\delta^{18}\text{O}$ with depth. (The same could be said about the apparent $^{15}\epsilon$ that has been observed in previous work on the EAIS as it is generally more negative and more variable than that predicted by theory, but the balance of evidence supports this being the photolytic imprint.) Still, we have removed the discussion of this potential phenomena.

Third, [Meusinger *et al.*, 2014] suggests that nitrate in snow grains can be categorized into two domains: photolabile nitrate and buried nitrate. Photolabile nitrate is nitrate in the surface of snow grain which is easily photolyzed and the photoproduct mainly escapes into the air; while the buried nitrate are in the snow grains, the photolysis of this nitrate leads to re-formation of nitrate in the condensed phase and depletion of oxygen isotopes due to exchange with water oxygen. The experiments in [Meusinger *et al.*, 2014] then suggest that the photolabile nitrate is quickly removed under UV radiation, and buried nitrate started to be photolyzed after photolabile nitrate is almost gone. Therefore, in the field, at surface, the photoproducts mainly escapes to the air (because nitrate are in the surface of snow grains) without significant re-oxidation in the condensed phase; but at depth, re-oxidation in the condensed phase becomes more important as where it is "buried nitrate" photolysis and the products stay in the condensed phase longer before escaping to the interstitial air. This means, as going deeper, NO_x is more difficult to escape (more re-oxidation in the condensed phase). This offsets the effect of re-oxidation of NO_x by O₃ on $\delta^{18}\text{O}$ of snow nitrate at greater depths, even the later indeed occurs.

Agreed. Based on the reviewer's concerns, we have removed the specific discussion regarding in situ (i.e. in snow) gas phase re-oxidation.

By the way, in the second paragraph in Page 31960, the authors are pretty much against themselves.

The text deserves clarification, but we are not sure how we go against ourselves here. Expecting that the isotopic composition should not change below the photic zone, and that the apparent fractionation factor be preserved with burial is, as discussed above, the starting assumption this study works under.

5. Section 4.3.: as discussed in the general comments, this section makes no sense. It is meaningless to apply this approach for depth below the photic zone, and give the time period the snowpit covers (300 cm, approximately 50 years), other factors have to be considered.

This is addressed in the general comments above, but we will also note here that the time period of coverage varies considerably across the pits; for example, Pit 4 only covers ~12-13 years. We are applying our understanding here across the pits in the context of what is captured by each. To clarify the timescale Table 1 from the supplement has been moved into the text and replaced by a figure (Fig. S2 in supporting information) suggested by anonymous referee #2 – please also see our response to referee #2 regarding adding timescales to the figures.

6. Section 4.4.: First, beside the discussion on stratospheric sources, it is unclear throughout this part which sources and how they shift. **Last paragraph in page 31965:** why the more stratospheric nitrate in the most recent winter in P1 is relate to the smaller ozone hole in the spring of 2012? Theoretically, chemical ozone loss in the stratospheric requires the growth of PSCs and which favors at lower temperature in polar winter (e.g., [Manney *et al.*, 2011]). Only severe cold promotes the growth of PSCs, when it grows big enough it starts to descend, leading to surface enhancement of nitrate. Lower ozone loss indicates probably less abundance / growth of PSCs in polar winter, and should be consistent with less stratospheric nitrate input. So the argument in this paragraph does not make sense.

We do think it's worth noting that these two events coincide even though a mechanistic link is not clear at this point. Also, significant HNO_3 exists in the lower stratosphere regardless of the presence of PSCs (i.e. PSC sedimentation is not the only source of nitrate, but the form of nitrate is very different when PSC chemistry is important).

First paragraph in page 31966: the authors claim that the high $\delta^{15}\text{N}$ values (31 per mil) in cold seasons indicate that stratospheric nitrate should be higher than [Savarino *et al.*, 2007] calculated. In Figure 7, in the season with the largest stratospheric nitrate contribution (the most recent one, as indicated by the largest $\delta^{18}\text{O}$ and $\delta^{17}\text{O}$ values), $\delta^{15}\text{N}$ is the lowest.

Not clear which peak the referee is looking at? The $\delta^{15}\text{N}$ for the most recent wintertime snow averages ~32 ‰ – so the connection here is that the $\delta^{15}\text{N}$ of stratospheric nitrate, which has been invoked to explain similarly high $\Delta^{17}\text{O}$ and $\delta^{18}\text{O}$ values in Savarino *et al.* (2007) may contribute values that are greater than the 19 ± 2 ‰ suggested in Savarino *et al.* (2007).

Therefore, it is not reasonable to attribute the high $\delta^{15}\text{N}$ values in the cold seasons to stratospheric influence alone, as if so $\delta^{15}\text{N}$ in the most recent cold season should be the highest. In addition, [Savarino *et al.*, 2007] measured seasonal atmospheric nitrate in a

coast regions of East Antarctica, which should be more directly influenced by stratospheric signals. The fact, that the snow nitrate in P1 possesses much higher $\delta^{15}\text{N}$ in all season compared to the atmospheric measurements [Savarino *et al.*, 2007] (though not in the same location, but if consider stratospheric signal, the spatial variability should be small), should not imply other process (e.g., post-depositional processing) in the air-snow interface plays a role? As a reminder, the stratospheric signals [Savarino *et al.*, 2007] measured in the boundary layer is less than 10 per mil for $\delta^{15}\text{N}$, while in the snow in this study is 31 per mil.

The discussion here seems counter to what is published in Savarino *et al.* (2007), and we limit our discussion to what appears in that work. We are looking to explain the very high $\Delta^{17}\text{O}$ and $\delta^{18}\text{O}$ that coincide with values of $\sim 32\text{‰}$ for $\delta^{15}\text{N}$. We offer several lines of evidence for why limited post-depositional loss is apparent in these coastal pits.

There are some other points:

1) P31946, line 16: the oxygen-17 anomaly reflects oxidants involved in nitrate production, not oxygen isotopes. NO_x itself and water vapor in the atmosphere also influence oxygen isotope in nitrate.

We agree with the reviewer. Corrected in the revised manuscript.

2) P31967, line 8-10: what are the problems?

We now cite literature that discusses this issue thoroughly. In the following paragraph we discuss how the data is very limited, how measurements of the $\delta^{15}\text{N}$ of NO_x from even the same source (e.g. vehicles) have reported values that vary from very negative to very positive, etc.

3) P31949, line 15-16: The sentence starts with "secondly..." is confusing. Does it mean that one sample was replicated 38 times?

Clarified.

4) P31949, line 23 to the end of this paragraph: when correct for oxygen isotope exchange with water, it seems only water in the sample matrix is considered. How about water in the bacterial media? or it is dry bacteria added to the liquid samples?

Clarified.

5) P31951, line 11-15: It must to make it clear that the 2.5 per mil underestimate without step 2 correction when using pre-concentration is only true for samples with nitrate at 35 nmol around; if there are 350 nmol nitrate in each sample, this effect will be much reduced to minor.

We agree with the reviewer that the blank effect *should* be reduced for a larger sample size, however, this effect has never been quantified by the other groups reporting measurements after concentrating. We have modified the text in section 2.2.

6) P31956, line 8: it is "sect. 4.1.3", not 4.1.2;

Corrected.

7) P31958, line 14: this is true at only low snow accumulation sites. Please make it clear.

Clarified.

8) P31958, line 25-26: This statement is not true according to table 2, as where it shows the relationship between d15N and nitrate concentration shifts from negative to positive, opposite to that between d18O and concentration.

This table has now been replaced with updated calculation based upon concerns raised above.

Shi et al. report in their study snow pit measurements of nitrate and its stable isotopes from an over-land traverse in East Antarctica and discuss potential contributions of post-depositional processing and the atmospheric source signal to the isotope ratios observed in the snow. The main findings are:

Nitrate concentrations and isotope ratios at low-accumulation sites in the interior of the continent ($<55 \text{ kg m}^{-2}\text{yr}^{-1}$) are found to be affected by post-depositional processing, i.e. nitrate concentrations decrease in the top few 10s of cm of snow, concurrent with enrichment in $\delta^{15}\text{N}(\text{NO}_3^-)$ and depletion in $\delta^{18}\text{O}(\text{NO}_3^-)$. The negative correlation between $\delta^{15}\text{N}$ and $\delta^{18}\text{O}$ in NO_3^- is consistent with the current understanding of post-depositional isotopic fractionation from nitrate photolysis, i.e. enrichment in $\delta^{15}\text{N}(\text{NO}_3^-)$ and depletion in $\delta^{18}\text{O}(\text{NO}_3^-)$. The latter is attributed to isotope exchange with a reservoir of small or negative oxygen isotope ratios during formation of secondary nitrate. However some of the low-accumulation sites show at depth a positive correlation between $\delta^{15}\text{N}$ and $\delta^{18}\text{O}$ in NO_3^- , which lead the authors to raise caution when interpreting the preserved isotope signal as a tracer of a single process, i.e. inversion of the preserved nitrate isotope signal to an atmospheric signal may be more complicated than only assuming nitrate photolysis and associated isotopic fractionation.

Sites with higher accumulation rates closer to the coast ($91\text{-}172 \text{ kg m}^{-2}\text{yr}^{-1}$) appear to preserve the atmospheric signal, as indicated by generally lower $\delta^{15}\text{N}(\text{NO}_3^-)$ and higher $\delta^{18}\text{O}(\text{NO}_3^-)$ values when compared to sites in the interior, and preservation of the seasonal variability in nitrate concentration and stable isotope ratios. The authors interpret the winter signal as a result of a stratospheric source, and the summer signal originating from a both tropospheric sources and chemical reactions.

Overall, the main merit of this study consists in reporting new spatially distributed data of nitrate and its stable isotopes in Antarctic surface snow, which is important to work towards a quantitative understanding of the Antarctic ice core signal of nitrate stable isotopes. Most findings and their interpretation are not really new, but rather confirm previous comprehensive (traverse) studies carried out in another sector of East Antarctica (Erbland et al., 2013; Frey et al., 2009; Savarino et al., 2007). Thus it's a bit disappointing that not more effort was undertaken to quantitatively compare the data to the existing literature, for example the dependence of the isotope ratios on site-specific accumulation rates or using an isotope fractionation model including recent progress in the lab (Berhanu et al., 2014). A more detailed and critical discussion of the data may well yield more insight into the complex topic of post-depositional processing of nitrate. The presentation of the material I find at times inaccurate (typos in table or equations) or lacking detail to follow the reasoning. Suggestions to rework the manuscript are included in the more detailed comments below.

We appreciate the time and attention to detail by referee 2. His/her constructive comments improve the manuscript in important ways. Please see below for point-by-point responses in blue following the referee's comments.

2 Detailed Comments

p31945/l9: or halogen radicals (XO)

Fixed, thank you.

p31945/l28: Cite here previous work, which found and discussed the relationship between isotope ratios and accumulation rate, as summarised in Fig.4 of Erbland et al. (2013).

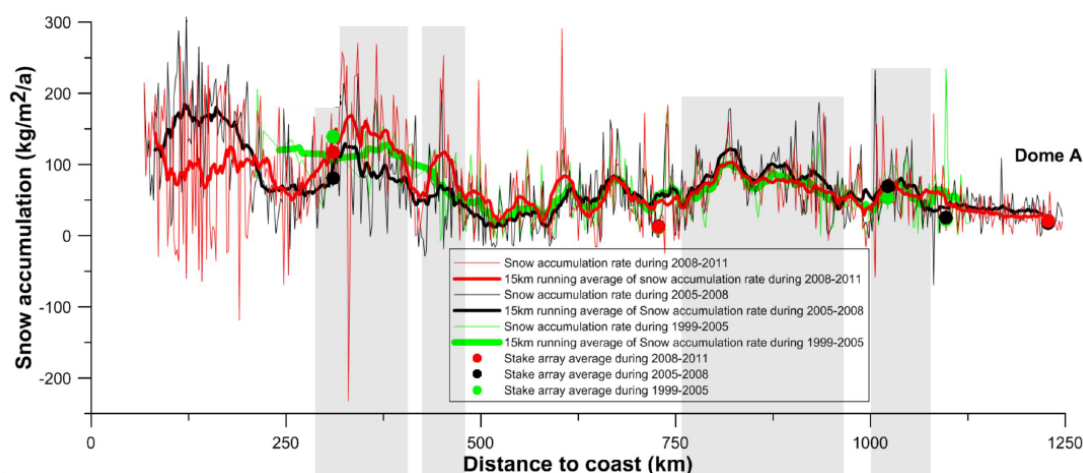
This has been updated and a figure similar to that of Erbland et al. (2013) Figure 4 was included in the supporting information of the manuscript (Fig. S1).

p31948/l2: The snow pit information given in Table S1 is very relevant to the discussion, e.g. accumulation rates, one of the key parameter for preservation of nitrate (e.g. Röthlisberger et al., 2002) as well as sampling depth resolution, and therefore needs to be moved from the Supporting Material section to the main manuscript. The method section needs also more detail from Ding et al. (2011) on the site-specific annual accumulation rate A : how was A determined? As the time series are likely too short to detect a trend state at least the inter-annual variability (standard deviation). Is there any information on the seasonality of A in the region?

The snow accumulation rates were determined using the standard stake technique, where changes in snow height over time are measured relative to fixed stakes, and density was measured using a density scoop with volume of 1000ml. For the details regarding the stake

measurements, please refer to Ding et al. (Ding et al., 2011. Spatial variability of surface mass balance along a traverse route from Zhongshan station to Dome A, Antarctica. *Journal of Glaciology* 57, 658-666.). There are not significant trends in the annual accumulation rates, and we considered this in terms of explaining the change in behavior in the isotopes over time/depth. Wang et al. (2013) (Wang, Y., H. Sodemann, S. Hou, V. Masson-Delmotte, J. Jouzel, and H. Pang (2013), Snow accumulation and its moisture origin over Dome Argus, Antarctica, *Climate Dynamics*, 40(3-4), 731-742, doi:10.1007/s00382-012-1398-9) have compiled existing stake and snowpit accumulation measurements from Dome A and show 1) little spatial variability (surrounding 50 km) and 2) stable accumulation rates over recent decades and since 1260 AD (1965-2009 = $21 \text{ kg m}^{-2} \text{ a}^{-1}$; 2005-2008 = $18 \text{ kg m}^{-2} \text{ a}^{-1}$; 2005-2009 = $19 \text{ kg m}^{-2} \text{ a}^{-1}$; 2008-2009 = $21 \text{ kg m}^{-2} \text{ a}^{-1}$; and 1260-2005 = 21.6 to $23 \text{ kg m}^{-2} \text{ a}^{-1}$). Automatic weather station measurements presented in the same work show somewhat higher accumulation in the spring and summer (roughly 6-7 mm per month) vs. fall and winter (roughly 3-6 mm per month) with fairly stable values in the warmer months.

The following figure show the accumulation rates on the traverse from the coast to Dome A during the three periods, 1998-2005, 2005-2008 and 2008-2011 (unpublished data, Ding et al., 2015, personal communication). Although this information is limited in time compared to some our snowpits, it also speaks to the idea that no significant trend in recent snow accumulation is apparent in the study region over the time period covered by the snowpits.



The CHINARE (Chinese National Antarctic Research Expedition) and ANARE ((Australian National Antarctica Research Expedition) have measured the annual average temperature using borehole (a well-established recorder of mean annual surface air temperature) or automatic weather station observations on the Zhongshan-Dome A traverse (Ding, M., et al., 2010. Distribution of $\delta^{18}\text{O}$ in surface snow along a transect from Zhongshan Station to Dome A, East Antarctica. *Chinese Science Bulletin* 55, 2709-2714.). The multiple regression plus Kriging was used to interpolate these data on this traverse at a 10^{-5} degree spatial resolution (about $4\text{e-}3 \text{ km}^2$), to estimate annual average temperature at different sampling sites, and there is good consistency between the observed and estimated values (Xiao, C., et al., 2013. Stable isotopes in surface snow along a traverse route from Zhongshan station to Dome A, East Antarctica. *Climate Dynamics* 41, 2427-2438.).

The information on the date of snowpit collection is provided in the updated table below and this was moved into the revised manuscript (Table 1). Much of the discussion above was also added to section 4.3.

Table - Summary information for the seven snowpits presented in this study.

Snowpit	Location	Elevation (m)	Distance from coast (km)	Mean annual accumulation (kg m ⁻² a ⁻¹) ¹⁾	Mean annual air temperature (°C) ²⁾	Depth (cm)	Sample resolution (cm)	Sampling date (DD.MM.YYYY)
P1	71.13°S 77.31°E	2037	200	172.0	-29.1	150	3.0	18.12.2012
P2	71.81°S 77.89°S	2295	283	99.4	-32.9	200	5.0	20.12.2012
P3	73.40°S 77.00°E	2545	462	90.7	-35.7	200	5.0	22.12.2012
P4	76.29°S 77.03°E	2843	787	54.8	-41.3	200	2.0	28.12.2012
P5	77.91°S 77.13°E	3154	968	33.3	-46.4	200	2.0	30.12.2012
P6	79.02°S 76.98°E	3738	1092	25.4	-53.1	200	2.5	02.01.2013
P7	80.42°S 77.12°E	4093	1256	23.5	-58.5	300	2.5	06.01.2013

1) Mean annual snow accumulation rates are obtained from stake height field measurements, updated to 2013 from Ding et al. (2011).

2) Mean annual surface air temperatures are derived from 10m borehole temperatures and automatic weather station observations (Ding et al., 2010; Xiao et al., 2013).

p31948/l7: what was the diameter of the vials?

The 20 mL vials are 23 mm in outer diameter and the 60 mL vials are 43 mm in outer diameter. All three comments (2 review + comments by Dr. Erbland) make clear that we needed to provide more information regarding the ability to measure only 5 nmol of nitrate, and additional information was added in the methods section and in the supplement. For completeness, here is the information provided in response to the comments by Dr. Erbland as well:

The denitrifying bacteria are prepared as described in the original methods paper by Sigman et al., 2001 (and this can be re-described/added to the manuscript). Indeed, the maximum injection volumes are near 55 mL for the method at Brown University (see the figure in responses to Reviewer#1). The autosampler carousel is designed to fit either 20 mL vials or 60 mL vials – both vials have the same size septa caps (see the figure below), and the purging needle is designed such that the carrier gas and sample outflow into the rest of the system near the very top of the vial (such that a volume near 60 mL can be achieved). We have tested the addition of high volume samples extensively,

and include additional information on this in the supplemental material. Below is an example table of data obtained from a 5 nmol run. It is critically important when running very low concentrations to include standards/reference materials that are very close in concentration to the samples (i.e. there is a small “volume” effect that is accounted for by using samples and standards of the same volume which yields similar area peaks on the mass spectrometer). Below is also a table of data obtained on internal quality controls (KNO_3 and a mix of USGS34/USGS35) that is now included in the supplement. These internal controls are used as a quality check. They have been run at different volumes in different runs and isotope values are corrected to reference materials in each run that are close in concentration (i.e. close in injection volume). As you can see both controls show excellent reproducibility over a variety of runs and ranges in (low) concentrations.

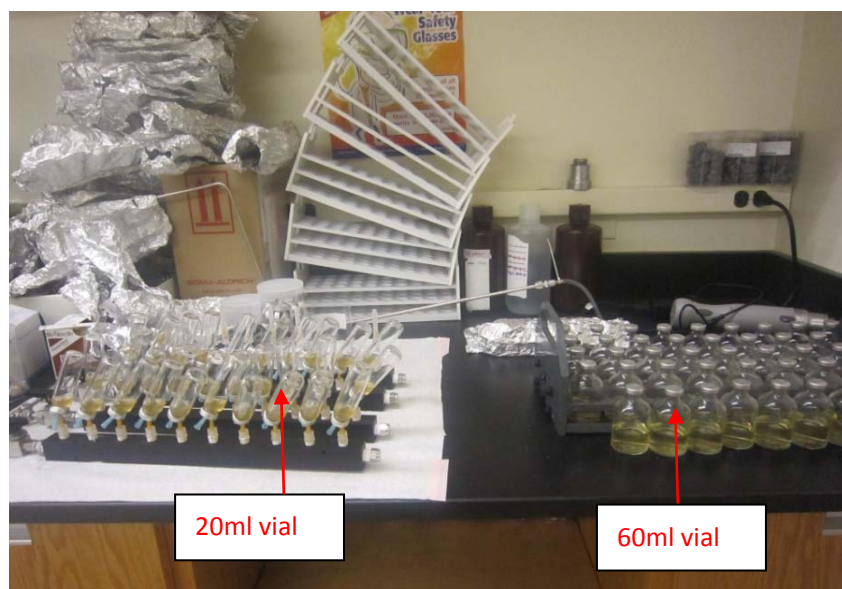


Figure: The two types of injection vials (e.g., 20ml and 60ml) used at Brown University.

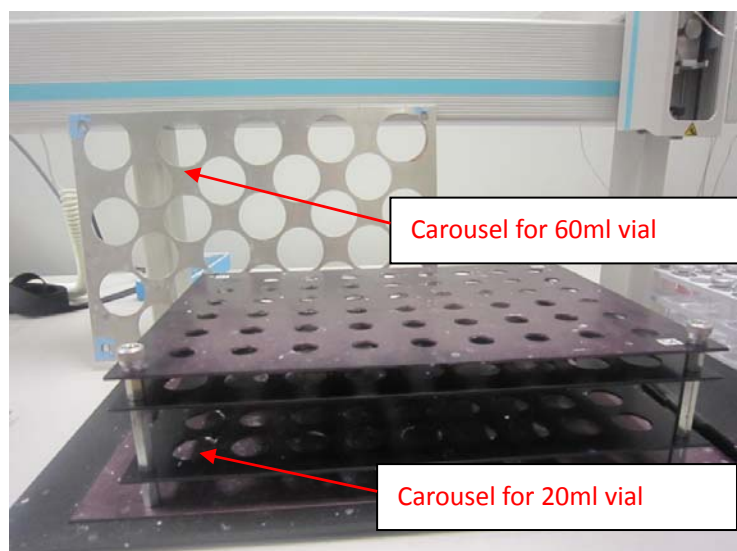


Figure: The autosampler carousel designed to fit either 20 mL vials or 60 mL vials

Table: Example raw data using 5nmol injections. Note that the “flush vial N₂O” is a vial filled with reference gas that serves as an additional quality check on the system prior to and after completing a sample run.

Sample/Standard	Injection volume, ml	Peak area, Vs	rd ¹⁵ N uncorrected	rd ¹⁸ O uncorrected
flush vial N ₂ O		22.1	-0.7	-0.2
flush vial N ₂ O		23.6	-0.9	-0.5
Blank		<0.2		
USGS 35	25.0	3.7	3.7	44.9
USGS 32	25.0	4.3	156.9	20.3
USGS 34	25.0	4.0	-3.5	-28.6
IAEA N3	25.0	4.2	3.7	17.7
Sample-2	24.5	3.8	271.6	40.2
Sample-4	24.5	4.4	299.1	35.8
Sample-7	25.1	4.5	323.3	35.2
Sample-8	22.1	4.3	299.0	36.5
Sample-9	23.6	4.2	290.3	37.2
IAEA N3	25.0	4.2	3.9	17.6
USGS 35	25.0	4.0	3.5	44.2
USGS 34	25.0	4.1	-3.0	-28.2
USGS 32	25.0	4.2	155.5	20.3
Sample-12	24.6	4.3	346.2	33.0
Sample-13	29.0	3.7	318.2	34.6
Sample-15	27.3	3.9	323.2	37.3
Sample-16	29.3	3.7	308.9	38.9
Sample-17	26.4	3.4	284.1	42.8
Sample-18	24.4	3.9	289.5	40.2
Sample-19	28.0	4.0	269.7	42.4
USGS 32	25.0	4.2	155.3	20.4
IAEA N3	25.0	4.4	3.9	17.4
USGS 35	25.0	3.9	3.4	44.7
USGS 34	25.0	4.0	-3.2	-28.8
flush vial N ₂ O		25.5	-1.1	-1.0

Table: Results of an internal quality control, KNO₃. The $\delta^{15}\text{N}(\text{NO}_3^-)$ mean is $58.37 \pm 0.62\text{‰}$, with the range of 57.52-59.59‰. The mean of $\delta^{18}\text{O}(\text{NO}_3^-)$ is $30.65 \pm 0.52\text{‰}$, with the range of 29.55-31.50‰.

$\delta^{15}\text{N}(\text{NO}_3^-)$	$\delta^{18}\text{O}(\text{NO}_3^-)$	Injected volume (mL)	Concentration (μM)
59.39	30.43	20.00	0.50
58.19	30.85	20.00	0.50
58.37	30.80	20.00	0.50
57.52	31.13	16.67	0.60
58.77	30.62	16.67	0.60
58.12	30.59	13.33	0.75

57.66	31.50	13.33	0.75
58.73	30.16	13.33	0.75
58.39	31.31	10.31	0.97
57.71	31.00	10.00	1.00
58.26	31.01	10.00	1.00
58.48	30.82	10.00	1.00
57.70	30.45	10.00	1.00
57.57	31.04	10.00	1.00
58.96	29.93	10.00	1.00
59.59	29.77	10.00	1.00
59.31	30.16	10.00	1.00
58.70	30.88	10.00	1.00
58.27	29.55	10.00	1.00
57.76	31.01	6.67	1.50

Table: Results of $\Delta^{17}\text{O}$ for USGS35/34 mixture, an internal quality control. The mean $\Delta^{17}\text{O}(\text{NO}_3^-)$ of $11.45 \pm 0.44\text{‰}$ and the range of 10.88-12.21‰.

$\Delta^{17}\text{O}(\text{NO}_3^-)$	NO_3^- amount (nmol)	Concentration (μM)	Injected volume (mL)
11.26	50.00	5.00	10.00
10.89	50.00	5.00	10.00
10.88	50.00	3.00	16.67
11.06	50.00	3.00	16.67
11.78	50.00	2.00	25.00
10.94	50.00	2.00	25.00
11.62	50.00	1.50	33.33
11.71	50.00	1.00	50.00
12.21	50.00	1.00	50.00
11.83	50.00	1.00	50.00
11.59	45.00	3.00	15.00
11.37	45.00	2.00	22.50
11.23	40.00	1.00	40.00
11.20	40.00	1.00	40.00
12.20	40.00	1.00	40.00

p31951/l20: A comparison of the snow pit statistics given in Table 1 is only meaningful if the parameters (mean, σ etc.) are calculated over the same snow depth interval, which is apparently not the case. For example, it would be interesting to see how the snow top layer (uppermost sample), the top 3-5 e-folding depths (e.g. 30-50cm) or top 150cm vary across sites; a graph (whisker plot) is even warranted to illustrate site variability e.g. as a function of A or distance from coast.

We agree with the referee that there should be a better way to capture a “picture” of the large amount of data included in this study. As suggested, a box and whisker plot is now included, displaying the mass fraction and isotope results, including the maximum, minimum, percentiles (5^{th} , 25^{th} , 75^{th} , and 95^{th}), mean and median plotted as a function of accumulation rate. This was included in the manuscript in place of (instead of) Table 1 (Fig. 2 in the revised manuscript).

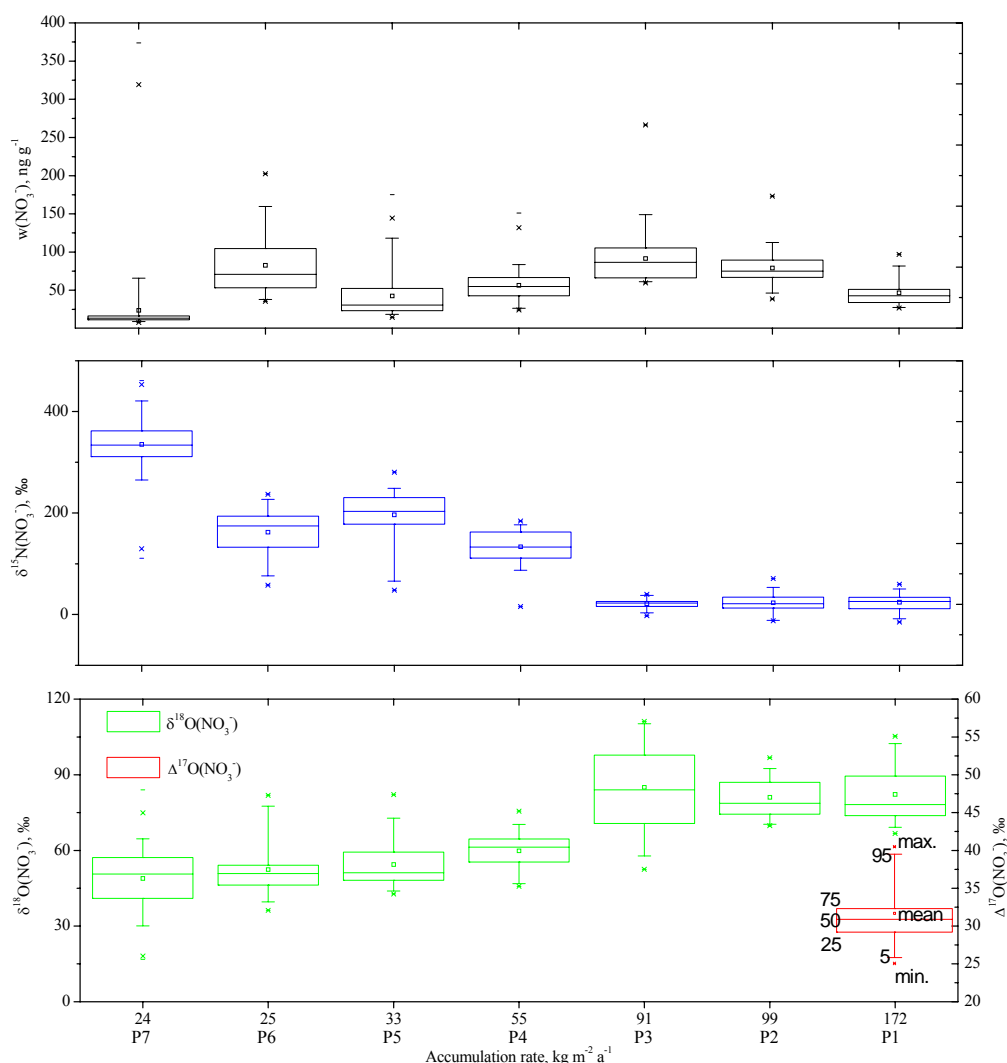


Figure: Statistics of mass fraction and isotopic compositions of NO_3^- for each snowpit (P1-P7), plotted as a function of snow accumulation rate. Box and whisker plots represent maximum (top x symbol for each box), minimum (bottom x symbol for each box), percentiles (5th, 25th, 75th, and 95th), and median (50th, solid line) and mean (open square near center of each box). It is noted that the data of $\Delta^{17}\text{O}(\text{NO}_3^-)$ are only available for P1 pit.

p31954/l11: But Table 2 states for P6 a $^{15}\epsilon$ value of -54.0‰. which one is correct?

This was a typo. The depths for which the apparent fractionation values were calculated have been updated based on the referee comments, and the new Table 2 and updated text are included in the revised manuscript.

p31954/l24-5: For completeness add also reactions of NO_2^- producing NO_x (photolysis and rxn with OH),

This has been added.

p31955/l8 ...: The theory of how to model ε values needs to be introduced properly in the method section, explaining advantages and limitations, as well as including the latest progress from lab experiments (e.g. Frey et al., 2009; Berhanu et al., 2014). For instance, the approach by Frey et al. (2009) is based on the Zero Point Energy shift (Δ ZPE) model, a general modelling framework developed originally to explain isotopic enrichment in stratospheric gas phase N_2O (Miller and Yung, 2000). A Δ ZPE of -44.8 cm is applied to the $\sigma_{^{14}\text{N}\text{O}_3^-}$ spectrum (measured in lab experiments) to obtain the unknown $\sigma_{^{15}\text{N}\text{O}_3^-}$ spectrum. While model predictions of $^{15}\varepsilon$ match field observations reasonably well, Berhanu et al. (2014) suggest an improved model based on their lab experiments. I suggest to update your calculation following these authors recommendations: use $\sigma_{^{14}\text{N}\text{O}_3^-}$ in the aqueous phase at 278 K (Chu and Anastasio, 2003) and model the ^{14}N to ^{15}N substitution by applying a four parameter analytical model (i.e. asymmetry factor 0.9, Δ C=-32.5 cm, width reduction factor 1%) (Berhanu et al., 2014). In addition state also boundary conditions for your TUV model runs, namely elevation, albedo and column ozone.

The ZPE model is an important choice for us as it allows us to calculate both $^{15}\varepsilon$ and $^{18}\varepsilon$. The text was updated to make clear the assumptions behind using it (e.g. that the isotopologues retain equal quantum yields and similar absorption curves (shape, peak), etc.) We contacted T. Berhanu and now provide comparison with the calculations using the Chu and Anastasio cross sections. Using the C/A data as discussed in the paper, $^{15}\varepsilon$ was calculated to be -45.3 ‰ at P1 and -48.0 ‰ at P7. Using the Berhanu 243K cross sections, $^{15}\varepsilon$ is calculated to be -48.9‰ at P1 and -52.8‰ at P7 (therefore, not changing any of our conclusions). For the TUV calculations, the elevations are those listed in the site descriptions table, which we now note in the text. We assumed clear sky conditions and no overhead SO_2 or NO_2 . Total overhead ozone was set to 300 DU for both sites. Albedo was set to 0.97 following Grenfell et al. (1994 (Grenfell, T. C., S. G. Warren, and P. C. Mullen (1994), Reflection of solar radiation by the Antarctic snow surface at ultraviolet, visible, and near-infrared wavelengths, J. Geophys. Res., 99(D9), 18669-18684, doi:10.1029/94jd01484).

p31955/l12: φ ? also it should be $d\lambda$

Thank you, these were errors associated with file transfer and have been fixed.

p31955/l13: $\Phi_{\text{NO}_3^-}$; note that the quantum yield of nitrate photolysis on ice or in the natural snow pack can be 10-100 times larger than the value based on the Chu and Anastasio (2003) experiments. Please comment in the context of the Meusinger et al. (2014) lab study.

The Meusinger et al. (2014) and Berhanu et al. (2014) studies had only recently been published when we submitted our study. We updated the text to better reflect these studies. The quantum yield, however, will not change the calculated fractionation factors as long as it is equal for the isotopologue pairs.

p31956/l10: as first observed in Dome C snow (Frey et al., 2009)

The observation of this decrease and its previous interpretation are discussed a few lines below in the original text.

p31957/l5: I suggest to introduce the Rayleigh model and equations under methods, i.e. using general equations as developed in Blunier et al. (2005).

This suggestion was taken into account, but we still find that the text is more complete if this remains as part of the discussion.

p31957/l8-15: This is an interesting detail: how does the extent of post-depositional O-exchange vary (in time and in between sites)? And does available information on the depositional environment yield an explanation? While there may be no definitive answer, I suggest to repeat the calculation done for P7 for the other sites (at least on the Plateau), making use of the concurrent $\delta^{18}\text{O}(\text{H}_2\text{O})$ measurements, and evaluate how much accumulative exchange of O atoms is needed to explain observations.

Indeed, the extent of post-depositional O-exchange varied among different sites. We use the discussion here as a “back of the envelope” type approach to hone in on the point we are making. The referee suggests estimating the amount of oxygen required to account for the changes in $\delta^{18}\text{O}$ across all of the inland snowpits. This is a complicated but important point from the perspective of understanding nitrate photolysis in snow, and to be accurate the initially deposited values prior to any post-depositional processing must be known. The following has been added to the discussion. For a simple mass balance approach where photolysis alone is assumed to be responsible for NO_3^- loss and isotopic alteration, a $\delta^{18}\text{O}(\text{NO}_3^-)$ is expected to be 161‰ at 25cm for P7 and thus an observed $\delta^{18}\text{O}$ of 38.4‰ requires that 55% of the O atoms in the remaining NO_3^- are derived from H_2O (if assumed to be the oxidant oxygen pool) for a $\delta^{18}\text{O}(\text{H}_2\text{O})$ of -60‰. For P4, P5 and P6, this exchange is estimated to be 48%, 36% and 2%, respectively. (It is noted that the exchange percent in P6 is rather small, associated with the small difference in concentrations and $\delta^{18}\text{O}$ of NO_3^- between the surface snow ($w(\text{NO}_3^-)=203 \text{ ng g}^{-1}$, $\delta^{18}\text{O}(\text{NO}_3^-)=70\text{‰}$) and the snow at depth ($w(\text{NO}_3^-)=155 \text{ ng g}^{-1}$, $\delta^{18}\text{O}(\text{NO}_3^-)=78\text{‰}$)). Overall, though, this would indicate that re-oxidation plays a very significant role in determining how the $\delta^{18}\text{O}$ of NO_3^- evolves in the snow. But this also raises a number of other difficult questions. For instance, using the exchange calculated at P7 would imply that, using a hypothetical starting $\Delta^{17}\text{O}$ of 32‰ (roughly similar to the top snowpit samples in Frey et al. and Erbland et al.) and $\Delta^{17}\text{O}(\text{H}_2\text{O})$ of 0‰, a $\Delta^{17}\text{O}$ of ~14‰ is predicted at 25 cm, which is far lower than what is observed previous work. A more complete assessment of this is the subject of current and future work in our group.

p31959/l4: If there was only a single process driving isotopic fractionation in snow ...

Thank you, fixed.

p31959/l4-22: I disagree with your interpretation. Changes at depth may not reflect ongoing change but rather changes in past deposition conditions, notably accumulation rates (see above, what is the variability/trend?) and recent changes in column ozone. Associated changes in spectrum and seasonal dose of incident UV in turn impact ϵ values as well as total nitrate loss from snow. Detailed modelling of your pit profiles is beyond the scope of this paper but at least comment. Adding to the pit profiles a 2nd y-axis with approximate snow age would help to discuss this aspect.

Thank you for pointing this out. Our purpose was to first consider changes based on the current understanding of the impact of photolysis on both $\delta^{15}\text{N}$ and $\delta^{18}\text{O}$; then consider how this varies with depth (i.e. time or additional in situ processes). This is now much better framed in the manuscript in sections 4.2 and 4.3. The changes in $\delta^{18}\text{O}$ with depth are different than would be expected, and intriguing. Even with “less” photolytic loss at some time point earlier, we cannot explain such higher values in $\delta^{18}\text{O}$, especially across snowpits

with differing accumulation rates and therefore representation of this signal at different times in history. In other words, if a significant change occurred in say, stratospheric chemistry this should influence the plateau around a similar time – not several years apart. It is a good suggestion to consider adding snow age to the y-axis, and we have added *approximate* timescales based on the accumulation rates (see below; now included in the supporting information Fig. S2). There is little to suggest significant trends in accumulation at the inland sites (described above) and the discussion below could be added to the text to clarify this. We do consider changes in the ozone layer as a way to assess changes in incident UV. Text has been re-organized and sections 4.2 and 4.3 have been extensively modified to better address the different hypotheses for explaining the trends in $\delta^{18}\text{O}$, and being clear which hypotheses have some evidence in their favor (and which do not).

Regarding the dating of P7 (the longest record) based on accumulation rate, the snow pit dug at Dome A in 2005 showed that accumulation was 2.3cm w.eq. a^{-1} during ~1965-2005 (pit dated with the aid of β -radioactivity peaks in 1964; Hou, et al., 2007)(Hou, S., Li, Y., Xiao, C., Ren, J., 2007. Recent accumulation rate at Dome A, Antarctica. Chinese Science Bulletin 52, 428-431.). The Dome A snow pit dug in 2010 showed that the accumulation rate was 2.37cm w.eq. a^{-1} during 1992-2010 (unpublished data, dated from the Pinatubo eruption nssSO_4^{2-} peak in 1992). The stake array observations showed that the snow accumulation at Dome A was 2.35cm w.eq. a^{-1} during 2009-2013. Combined with the discussion above, there is little to support any recent trend in snow accumulation at Dome A. This also speaks to why it is unlikely that the changes in $^{18}\epsilon_{\text{app}}$ can be explained by variation in snow accumulation.

If it is *assumed* that the snow accumulation is constant for 4 inland sites (also see the figure above lending confidence to this assumption), then the snowpit could be dated roughly following the measured accumulation and snow density, as shown below in the figure. We can add this to manuscript, and make clear both the assumption of constant accumulation and the existing data that would indicate this.

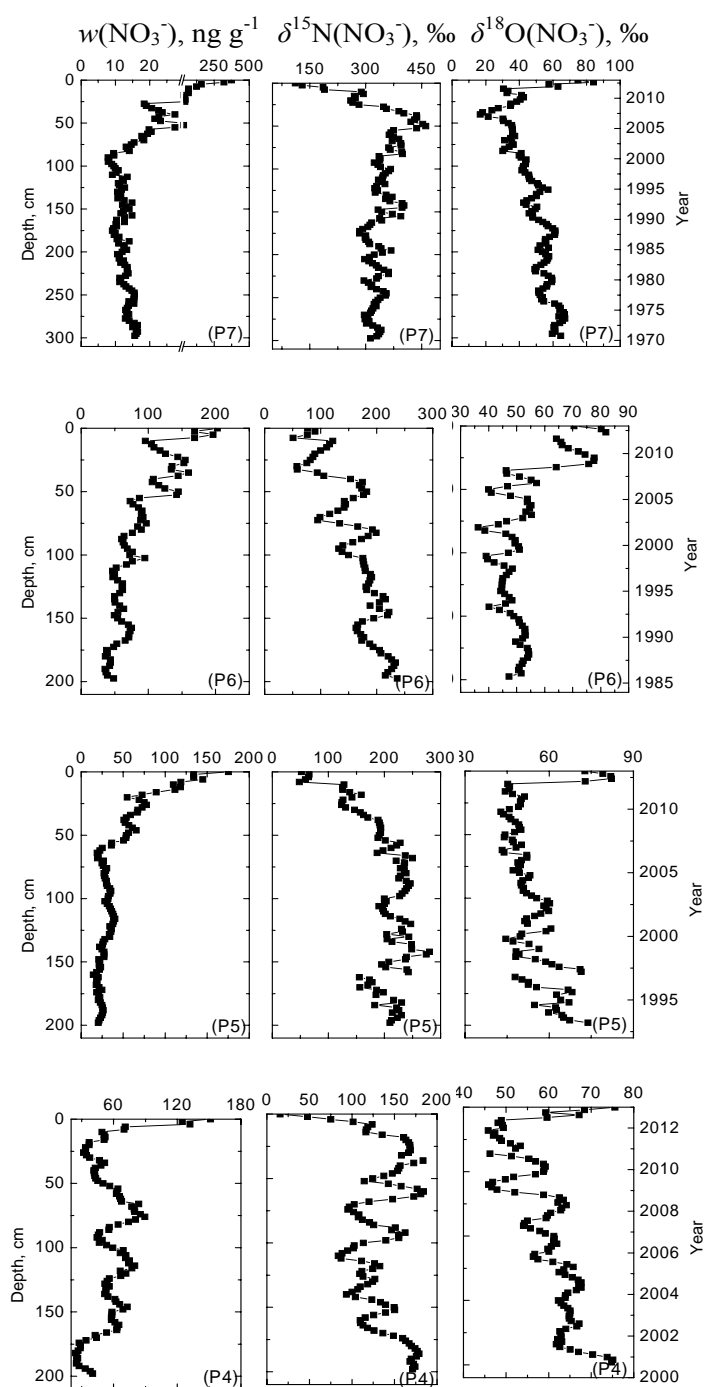


Figure: Rough dating of the group II inland snowpits, from measured snow accumulation rate and snow density (for details see the main text).

p31960/l2: "This can explain ..." is redundant with p31959/l26-7

Changed to "This is consistent with..."

p31960/l3-9 and below: Your suggestion to explain negative correlations between $w(\text{NO}_3^-)$ and $\delta^{18}\text{O}(\text{NO}_3^-)$ at 100-200cm depth through the dark reaction $\text{NO}_2 + \text{O}_3$ needs a more critical evaluation. (i) this process depends on O_3 and NO_2 mixing ratios in firn air at a particular snow depth. One would expect this process to occur at all sites, but why do you observe it only at P4-P7? Comparing the respective snow age with estimates of re-oxidation rates might yield further insight. (ii) in general the gas phase oxidation of NO_x contributes only small amounts of nitrate, and thus must be going on for quite some time to make a significant change in the isotope signature of a very large nitrate reservoir; e.g. taking Dome C firn air observations from the top meter of snow (as an upper limit) for NO_x ($\sim 4\text{ppbv}$) and O_3 ($\sim 16\text{ppbv}$) (Frey et al., 2014), along with typical snow density of 0.3 g cm^{-3} and assuming that the O_3 would oxidise all NO_2 then one obtains roughly $0.4\text{ nmol L}_{\text{H}_2\text{O}}^{-1}$ additional nitrate, contributing only a few ‰ to snow nitrate (typically a few tens of ng g^{-1}). While not impossible, it requires downward redistribution of nitrate, thus in the opposite direction of what is commonly assumed during snow denitrification. (iii) At the driest sites snow at 100-200 cm depth and below may have been deposited during the pre-O3 hole era, when boundary conditions for photolysis were different (see above). Please comment.

This is a very good point regarding the firn air measurements and we have removed discussion of the in situ gas phase oxidation as there is little support for it. As we noted in the text, these types of measurements are critical but have been very limited to date, and the Frey et al. (2014) OPALE paper was not yet published when we submitted our manuscript. As for why the correlations are more apparent in the plateau pits, the photolytic imprint is much less pronounced in the coastal pits due to the higher accumulation (shorter residence time in the photic zone), thus allowing for greater expression of seasonality which obscures a (more limited) post-depositional signature in the isotopic relationships at these sites.

As for changes in the ozone hole, we now more clearly address changing boundary conditions, but a connection to recent ozone depletion is not straightforward. Below are stratospheric ozone plots that help illustrate this. Based on the approximate dating in plots above, P7 overlaps with the pre-ozone hole era (generally considered prior to ~ 1980), but there is no obvious change in the nitrate isotope observations. Also, the shift at which $\delta^{18}\text{O}$ starts increasing with depth and changes in its relationship with $\delta^{15}\text{N}$ occurs roughly between 2000 and 2007 depending on the pit, yet there is also no clear correspondence to a change in ozone. Nor is there a signal reflecting when the ozone hole plateaus in the mid/early 1990s (for pits which overlap). This is not to say that the observed changes aren't related to changing boundary conditions (influence on photolysis or source), but that a link to ozone is not obvious based on a simple comparison. Also, it is notable that the DC07 and DC04 pits from Frey et al. (2009) cover 8-10 years and thus overlap with our observations, yet they do not show any increasing $\delta^{18}\text{O}$ with depth (or decreasing $\delta^{15}\text{N}$ in P7). The depths at which we observe this are also covered by the DC04 and DC07 pits ($\sim 70\text{ cm}$). Given the large spatial influence of the stratospheric ozone on surface irradiance in Antarctica, it seems unlikely that Dome A and its surrounding region would be affected by this process and not Dome C. So something clearly more regional, or local, is at play in our observations. One suggestion was different in situ chemistry. We revisit our explanation, however, and consider other factors, such as possible changes in source and snow chemistry. For ozone, the changes in the boundary conditions should be most influential, and mostly confined, to spring, despite the majority of photolysis occurring in summer.

Minimum springtime ozone at Halley

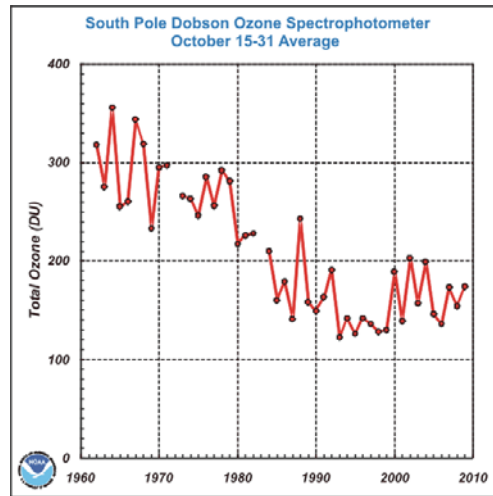
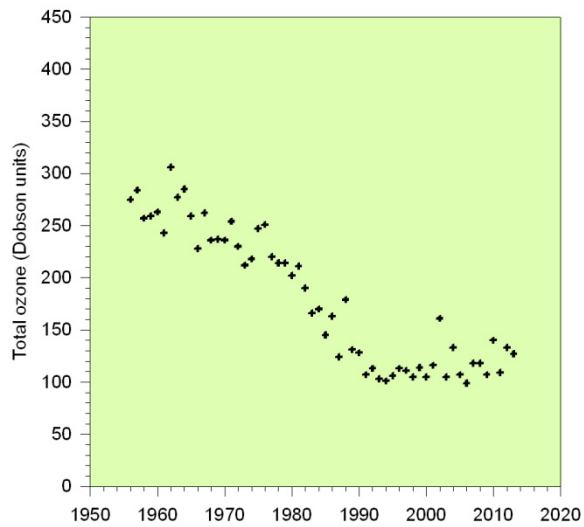
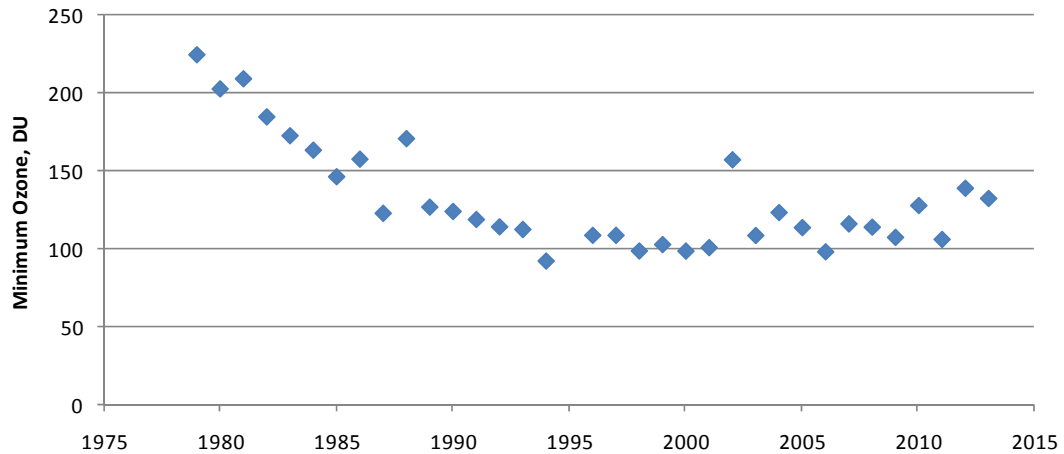


Figure 17. Mean total ozone amount between October 15-31 measured by the Dobson spectrophotometer at the NOAA South Pole station.

Sources: <http://www.antarctica.ac.uk/met/jds/ozone/graphs.html>;

http://www.cpc.noaa.gov/products/stratosphere/winter_bulletins/sh_09/



Minimum daily Southern Hemisphere total overhead ozone from TOMS/OMI measurements.

Data from: http://ozonewatch.gsfc.nasa.gov/statistics/annual_data.html.

p31961/l5-8: An important assumption is also that the boundary conditions of deposition (i.e. for photolysis) remain constant.

Agreed, and based on the comments here and in the other reviews we have extensively modified the discussion to better address this.

p31963/l3-5: Note that photolytic loss (or redistribution) is expected to occur throughout the sunlit season, while deposition of nitrate spikes may depend also on other factors such as the timing of snow fall.

Noted.

p31963/l21: describe dating of the snow pit(s) (along with the accumulation rate measurement) in the method section

This was added along with the table that was originally in the supplement, and is also discussed in section 4.3 now.

p31964/l4: Nitrate profiles in snow and firn show occasionally also winter spikes; for a discussion see Wolff et al. (2008).

In general, the nitrate peaks in surface snow at Halley were present in summertime (Wolff et al., 2008). However, there was also *one prominent peak* in snow concentration of nitrate observed in winter 2004 (see the figure below). Wolff et al. argued that the high concentrations in winter surface snow appear to have been associated with an enhancement of partitioning of nitrate to aerosol, without definitively attributing a cause. In comparison with summertime nitrate peaks, the winter peak was small. Overall, the results in Wolff et al. (2008) are consistent with our findings and we re-phrase this point as “Previous observations at Antarctic coastal sites suggested that NO_3^- concentrations were generally higher in summer and lower in winter (Mulvaney et al., 1998; Wagenbach et al., 1998; Wolff et al., 2008), which is consistent with our findings.”

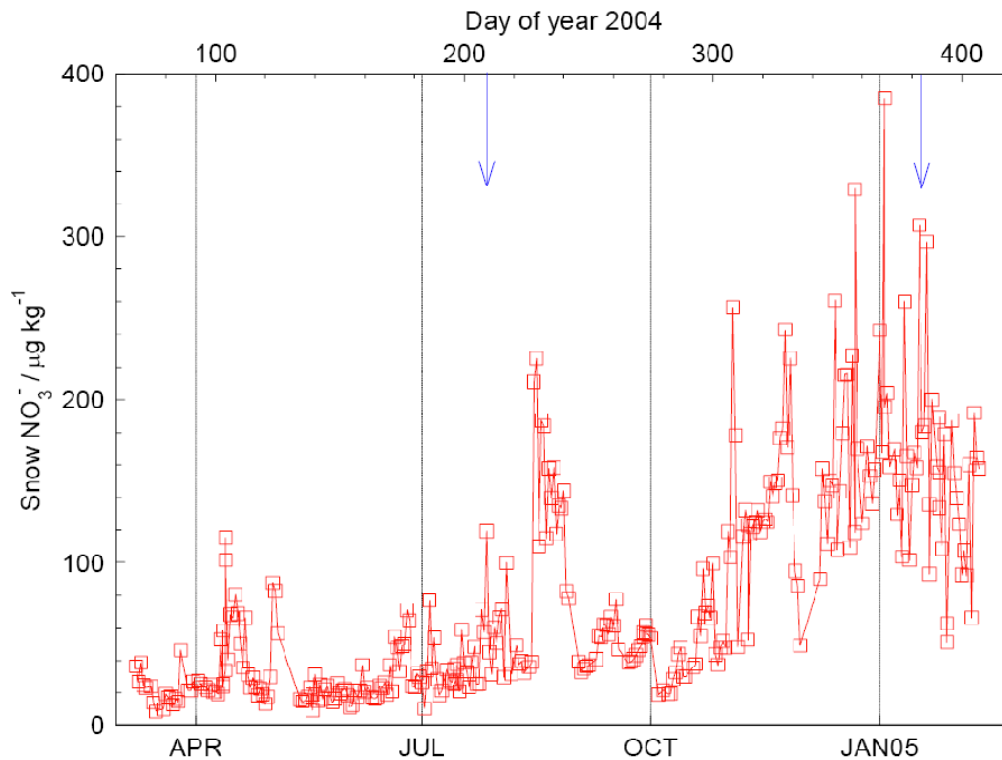


Figure - Nitrate concentrations measured in surface snow samples collected approximately daily at Halley, Antarctica, in 2004 and early 2005. (From Wolff et al., 2008).

(Wolff, E.W., et al., 2008. The interpretation of spikes and trends in concentration of nitrate in polar ice cores, based on evidence from snow and atmospheric measurements. *Atmospheric Chemistry and Physics* 8, 5627-5634.).

p31965/l22 ... : Please explain your hypothesis, i.e. why do you expect larger oxygen isotope values in snow nitrate when the ozone hole area is smaller and column ozone minimum larger? e.g. McCabe et al. (2007) found the opposite, a negative correlation between $\Delta^{17}\text{O}(\text{NO}_3^-)$ and spring time column ozone.

In McCabe et al. (2007), $\Delta^{17}\text{O}(\text{NO}_3^-)$ in snow anti-correlates with the October-November-December column ozone. Two possibilities were proposed there, 1) the nitrate oxygen isotopes are being primarily affected by increases in tropospheric ozone levels because of increased UV from decreased springtime column ozone levels, or 2) the oxygen isotopes are recording increases in the stratospheric nitrate flux during years of reduced column ozone.

In South Pole, nitrate in ice preserves 25% of the original stratospheric isotopic composition, where 75% possess the tropospheric isotopic composition, due to nitrate produced from the photochemically recycled NO_x on the polar plateau (McCabe et al., 2007).

The situation is really different at our coastal site P1, where the photolysis imprint is rather minor. For the snow nitrate in cold season at P1, the higher $\delta^{18}\text{O}(\text{NO}_3^-)$ and $\Delta^{17}\text{O}(\text{NO}_3^-)$ were observed, corresponding to the smaller ozone hole (i.e., column ozone is higher). We were aiming to give McCabe et al. (2007) credit for the previous findings and we have added the above discussion in the text.

p31966/l12: State R^2 and p values for the correlation.

Added to the text: $R^2=0.77$, $p<0.01$.

p31967/l24 - p31968/l10: Cite here again previous work on the East Antarctic Plateau which reached the same conclusions.

These lines discuss the purpose of the study here and summarize the findings in *this study*. Throughout the text we consistently give credit to the previous work done on the EAIS. The latter part of that section also discusses the relationship between $w(\text{NO}_3^-)$ and $\delta^{18}\text{O}$, which has not been previously pointed out.

Table 1: I recommend to compare profile statistics over a common depth interval (see comment above).

See response above and new tables as suggested by the referee.

Figure 6: I suggest plotting as a function of accumulation rate (or its inverse) to compare to other studies (see comment above).

Thank you for the suggestion. The previous figure 6 is now replaced by comparison of the full profile of observations for the snowpit with the asymptotic calculated profiles.

Dr. Erbland

We thank Dr. Erbland for his careful and thoughtful review of our work. Please see below for point-by-point responses in blue following Dr. Erbland's comments.

Shi et al. report 7 profiles of nitrate mass fraction and isotopic composition (mostly $\delta^{15}\text{N}$ and $\delta^{18}\text{O}$. $\Delta^{17}\text{O}$ is measured for P1 only) from 2 to 3 meters depth snow pits dug along the Chinese traverse from Zhongshan station to Dome A in East Antarctica. I congratulate the authors for compiling these amazing datasets both in terms of spatial coverage and depth range.

The datasets are exciting for three reasons. First, because the snow pits were dug in a sector which has never been sampled for this purpose before (to the best of my knowledge) and which includes Dome A, the summit of the East Antarctic ice sheet. Second, because continuous profiles are available below the photic zone. Third, because this study probably reports the highest $\delta^{15}\text{N}(\text{NO}_3^-)$ value (+461 ‰) ever measured in Antarctic snow.

It is disappointing to see that in this study, the Zhongshan – Dome A transect is treated as if it was in a different environment compared to the D10 – Dome C – Vostok transect documented in other recent studies (Frey et al., 2009; Erbland et al., 2013). Both transects are part of the East Antarctic ice sheet and cover similar ranges of elevations, snow accumulation rates, temperatures... I think that these facts are sufficient to encourage a proper comparison of the new datasets obtained to those previously published. To me, the first goal of this paper should be to compare to and confirm other observations on the East Antarctic ice sheet. For instance, Fig. 4 in Erbland et al. (2013) could be reproduced with the new datasets published in the present study.

We agree that the text should include more comparison with the Erbland dataset. We have reproduced the suggested figure (see below) and is now included in the supplement. The snow samples on the traverse of D10-Dome C-Vostok (referred to as DDV in following) were collected only to the depth of ca. 20cm for most of the snowpits (Frey et al., 2009; Erbland et al., 2013). We thus only compare the apparent fractionation constants (ϵ_{app}) and asymptotic values (as.) from the depth interval of 0-20cm to make a direct comparison with those in Erbland et al. (2013). It is noted that all of the data from Erbland et al. (2013) were used to make the figure. For the apparent fractionation constants, all of the seven pits in this study were included in the figure, with red squares and green triangles representing $p < 0.05$ and $p > 0.05$, respectively (we do not know the p-values for the data reported in the Erbland et al. study). In terms of the asymptotic values, based on the fact that $w(\text{NO}_3^-)$, $\delta^{15}\text{N}(\text{NO}_3^-)$ and $\delta^{18}\text{O}(\text{NO}_3^-)$ varied significantly along the profiles in the pits P1-P3 (Figure 2 in the manuscript), the calculation of asymptotic values were not performed for P1-P3. The asymptotic values of P4-P7 were included in the figure, with red squares and green triangles representing $p < 0.05$ and $p > 0.05$, respectively.

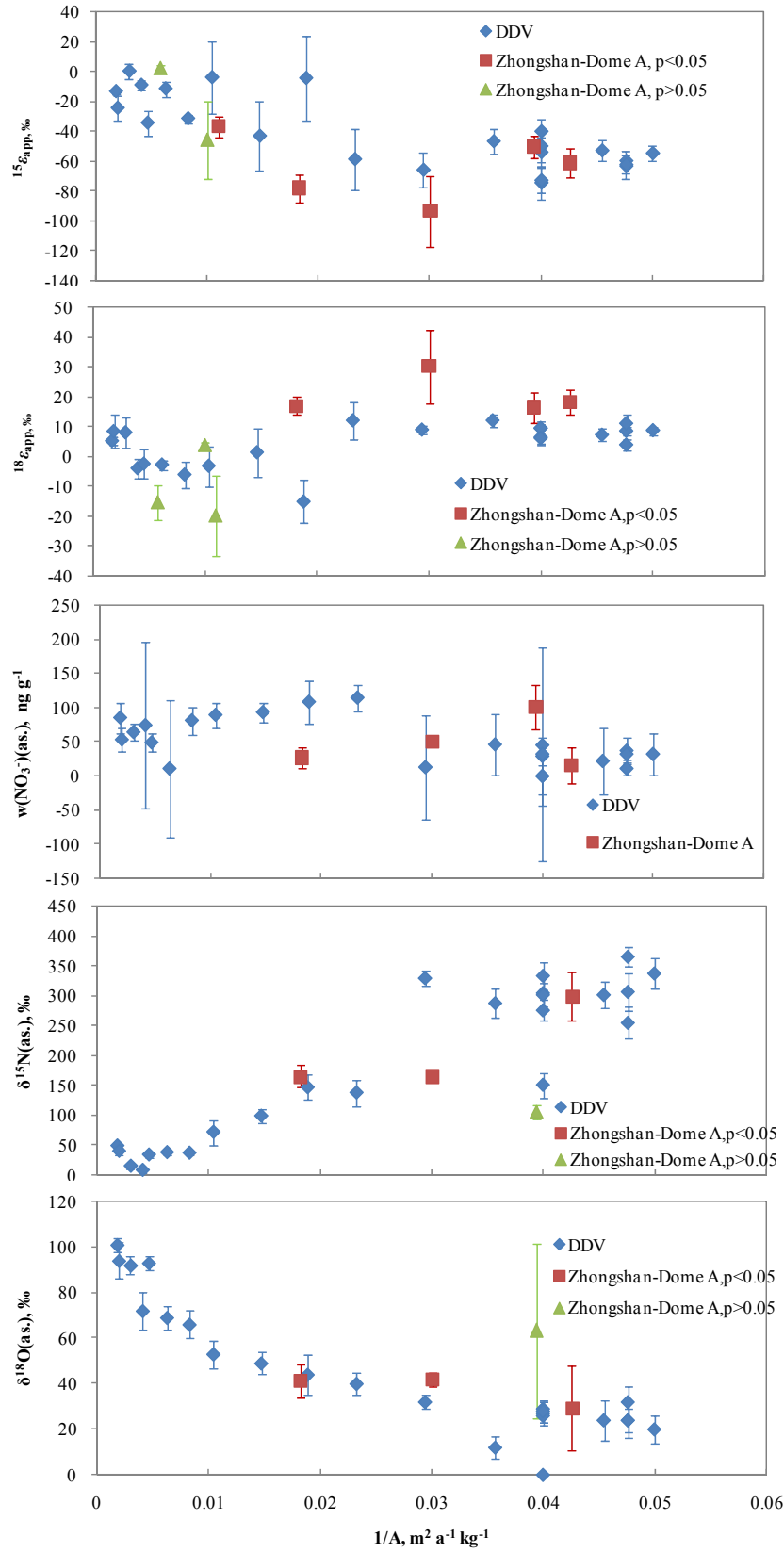


Figure – Comparison of current study data with Erbland et al. (2013) Figure 4. Now, this figure was included in the supporting information, Fig. S1.

Unfortunately, the oxygen isotope anomaly ($\Delta^{17}\text{O}$), which is of great interest to track the oxidation of NO_x , has not been measured for 6 of the 7 snow pits. I understand that the measurement of $\Delta^{17}\text{O}(\text{NO}_3^-)$ was not possible because of the small nitrate amounts in most of the snow pits. However, the discussion of this single $\Delta^{17}\text{O}$ profile for one snow pit only has confused me at the end of the manuscript. I wonder if this dataset is at its place in the present manuscript.

Based on referee #2, we have now included a box and whisker plot of all of the data (instead of the previous table of data). Along with this we have included the P1 $\Delta^{17}\text{O}$ data (and there is discussion of this in the methods section). We feel this will better prepare the reader for what is to come.

In agreement with Anonymous Reviewer #1, I do not agree with the treatment of the profiles 1 below the photic zone (see my comment below). Also, I wonder if those data could not be placed in a different manuscript or this manuscript could be revisited. Indeed, the profiles below the photic zone speak less than do profiles in the photic about the nature of the loss process at play in the top decimeters but more about the variability of the surface loss process with time. This specific point could a model framework which has recently been submitted to as a companion to Erbland et al. (2013) (Erbland et al., 2015, not available online yet).

While we appreciate this concern, we do not feel it is appropriate to report separately the data above and below the photic zone. Part of the purpose of our study, and indeed the reason it is different than previous work by Dr. Erbland and others, is to test our understanding of what happens to nitrate (isotopically) in the photic zone and how buried nitrate can be interpreted in this context. Now, we noticed that the a companion to Erbland et al. (2013) is available (Erbland, J., Savarino, J., Morin, S., France, J. L., Frey, M. M., and King, M. D.: Air-snow transfer of nitrate on the East Antarctic plateau -Part 2: An isotopic model for the interpretation of deep ice-core records, *Atmos. Chem. Phys. Discuss.*, 15, 6887-6966, 10.5194/acpd-15-6887-2015, 2015.).

Major comments

In agreement with Anonymous Reviewer #1, my main concern is about the authors' interpretation of the data analysis of the Erbland et al. (2013) study. In this work, an attempt was made to systematically characterize the mass fraction and isotopic composition values attained by nitrate immediately below the photic zone. Below this zone, nitrate can be considered inert with respect to photo-processes. The characterization is achieved by assuming that the post-depositional processing of nitrate is constant throughout the residence of a snow layer in the photic zone. Therefore, the mass fraction and isotopic composition of nitrate in the photic zone were assumed to follow exponential behavior whose decay parameter was fitted in the 1-30 cm range. In Erbland et al. (2013), a few samples were collected below a depth of 60 cm, i.e. 3 times the e-folding attenuation depth (as modelled by Zatko et al., 2013, for remote 19 plateau sites). Those

samples share as follows : 8 in DC04 (DC pit) and one in each of the IV, 20 VI, VIII, X, XII, XIV, XVI, XVIII, XX and XXII snow pits (from DC to the coast). Although those samples were not sampled below a depth of 1 m, I acknowledge that it would have been more suitable not to consider them in the calculation of the asymptotic values. However, taking them into account does not lead to significant differences as one can observe from the DC04 snow pit (Fig. 14 in Erbland et al., 2013). Last, I add that if any main deviation from the exponential fit may have appeared, this would have been accounted for in the calculation of the uncertainty in $\omega(\text{as.})$, $\delta^{15}\text{N}(\text{as.})$, $\Delta^{17}\text{O}(\text{as.})$ and $\delta^{18}\text{O}(\text{as.})$.

We appreciate Dr. Erbland sharing additional insight, but it still stands that the published work includes the samples below the photic zone. And while this does not appear to make a significant difference at DC04, this is the pit with the most information (i.e. nitrate sampled well below the photic zone), and this can indeed make a significant difference at the rest of the sites as proven in our study. We clearly needed to better address the starting assumptions in our work (which are the same assumptions made in Erbland et al. and Frey et al.) and more directly set out what questions we are testing. Both sections 4.2 and 4.3 have been extensively modified. Over what depth is it appropriate to calibrate the exponential decay (i.e. asymptotic) relationship? We are in fact showing that it is important to understand this and are questioning how to best use this relationship. The uncertainty as measured by standard deviation or standard error alone is incomplete without consideration of the importance of the relationships found, which we are measuring by significance (p-values) and by “fit” (r^2 values).

By no means must the exponential fits be used to predict the mass fraction and isotopic composition of nitrate at depths well below the photic (e.g. below 1 meter). Indeed, nitrate below the active zone of snow photochemistry may vary both in terms of mass fraction and isotopic composition as a result of varying conditions in its post-depositional processing. For example, the residence time of nitrate in the photic zone could vary under the effect of variations in the local snow accumulation rates (which greatly vary at the decimeter scale, Libois et al., 2014). Also the photochemical rates and $^{15}\text{N}/^{14}\text{N}$ fractionation constant could change with time mostly under the effect of changes in the ozone column above site.

Similarly to the calculation of the asymptotic values, apparent fractionation constants should be calculated for samples in the photic zone (say the top 60 cm). By the way, I recommend that the author should differentiate the apparent fractionation constants (which could be denoted “ $^{15}\epsilon$ ”) and the fractionation constants associated with a specific process (e. g. “ $^{15}\epsilon_{\text{pho}}$ ” for the $^{15}\text{N}/^{14}\text{N}$ fractionation constant associated with the photolysis of nitrate).

We have recalculated the apparent fractionation factors ($^{15}\epsilon_{\text{app}}$ and $^{18}\epsilon_{\text{app}}$) over the depth intervals of 0-20cm, 0-40cm, and 0-60cm, to better represent our aim. If indeed nothing changes under the photic zone, then the apparent fractionation constant that is derived over an interval below the photic zone, should reflect that for an interval near the surface. In other words, as the nitrate moves out of the photic zone the impact of the photolysis

(fractionation constant) should be “locked in.” So if that apparent fractionation constant changes with the depth interval over which it is calculated, why would this be? Our paper aim is to consider this question and test our current understanding of how we explain the changes in the isotopes of nitrate with depth. We have now included a more complete discussion of how the modeled fractionation factors and rate constants change for different boundary conditions. (And see the discussion in our response to reviewer 2 regarding ozone.) We also aim to consider how to effectively use the asymptotic relationships to understand how much the nitrate has varied over time outside of the expectation of the photolytic change alone. Again, the discussion of this in the manuscript (and distinction of the fractionation factors for different processes) is much improved based upon the concerns raised by Dr. Erbland.

Some additional questions and comments (not comprehensive)

Methods. What is the maximum sample volume that you can inject to the denitrifying bacterial? Line 2 Page 31949, I read that samples with nitrate mass fractions as low as 6.0 ng g⁻¹ can be analyzed. This means that, if you aim for a minimum amount of 5 nmol of nitrate (Line 1 P 15 31949), your injected sample volume is 51.5 ml. Can you explain how you deal with such a high volume? How do you prepare the denitrifying bacteria?

The maximum injection volumes are near 55 mL for the method at Brown University (see the figure below). The autosampler carousel is designed to fit either 20 mL vials or 60 mL vials – both vials have the same size septa caps (see the figure below), and the purging needle is designed such that the carrier gas and sample outflow into the rest of the system near the very top of the vial (such that a volume near 60 mL can be achieved). We have tested the addition of high volume samples extensively, and have included additional information in the text and in the supplemental material. As requested by the referee, below is an example table of data obtained from a 5 nmol run. It is critically important when running very low concentrations to include standards/reference materials that are very close in concentration to the samples for correcting the data (i.e. there is a small “volume” effect such that is accounted for by using samples and standards of the same volume), and we apologize for not including detailed information on this originally. Below are also two additional tables of data (now included) obtained on internal quality controls. The first is a mix of USGS 35+USGS 34, and the second is KNO₃. Both are used as internal controls for quality purposes (they are treated as samples and corrected to reference materials in each run). Each has been injected for different volumes in different runs and its isotope values corrected to reference materials in each run that are close in concentration (i.e. close in injection volume). As you can see this also shows excellent reproducibility over a variety of runs and range in (low) concentrations for $\Delta^{17}\text{O}$, $\delta^{15}\text{N}$, and $\delta^{18}\text{O}$.

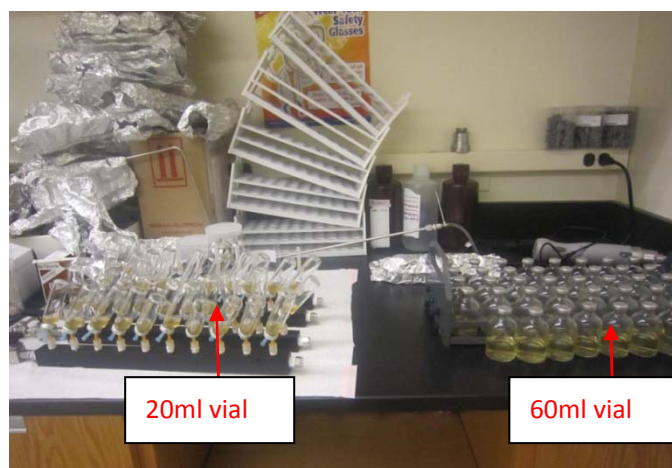


Figure: The two types of injection vials (e.g., 20ml and 60ml) used at Brown University.

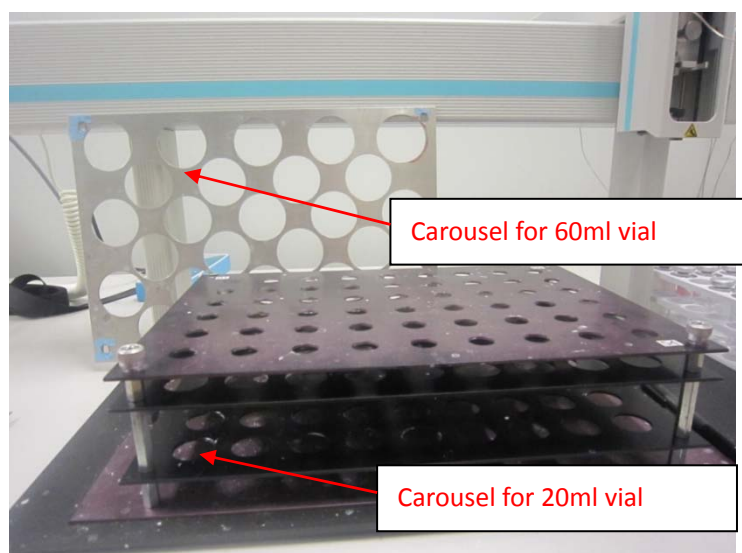


Figure: The autosampler carousel designed to fit either 20 mL vials or 60 mL vials

Table: Example raw data using 5nmol injections. Note that the “flush vial N₂O” is a vial filled with reference gas that serves as an additional quality check on the system prior to and after completing a sample run.

Sample/Standard	Injection volume, ml	Peak area, Vs	rd ¹⁵ N uncorrected	rd ¹⁸ O uncorrected
flush vial N ₂ O		22.1	-0.7	-0.2
flush vial N ₂ O		23.6	-0.9	-0.5
Blank		<0.2		
USGS 35	25.0	3.7	3.7	44.9
USGS 32	25.0	4.3	156.9	20.3
USGS 34	25.0	4.0	-3.5	-28.6
IAEA N3	25.0	4.2	3.7	17.7
Sample-2	24.5	3.8	271.6	40.2
Sample-4	24.5	4.4	299.1	35.8

Sample-7	25.1	4.5	323.3	35.2
Sample-8	22.1	4.3	299.0	36.5
Sample-9	23.6	4.2	290.3	37.2
IAEA N3	25.0	4.2	3.9	17.6
USGS 35	25.0	4.0	3.5	44.2
USGS 34	25.0	4.1	-3.0	-28.2
USGS 32	25.0	4.2	155.5	20.3
Sample-12	24.6	4.3	346.2	33.0
Sample-13	29.0	3.7	318.2	34.6
Sample-15	27.3	3.9	323.2	37.3
Sample-16	29.3	3.7	308.9	38.9
Sample-17	26.4	3.4	284.1	42.8
Sample-18	24.4	3.9	289.5	40.2
Sample-19	28.0	4.0	269.7	42.4
USGS 32	25.0	4.2	155.3	20.4
IAEA N3	25.0	4.4	3.9	17.4
USGS 35	25.0	3.9	3.4	44.7
USGS 34	25.0	4.0	-3.2	-28.8
flush vial N ₂ O		25.5	-1.1	-1.0

Table: Results of an internal quality control, KNO₃. The $\delta^{15}\text{N}(\text{NO}_3^-)$ mean is $58.37 \pm 0.62\text{‰}$, with the range of 57.52-59.59‰. The mean of $\delta^{18}\text{O}(\text{NO}_3^-)$ is $30.65 \pm 0.52\text{‰}$, with the range of 29.55-31.50‰.

$\delta^{15}\text{N}(\text{NO}_3^-)$	$\delta^{18}\text{O}(\text{NO}_3^-)$	Injected volume (mL)	Concentration (μM)
59.39	30.43	20.00	0.50
58.19	30.85	20.00	0.50
58.37	30.80	20.00	0.50
57.52	31.13	16.67	0.60
58.77	30.62	16.67	0.60
58.12	30.59	13.33	0.75
57.66	31.50	13.33	0.75
58.73	30.16	13.33	0.75
58.39	31.31	10.31	0.97
57.71	31.00	10.00	1.00
58.26	31.01	10.00	1.00
58.48	30.82	10.00	1.00
57.70	30.45	10.00	1.00
57.57	31.04	10.00	1.00
58.96	29.93	10.00	1.00
59.59	29.77	10.00	1.00
59.31	30.16	10.00	1.00
58.70	30.88	10.00	1.00
58.27	29.55	10.00	1.00
57.76	31.01	6.67	1.50

Table: Results of $\Delta^{17}\text{O}$ for USGS35/34 mixture, an internal quality control. The mean $\Delta^{17}\text{O}(\text{NO}_3^-)$ of $11.45 \pm 0.44\text{‰}$ and the range of 10.88-12.21‰.

$\Delta^{17}\text{O}(\text{NO}_3^-)$	NO_3^- amount (nmol)	Concentration (μM)	Injected volume (mL)
11.26	50.00	5.00	10.00
10.89	50.00	5.00	10.00
10.88	50.00	3.00	16.67
11.06	50.00	3.00	16.67
11.78	50.00	2.00	25.00
10.94	50.00	2.00	25.00
11.62	50.00	1.50	33.33
11.71	50.00	1.00	50.00
12.21	50.00	1.00	50.00
11.83	50.00	1.00	50.00
11.59	45.00	3.00	15.00
11.37	45.00	2.00	22.50
11.23	40.00	1.00	40.00
11.20	40.00	1.00	40.00
12.20	40.00	1.00	40.00

Calculation of $15\epsilon_{\text{pho}}$. I agree with Anonymous Reviewer 2 who questions the calculation of $15\epsilon_{\text{pho}}$. Could you please give more details about your calculation? Which absorption cross section have you used for $\sigma(^{15}\text{NO}_3^-)$ and for $\sigma(\text{N}_2\text{O})$? Also, how have you obtained the actinic flux at the different sites and for solar noon at summer solstice? Have you measured it or have derived it from a radiative transfer model? In the latter case, which ozone column value have you obtained? I also suggest the use of the $\sigma(^{14}\text{NO}_3^-)$ and $\sigma(^{15}\text{NO}_3^-)$ spectrums recommended by Berhanu et al. (2014).

As we noted in the text, the actinic flux was calculated using the TUV (5.0) model for each site, and the fractionation factor calculation used the Chu and Anastasio cross sections and quantum yields. We have now more completely described the inputs, however. We assumed clear sky conditions and no overhead SO_2 or NO_2 . Total overhead ozone was set to 300 DU for both sites. Elevation was that listed in the site descriptions table, which we now note in the text. Albedo was set to 0.97 following Grenfell et al. (1994) (Grenfell, T. C., S. G. Warren, and P. C. Mullen (1994), Reflection of solar radiation by the Antarctic snow surface at ultraviolet, visible, and near-infrared wavelengths, *J. Geophys. Res.*, 99(D9), 18669-18684, doi:10.1029/94jd01484). We now also provide comparison to using the Berhanu modeled cross sections at 243K to calculate the fractionation factors. In brief, using the C/A data as discussed in the paper, $^{15}\epsilon$ was calculated to be -45.3‰ at P1 and -48.0‰ at P7. Using the Berhanu 243K cross sections, $^{15}\epsilon$ is calculated to be -48.9‰ at P1 and -52.8‰ at P7. Using the Berhanu cross section does not change any of our conclusions.

Lines 5 P 31954: Zatko et al. (2013) report a modelled e-folding depth of 18-22 cm which makes the photic zone ca. 60 cm. Why do you then calculate the apparent

fractionation constants in the upper 25 cm only?

We have re-calculated the apparent fractionation factors ($^{15}\epsilon_{\text{app}}$ and $^{18}\epsilon_{\text{app}}$) over the depth intervals of 0-20cm, 0-40cm, and 0-60cm, to better represent our aim of understanding changes in the apparent fractionation with depth. Dr. Erbland also points out in comments below the need for calculating uncertainty and that is included here as well (note the +/- 1 standard error) in updated tables and figures. The observed fractionation ϵ was obtained from the linear fit of $\ln(\delta_{\text{snow}}+1)$ vs. $\ln(w_{\text{snow}})$. The software package Origin 7.5 was used for the linear fitting and calculation of the standard error.

Table. Observed fractionation constants for ^{15}N and ^{18}O of NO_3^- ($^{15}\epsilon_{\text{app}}$ and $^{18}\epsilon_{\text{app}}$) calculated for different snow layer depths from the linear regression of $\ln(\delta_{\text{snow}}+1)$ vs. $\ln(w_{\text{snow}})$ in Eq. (2). Four different depth intervals were selected for calculating ϵ_{app} : 0-20cm, 0-40cm, 0-60cm, 100-bottom and the entire pit. Also given are the standard error (1σ), r^2 values and the significance level, p , where bolded values represent $p < 0.05$.

Snow pit	Depth	^{15}N			^{18}O		
		$^{15}\epsilon_{\text{app}} \pm 1\sigma$, ‰	p	r^2	$^{18}\epsilon_{\text{app}} \pm 1\sigma$, ‰	p	r^2
P1	0-20cm	2.4±2.0	0.379	0.157	-15.3±6.0	0.044	0.588
	0-40cm	-0.4±5.0	0.943	0.000	-8.7±7.0	0.248	0.109
	0-60cm	-3.9±14.0	0.785	0.004	-9.4±10.0	0.368	0.043
	100-Bottom	17.2±14.0	0.248	0.094	-6.5±5.0	0.175	0.127
	Entire	-11.8±7.0	0.098	0.056	-3.7±4.0	0.390	0.015
P2	0-20cm	-45.5±26.0	0.184	0.497	4.0±1.0	0.017	0.887
	0-40cm	0.8±10.0	0.936	0.001	-4.2±4.0	0.274	0.167
	0-60cm	4.1±15.0	0.789	0.007	-2.1±4.0	0.647	0.020
	100-Bottom	21.5±16.0	0.197	0.091	11.2±4.2	0.015	0.287
	Entire	11.9±9.1	0.198	0.043	7.0±3.6	0.060	0.090
P3	0-20cm	-36.8±6.7	0.012	0.909	-19.8±13.5	0.237	0.420
	0-40cm	-27.5±11.0	0.036	0.488	-15.4±11.0	0.188	0.233
	0-60cm	-28.8±9.1	0.009	0.476	-14.0±8.7	0.135	0.192
	100-Bottom	12.3±12.0	0.318	0.059	13.5±18.6	0.478	0.030
	Entire	-1.2±4.9	0.811	0.002	15.4±8.0	0.061	0.092
P4	0-20cm	-77.8±9.2	0.000	0.888	17.1±3.1	0.000	0.778
	0-40cm	-81.6±7.5	0.000	0.868	14.0±2.1	0.000	0.706
	0-60cm	-73.3±9.8	0.000	0.665	11.4±2.5	0.000	0.419
	100-Bottom	-56.0±5.3	0.000	0.703	-3.4±1.3	0.011	0.126
	Entire	-58.7±5.0	0.000	0.584	1.4±1.8	0.433	0.006
P5	0-20cm	-93.1±23.6	0.003	0.633	30.2±12.3	0.036	0.401
	0-40cm	-92.1±10.8	0.000	0.791	24.9±5.5	0.000	0.522
	0-60cm	-92.5±8.1	0.000	0.820	16.0±3.6	0.000	0.412
	100-Bottom	27.3±13.7	0.053	0.083	-9.6±4.0	0.022	0.114
	Entire	-56.9±5.0	0.000	0.577	0.0±1.6	0.985	0.000
P6	0-20cm	-50.2±7.3	0.000	0.889	16.7±5.1	0.017	0.638
	0-40cm	-63.0±21.0	0.010	0.390	16.2±12.1	0.201	0.114

	0-60cm	-70.8±25.1	0.010	0.265	17.9±9.3	0.066	0.145
	100-Bottom	-61.3±8.0	0.000	0.605	-7.8±2.4	0.003	0.216
	Entire	-76.8±5.8	0.000	0.694	11.3±2.1	0.000	0.265
P7	0-20cm	-61.3±9.8	0.000	0.849	18.4±4.1	0.003	0.738
	0-40cm	-73.9±8.5	0.000	0.834	16.4±2.4	0.000	0.753
	0-60cm	-81.0±8.7	0.000	0.789	15.2±1.9	0.000	0.728
	100-Bottom	20.7±14.4	0.154	0.026	10.0±4.5	0.051	0.060
	Entire	-31.5±5.0	0.000	0.251	-0.7±1.7	0.690	0.001

Lines 13-14 P 31957: “This is a substantial exchange of O atoms, indicating that re-oxidation plays a major role in determining the $\delta_{18}\text{O}$ of NO_3^- in the upper snowpack”. I find this statement a little daring. Indeed, what do you mean by “the upper snowpack”? It is the top few centimeters? The top decimeters? If the top few centimeters are considered, $\delta_{18}\text{O}$ of NO_3^- in this part of the snowpack must be close to that in the atmosphere as it is the case when considering, at the extreme, the skin layer (the top 4 mm of the snowpack) (Erbland et al., 2013).

This section has been re-named and text is added to clarify that we are describing the re-oxidation of nitrate in the condensed phase. The oxygen exchange estimate in the paragraph Dr. Erbland refers to was for the observed changes in the top 25cm, as was noted in the text. This is what “upper snowpack” was meant to refer to. This has been clarified. We agree that as observed by Erbland et al. (2013) the oxygen isotopic composition of nitrate in the skin layer, or that produced locally in the gas phase, would be expected to be in equilibrium with local oxidants.

Section 4.2: I don’t understand the author’s goal in this section. Perhaps denoting the quantities with better care will help to understand the point made in this section. Indeed, quantities of interest calculated so far are the apparent fractionation constants (which I suggest to denote with an “app” subscript). The authors decided to calculate those quantities in the 0-25 cm range. As I wrote above, I do not agree with this choice since the loss occurs in the whole photic zone, i.e. ca. 60 cm when considering 95 % of UV radiation extinction (3 times the attenuation depth). Fractionation constants using the data below the photic zone (such as 25-100 cm range or 100 cm to pit base range) could be calculated although I do not see what information are obtained from them. Indeed, the assumption of constant post-depositional conditions is difficult to make depending on the considered depth range. However, if such choice of calculating fractionation constants below the photic zone is made, I recommend to use a different denomination than “apparent” to avoid confusing. The quality of the information obtained from the calculation of apparent fractionation constants depends on the uncertainty linked with each of them. I recommend that the calculated fractionation constants are given with the corresponding uncertainty (e.g. $\pm 1\sigma$) as in Frey et al. (2009) and Erbland et al. (2013). Indeed, this will test the limitations of the assumed single-step one-way Rayleigh model. I note the authors’ effort to report values of statistical interest (e. g. Tab. 2). I observe that

those question the approach presented in Fig. 4. Indeed, to me r^2 is a better measure than p to determine the relevance of the calculated fractionation constant. Let's take the example of the $^{15}\epsilon$ and $^{18}\epsilon$ values calculated for the 25-100 cm and 100-bottom ranges as well as for the entire snowpack (Tab. 2). I observe that the ϵ values which significantly differ from those calculated in the 0-25 cm range (i.e. $^{15}\epsilon$ in the 25-100 cm and 100-bottom ranges and the entire snowpack in P7) almost systematically feature low (< 0.5) r^2 values. If uncertainties ($\pm 1\sigma$) were calculated as in the aforementioned studies, I am pretty sure that those would be high when r^2 is low. In other words, I recommend to the author that they use a better measure of the uncertainty in the calculation of fractionation constants in order to conduct their depth dependency analysis (Figure 4).

Thank you for the suggestions, all of these are incorporated to better distinguish the different quantities and clarify the discussion in the text. We have re-calculated both the apparent fractionation constants and the asymptotic relationships as shown in the response above for 0-20cm, 0-40cm, and 0-60cm, etc. Table 2 has been updated above and now also includes the standard error. The standard errors are not necessarily larger when the relationships are not statistically significant. We therefore feel it is a better measure of “fit” to consider the r^2 and significance values before considering the standard error in evaluating the robustness of this approach for reconstructing the isotopic values of nitrate with depth. For comparison, it would be useful if future work follows the standard practice of reporting the statistical significance of a linear regression in addition to the error for the coefficient of interest.

Section 4.3: The use of exponential fits as in Erbland et al. (2013) is misunderstood (see main 4 comments above).

Please see comments and responses above.

Section 4.4: It seems to me that parts of the discussion in this section rely on the assumption that the $\delta^{15}\text{N}$ signature is conserved at the air-snow interface, in other words, that $\delta^{15}\text{N}$ in skin layer nitrate is the same than $\delta^{15}\text{N}$ in atmospheric nitrate. However, the $\delta^{15}\text{N}$ values measured at the air-snow interface at Dome C show that the annual weighted average in $\delta^{15}\text{N}$ in skin layer nitrate is 24.7 ‰ than that in atmospheric nitrate. A fraction of this observed shift may be linked to a fractionation of the nitrogen isotopes of nitrate during the deposition of this compound from the atmosphere to the snow (Erbland et al., 2013).

Agreed that this is not necessarily a valid assumption and we now include the observation at Dome C in our discussion as it may also help to explain the greater than expected values from stratospheric nitrate as compared to that in Savarino et al. (2007). The observed difference between the skin layer and that in atmospheric nitrate at Dome C, however, is a unique finding. We should indeed consider that this difference may apply in the coastal zone, but note that the partitioning between the atmosphere and skin layer at

Dome C might be different in a very different environment.

Line 25 Page 31964: I recommend the authors to consider the $\delta^{15}\text{N}_{\text{phy}}$ value measured at $-20\text{ }^{\circ}\text{C}$ (Erland et al., 2013) with care. Indeed, only little nitrate mass fractions changes were observed during this two-week experiment.

Thank you for this comment. Our purpose here was to review the state of the science and consider both the theoretical and the experimental results in terms of our observations. The wording in the manuscript needs to be modified to better reflect this.

Tables 2 and 3: See comment above. Can you give an estimate of the uncertainty in the fractionation constants and asymptotic values?

Please see the updated Table 2 and figures in the responses above.

Figure 2: the different scales and broken axis (for nitrate mass fractions in P7) are confusing.

It is important to us to show all of the snowpit data and it is difficult given the significant differences in ranges. We felt this was the best compromise to include a broken axis. The split axes was clearly pointed out in the figure caption.

Figure 3: it is confusing here that $\delta^{15}\text{N}$ and $\delta^{18}\text{O}$ data are represented against $\omega(\text{NO}_3^-)$ and that slopes are calculated. Indeed, those may confuse the reader who may consider the slopes as fractionation constants (normally derived in the $\ln(\delta + 1)$ versus $\ln(\omega(\text{NO}_3^-))$ space).

We will take care to point out this difference from the fractionation constants calculation in the text and figure caption. The point here was that the simple relationship between concentration and the isotopes were changing with depth and we feel it is illustrative of the point directly without converting to the log scales.

Figure 4: See comment above. A precise estimate of the uncertainty associated with the calculation of $\delta^{15}\text{N}$ and $\delta^{18}\text{O}$ is needed.

Please see the new figure in response above.

Table S1 (Supplementary): I agree with the other reviewers, this table should be placed in the main text. How were the snow accumulation rates computed? From the bamboo sticks you obtain the accumulated snow thickness. Have you made an assumption on the snow density? The accuracy of the mean annual temperatures does not seem sound to me. The sampling date format which is displayed is “YYYYMM” and not “YYMM”. By the way, could you provide the day when the pits were dug? Only the month and year are available.

The table has been updated (see below) and is now included in the main text as Table 1. Please refer to our response to the second reviewer regarding accumulation and temperature.

Table . Summary information for the seven snowpits presented in this study.

Snowpit	Location	Elevation, m	Distance from coast, km	Mean annual accumulation, $\text{kg m}^{-2} \text{a}^{-1}$ ¹⁾	Mean annual Temperature, $^{\circ}\text{C}$ ²⁾	Depth, cm	Sampling resolution, cm	Sampling date, DD.MM.YYYY
P1	71.13°S, 77.31°E	2037	200	172.0	-29.12	150	3.0	18.12.2012
P2	71.81°S, 77.89°E	2295	283	99.4	-32.87	200	5.0	20.12.2012
P3	73.40°S, 77.00°E	2545	462	90.7	-35.72	200	5.0	22.12.2012
P4	76.29°S, 77.03°E	2843	787	54.8	-41.28	200	2.0	28.12.2012
P5	77.91°S, 77.13°E	3154	968	33.3	-46.37	200	2.0	30.12.2012
P6	79.02°S, 76.98E	3738	1092	25.4	-53.13	200	2.5	02.01.2013
P7	80.42°S, 77.12°E	4093	1256	23.5	-58.50	300	2.5	06.01.2013

1) Mean annual snow accumulation rates are obtained from bamboo stick field measurements, updated to 2013 from Ding et al. (2011).

2) Mean annual temperatures are derived from 10m borehole temperatures and automatic weather station observations (Ding et al., 2010; Xiao et al., 2013).

Minor comments (not comprehensive)

Line 9 P 31953: Wagenbach (not Vagenbach)

Wagenbach is correct, thanks.

1 **Investigation of post-depositional processing of nitrate in East**
2 **Antarctic snow: Isotopic constraints on photolytic loss, re-oxidation,**
3 **and source inputs**

4 **Short title:** Isotopes of nitrate in East Antarctic snow

5
6 G. Shi^{1,2}, A. M. Buffen², M. G. Hastings², C. Li³, H. Ma¹, Y. Li¹, B. Sun¹, C. An¹, S.
7 Jiang¹

8
9 ¹ Key Laboratory for Polar Science of State Oceanic Administration, Polar Research
10 Institute of China, Shanghai 200062, China

11 ² Department of Earth, Environmental and Planetary Sciences and Institute at Brown for
12 Environment and Society, Brown University, Providence, Rhode Island 02912, USA.

13 ³ The State Key Laboratory of the Cryospheric Sciences, Cold and Arid Regions
14 Environmental and Engineering Research Institute, Chinese Academy of
15 Sciences, Lanzhou 730000, China

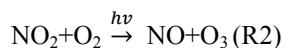
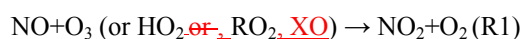
16
17 **Correspondence to: M.G. Hastings (meredith_hastings@brown.edu)**
18
19

Abstract

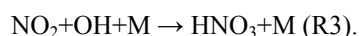
Snowpits along a traverse from coastal East Antarctica to the summit of the ice sheet (Dome Argus) are used to investigate the post-depositional processing of nitrate in snow. Seven snowpits from sites with accumulation rates between 24 and 172 kg m⁻² a⁻¹ were sampled to depths of 150 to 300 cm. At sites from the continental interior (low accumulation, <55 kg m⁻² a⁻¹), nitrate mass fraction is generally >200 ng g⁻¹ in surface snow and decreases quickly with depth to <50 ng g⁻¹. Considerably increasing values of $\delta^{15}\text{N}$ of nitrate are also observed (16-461‰ vs. air N₂), particularly in the top 20 cm, which is consistent with predicted fractionation constants for the photolysis of nitrate. The $\delta^{18}\text{O}$ of nitrate (17-84‰ vs. VSMOW), on the other hand, decreases with increasing $\delta^{15}\text{N}$, suggestive of secondary formation of nitrate in situ (following photolysis) with a low $\delta^{18}\text{O}$ source. Previous studies have suggested that $\delta^{15}\text{N}$ and $\delta^{18}\text{O}$ of nitrate at deeper snow depths should be predictable based upon an exponential decrease derived near the surface. At deeper depths sampled in this study, however, the relationship between nitrate mass fraction and $\delta^{18}\text{O}$ changes, with increasing $\delta^{18}\text{O}$ of nitrate observed between 100-200cm. Predicting the impact of post-depositional loss, and therefore changes in the isotopes with depth, is highly sensitive to the depth interval over which an exponential decrease is assumed. In the snowpits collected closer to the coast (accumulation >91 kg m⁻² a⁻¹), there are no obvious trends detected with depth and instead seasonality in nitrate mass fraction and its isotopic composition is found. In comparison to the interior sites, the coastal pits are lower in $\delta^{15}\text{N}$ (-15-71‰ vs. air N₂) and higher in $\delta^{18}\text{O}$ of nitrate (53-111‰ vs. VSMOW). The relationships found amongst mass fraction, $\delta^{15}\text{N}$, $\delta^{18}\text{O}$ and $\Delta^{17}\text{O}$ ($\Delta^{17}\text{O} = \delta^{17}\text{O} - 0.52 \times \delta^{18}\text{O}$) of nitrate cannot be explained by local post-depositional processes, and are instead interpreted in the context of a primary atmospheric signal. Consistent with other Antarctic observational and modeling studies, the isotopic results are suggestive of an important influence of stratospheric chemistry on nitrate formation during the cold season and a mix of tropospheric sources and chemistry during the warm season. Overall, the findings in this study speak to the sensitivity of nitrate isotopic composition to post-depositional processing and highlight the strength of combined use of the nitrogen and oxygen isotopes for a mechanistic understanding of this processing.

1 Introduction–

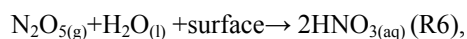
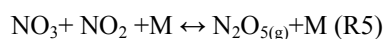
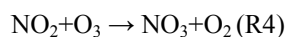
Nitrate (NO_3^-) is one of the major ions measured in Antarctic snow and ice. In the atmosphere, NO_3^- is formed by oxidation of NO and NO_2 , which are collectively referred to as NO_x . In the presence of sunlight, NO and NO_2 recycle rapidly with ozone (O_3), peroxy radical (HO_2), ~~or~~ an organic radical (RO_2 , where R=organics), or halogen radicals (XO , where X=Br, Cl or I) according to the following reactions:



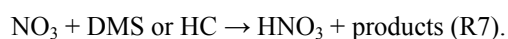
During the day, i.e., when sunlight is present, oxidation of NO_2 by the hydroxyl radical (OH) produces nitric acid (HNO_3):



At night and in colder environments, oxidation of NO_2 by O_3 is promoted and HNO_3 can be formed from hydrolysis of dinitrogen pentoxide (N_2O_5),



or by abstraction of a hydrogen atom by the nitrate radical (NO_3) from dimethyl sulfide (DMS) or a hydrocarbon (HC),



Important NO_x inputs to the troposphere include fossil fuel combustion, biomass burning, soil microbial activity, lightning, and injection from the stratosphere (Delmas et al., 1997; Lee et al., 1997). There has been interest in using ice core NO_3^- records to reconstruct past atmospheric NO_x sources, and atmospheric loading and variability in concentrations ~~and variability~~ over time. Increasing NO_3^- concentrations in Greenland ice core records ~~correspond~~ has been linked to increasing ~~fossil fuel and/or agricultural~~ anthropogenic emissions (fossil fuel and/or agricultural) since the Industrial Revolution (Mayewski and Legrand, 1990; Hastings et al., 2009). In contrast, such increases in NO_3^- have not been observed in Antarctica (Wolff, 1995; Wolff et al., 2012), suggesting that concentrations in snow are mainly controlled by natural sources.

The partitioning of NO_x inputs using ice core NO_3^- concentrations is difficult, however, since concentration alone cannot identify specific NO_x sources and NO_3^- can be lost from snow by post-depositional processes such as photolysis and possibly volatilization as HNO_3 (Wolff, 1995; Röthlisberger et al., 2000; Frey et al., 2009). Measurements of nitrogen and oxygen stable isotope ratios in NO_3^- provide further constraints for past NO_x sources and oxidation chemistry (Alexander et al., 2004; Hastings et al., 2009; Hastings, 2010). In the atmosphere, the oxygen isotopes in NO_3^- reflect the ~~isotopic compositions of the oxidants contributing to oxidants involved in~~ the production of NO_3^- (e.g., R1-R7 above; Hastings et al., 2003; Michalski et al., 2003; Alexander et al., 2009), and the nitrogen isotopes can reflect NO_x sources and possible imprints of transport and chemistry (Hastings et al., 2003; Elliott et al., 2007; Savarino et al., 2007; Morin et al., 2008; Altieri et al., 2013). However, post-depositional processing in snow can modify the isotopic composition of NO_3^- . At Dome C in East Antarctica (where the snow accumulation rate is roughly $25 \text{ kg m}^{-2} \text{ a}^{-1}$, i.e., $<10 \text{ cm snow a}^{-1}$), NO_3^- mass fractions decrease from hundreds of ng g^{-1} in surface snow to tens of ng g^{-1} at a depth of 10cm and this decrease corresponds to large changes in isotopic composition (Röthlisberger et al., 2000; Blunier et al., 2005; Frey et al., 2009; Erbland et al., 2013) such that this processing should be identifiable where it occurs. The influence of

post-depositional alteration on NO_3^- , however, appears closely related to annual snow accumulation and at sites with higher accumulation rates, such as Summit, Greenland ($200 \text{ kg m}^{-2} \text{ a}^{-1}$, i.e., $\approx 60 \text{ cm snow a}^{-1}$; Dibb and Fahnstock, 2004), the post-depositional effects are rather minor, and the atmospheric signal appears to be preserved (Hastings et al., 2004; Fibiger et al., 2013 [and references therein](#)).

In recent studies, the spatial variability of photolytic and volatile NO_3^- loss in East Antarctic upper snow has been investigated (Frey et al., 2009; Erbland et al., 2013), and represents important progress in understanding air-snow transfer of NO_3^- . However, there are still a number of questions regarding the interpretation of NO_3^- isotopes due to the complicated post-depositional behavior of NO_3^- . Distinguishing the form, extent and relative importance of the different possible isotope effects associated with post-depositional processes is critical for understanding what NO_3^- in an ice core represents.

In this study, samples from 150 to 300 cm-deep snowpits, have been collected at seven sites along a traverse from the East Antarctic coast to Dome Argus (Dome A: the summit of the Antarctic ice sheet), and NO_3^- mass fraction and isotopic composition were determined. The key objectives of this study are: (1) to investigate the effects of post-depositional processes on isotopic composition of NO_3^- at different depths in the snowpack; and (2) to understand the variation of NO_3^- isotopes in different environments across the East Antarctic Ice Sheet (EAIS). The results of this study are of significance to a further understanding of post-depositional processing of snow NO_3^- and the interpretation of NO_3^- isotopic composition archived in ice cores.

2 Materials and methods

2.1 Sample collection

The Chinese National Antarctic Research Expedition (CHINARE) team conducts an annual inland traverse from the coastal Zhongshan Station (Indian Ocean sector) to Dome A in East Antarctica (Fig. 1). This traverse covers a distance of 1250 km. On the traverse route from Zhongshan to Dome A, seven snowpits were excavated during the 2012/2013 austral summer season (Fig. 1). Full information about each pit, including location, snow depth, sampling resolution, collection date, [mean annual snow accumulation](#), etc., is summarized in Table S1.

Snowpits were excavated manually and one snow wall was scraped clean and flat with a high-density polyethylene (HDPE) scraper. Snow samples were collected using 250ml narrow-mouth HDPE vials pushed horizontally into the snow wall beginning at the bottom of the pit and moving upwards. The scraper and vials were pre-cleaned with Milli-Q ultrapure water ($>18.2 \text{ M}\Omega$), dried in a class 100 super clean hood at 20°C and then sealed in the clean polyethylene (PE) bags that were not opened until the field sampling started. Field blanks consisting of sampling bottles filled with Milli-Q water were analyzed for ion concentrations. All personnel wore PE gloves and face masks and the pit sites were generally 1 km away from the traverse route to avoid possible contamination from expedition team activities. After collection, the vials were again sealed in clean PE bags and preserved in a clean insulated cabinet. All together, 530 snow samples were collected. All samples were transported to China in a freezer at -25°C and then shipped frozen to Brown University in Providence, RI.

2.2 Sample analysis

Snow NO_3^- mass fractions (denoted as $w(\text{NO}_3^-)$ in the following context) were determined using a Westco

Scientific SmartChem 200 discrete chemistry analyzer. The SD (standard deviation) of $w(\text{NO}_3^-)$ of 55 field blanks run within sets of samples was 0.8 ng g^{-1} , which is comparable to blank Milli-Q water run on the same system. The pooled standard deviation of samples run in replicate ($n=50$) in different sample sets is 1.5 ng g^{-1} .

Snow NO_3^- isotopic compositions were measured according to the denitrifier method by using denitrifying bacteria to convert NO_3^- to N_2O gas, which is collected and injected into a stable isotope ratio mass spectrometer (Thermo Scientific DELTA V Plus; Sigman et al., 2001; Casciotti et al., 2002; Kaiser et al., 2007). At Brown, a minimum of 5 nmol of NO_3^- is required for an accurate isotopic determination of $^{15}\text{N}/^{14}\text{N}$ and $^{18}\text{O}/^{16}\text{O}$ ratios in snow samples with $w(\text{NO}_3^-)$ as low as 10.0 ng g^{-1} , which can be analyzed directly without a pre-concentration step (i.e. for a 5 nmol NO_3^- run, a sample of 10.0 ng g^{-1} requires a 31 mL injection).

NO_3^- isotopic ratios ($\delta^{15}\text{N}(\text{NO}_3^-)$, $\delta^{17}\text{O}(\text{NO}_3^-)$ and $\delta^{18}\text{O}(\text{NO}_3^-)$) are defined as

$\delta = R_{\text{sample}}/R_{\text{standard}} - 1$ (Eq. 1),

where R is $^{15}\text{N}/^{14}\text{N}$, $^{17}\text{O}/^{16}\text{O}$, or $^{18}\text{O}/^{16}\text{O}$. $\delta^{15}\text{N}(\text{NO}_3^-)$ and $\delta^{18}\text{O}(\text{NO}_3^-)$ values are reported in per mil (‰) relative to atmospheric N_2 ($\delta^{15}\text{N}_{\text{air}}=0\text{‰}$) and Vienna Standard Mean Ocean Water (VSMOW $\delta^{18}\text{O}=0\text{‰}$), respectively. All of the isotopic data were calibrated using the international reference materials IAEA-NO-3, USGS-35, USGS-34 and USGS-32 (Michalski et al., 2002; Böhlke et al., 2003). Determining the isotopic composition in large volume samples has been extensively tested in the laboratory, and it is critical to run reference materials very close to the same concentrations (i.e. same volume injections) as samples, to eliminate any potential volume effects. Included in the supplementary materials are data from internal working standards that show excellent reproducibility over a variety of injection volumes in different runs (Tables S1 and S2). Precision of the isotopic analyses was-is calculated in two ways. First, the pooled standard deviation ($1\sigma_p$) of all standards run within individual sample sets was calculated, as used in a previous study (Buffen et al., 2014). For $\delta^{15}\text{N}(\text{NO}_3^-)$, the $1\sigma_p$ of standards is 0.3‰ (IAEA-NO-3, $n=80$), 0.3‰ (USGS-34, $n=80$), 1.1‰ (USGS-32, $n=53$); and for $\delta^{18}\text{O}(\text{NO}_3^-)$ this is 0.6‰ (IAEA-NO-3, $n=80$), 0.6‰ (USGS-34, $n=80$) and 0.7‰ (USGS-35, $n=80$). ~~Secondly~~, the pooled standard deviation of all replicate samples run in at least two different sets was examined ($n=38$ pairs of samples) and yielded 0.8‰ for $\delta^{15}\text{N}(\text{NO}_3^-)$ and 0.5‰ for $\delta^{18}\text{O}(\text{NO}_3^-)$. The pooled standard deviation of the replicate samples is probably the most representative measure of precision as it accounts for the total variation within the denitrifier method (i.e., from sample preparation to isotopic determination), and the variance is not diluted compared to the much higher number of standards that are pooled across sample sets (compared to individual samples that are only run once or twice).

During the NO_3^- reduction by bacteria, a small number of oxygen atoms may be exchanged between water and the intermediates of denitrification (e.g., NO_2^-) and must be corrected for the isotopic determination. In general, this exchange is $< 10\%$, and typically $< 3\%$, of the total O atoms in the produced N_2O and is corrected for using the measured ~~snow~~-oxygen isotope compositions of snow ($-\delta^{18}\text{O}(\text{H}_2\text{O})$) and water in the bacteria/media (see Casciotti et al., 2002; Kaiser et al., 2007 for correction schemes). $\delta^{18}\text{O}(\text{H}_2\text{O})$ was determined using the standard CO_2 equilibration method (Johnsen et al., 1997). The standard deviation of reference (VSMOW) measurements ($n=20$) was 0.10‰ . Full snowpit profiles of $\delta^{18}\text{O}(\text{H}_2\text{O})$ were only completed for P1 and P7, while only surface snow samples (3 cm) were measured for P2-P6.

A correction is also needed for $\delta^{15}\text{N}(\text{NO}_3^-)$ to account for the contribution of the $^{14}\text{N}^{14}\text{N}^{17}\text{O}$ isotopologue to the m/z 45 signal measured by the IRMS (Kaiser et al., 2007). Because atmospheric NO_3^- contains a non-zero $\Delta^{17}\text{O}$ (i.e., $\Delta^{17}\text{O} = \delta^{17}\text{O} - 0.52 \times \delta^{18}\text{O} > 0\text{‰}$), simply assuming $\delta^{17}\text{O} = 0.52 \times \delta^{18}\text{O}$ can yield an overestimate of the true $\delta^{15}\text{N}(\text{NO}_3^-)$ by as much as $1\text{--}2\text{‰}$ (Sigman et al., 2001; Hastings et al., 2003;

Savarino et al., 2007). To account for this contribution, a measured or estimated $\Delta^{17}\text{O}(\text{NO}_3^-)$ is used to correct the $\delta^{15}\text{N}(\text{NO}_3^-)$ values. Previous East Antarctic investigations have shown that $\Delta^{17}\text{O}(\text{NO}_3^-)$ mainly ranges from 25 to 35‰ in snow NO_3^- (Erbland et al., 2013) and we find a similar range for P1 in our study (see below). For P1, the measured $\Delta^{17}\text{O}(\text{NO}_3^-)$ values reported below were used to correct $\delta^{15}\text{N}(\text{NO}_3^-)$, while a mid-range value of $\Delta^{17}\text{O}(\text{NO}_3^-)=30\text{‰}$ was used for P2-P7. Using this mid-range value of $\Delta^{17}\text{O}(\text{NO}_3^-)=30\text{‰}$ leads to an average $\delta^{15}\text{N}(\text{NO}_3^-)$ difference of 1.6‰ compared to using $\Delta^{17}\text{O}(\text{NO}_3^-)=0\text{‰}$. A difference of $\pm 5\text{‰}$ in the $\Delta^{17}\text{O}(\text{NO}_3^-)$ used to correct the data (i.e., $\Delta^{17}\text{O}(\text{NO}_3^-)=25\text{‰}$ ~~to~~ or 35‰) results in a $\delta^{15}\text{N}(\text{NO}_3^-)$ difference of 0.3‰, which is comparable to our reported analytical precision and is negligible when compared to the range of sample $\delta^{15}\text{N}(\text{NO}_3^-)$ values.

For determination of $\Delta^{17}\text{O}(\text{NO}_3^-)$, the sample N_2O produced by the denitrifier method was thermally decomposed to N_2 and O_2 in a heated gold tube, and the O_2 was then measured at m/z 32 and 33 signals on the IRMS (Kaiser et al., 2007). A minimum of 35 nmol NO_3^- is needed for the analysis, but the low $w(\text{NO}_3^-)$ and low sample volumes available in this study limited the measurement of both $\Delta^{17}\text{O}(\text{NO}_3^-)$ and $\delta^{15}\text{N}$ and $\delta^{18}\text{O}$ on the same sample. A pre-concentration procedure is needed for the measurement of $\Delta^{17}\text{O}(\text{NO}_3^-)$ (e.g., Morin et al., 2008; Frey et al., 2009; Erbland et al., 2013). Briefly, NO_3^- was trapped in an anion exchange resin, and then eluted by a 1M NaCl solution. A variety of NaCl salts were tested and found to contain NO_3^- , and thus procedural blanks were determined for each batch of NaCl used. (Note that NO_3^- was found in every batch of NaCl (Fisher Scientific) tested, ranged from 478 to 547 ng g^{-1} , and was different even for bottles with the same lot number.) For the samples from P1, 28 ng g^{-1} was measured for the 1M solution of NaCl used for elution. During the concentrating procedure, one Milli-Q water blank and two sets of standards (USGS-34 and USGS-35) with similar $w(\text{NO}_3^-)$ to the snow samples were processed simultaneously. The measured $\Delta^{17}\text{O}(\text{NO}_3^-)$ was then corrected by two steps: (1) $\Delta^{17}\text{O}(\text{NO}_3^-)$ in concentrated samples was linearly corrected using the standards USGS-34 and USGS-35 run within individual sample sets; and (2) the output of step (1) was further corrected by the standards used during the concentration procedure to account for the impact of procedural influence (e.g., the NaCl blank). A mean difference of 2.5‰ for $\Delta^{17}\text{O}(\text{NO}_3^-)$ was obtained without the step (2) correction. Precision for repeated measurement of $\Delta^{17}\text{O}(\text{NO}_3^-)$ is only 0.44‰ (see also Table S2), but without correcting for the blank associated with the eluent NaCl, we find that ~~which means that~~ the pre-concentration method can result in an underestimation at least on the order of 2.5‰ for $\Delta^{17}\text{O}(\text{NO}_3^-)$.

3 Results

3.1 Snowpit $w(\text{NO}_3^-)$

A Summary for all measurements of statistics for $w(\text{NO}_3^-)$, $\delta^{15}\text{N}(\text{NO}_3^-)$ and $\delta^{18}\text{O}(\text{NO}_3^-)$ in each snowpit ~~are~~ is given in ~~Table 1~~ Fig. 2 and the detailed profiles with depth are illustrated in Fig. 23. In general, $w(\text{NO}_3^-)$ is lower than 200 ng g^{-1} in P1 and P2, which are characterized with higher annual snow accumulation (see Fig. 1), and large, quasi-regular fluctuations of $w(\text{NO}_3^-)$ are present in both pits. In contrast, pits P4-P7 from the lower snow accumulation sites show the highest $w(\text{NO}_3^-)$ in surface snow, which falls sharply from >200 ng g^{-1} near the surface to below 50 ng g^{-1} within the top meter, and do not contain regular fluctuations. The markedly decreasing trend of $w(\text{NO}_3^-)$ with depth seems to fit an exponential model as has been done previously (Traversi et al., 2009).

3.2 Isotopic compositions of NO_3^-

For $\delta^{15}\text{N}(\text{NO}_3^-)$ and $\delta^{18}\text{O}(\text{NO}_3^-)$, the coastal and inland pits differ greatly in terms of the average values and the variability with depth. For the coastal sites P1-P3, $\delta^{15}\text{N}(\text{NO}_3^-)$ is generally lower than in the inland snowpits P4-P7, varying between -14.8 and 70.8‰, while $\delta^{15}\text{N}(\text{NO}_3^-)$ in the inland pits ranges from 15.5 to 460.8‰ (Table 1; Figs. 2 and 3). This high value of 460.8‰ in pit P7 (which is at Dome A) is the highest natural $\delta^{15}\text{N}(\text{NO}_3^-)$ on Earth so far reported to our knowledge. In the inland pits (P4-P7), $\delta^{15}\text{N}(\text{NO}_3^-)$ is lower in the uppermost layers and strongly increases deeper in the snowpack, with most of the increase occurring in the top 25 cm.

In contrast to $\delta^{15}\text{N}(\text{NO}_3^-)$, $\delta^{18}\text{O}(\text{NO}_3^-)$ is higher on average in the coastal pits (P1-P3), ranging between 52.5 and 111.2 ‰, compared to the inland sites (P4-P7) where $\delta^{18}\text{O}(\text{NO}_3^-)$ varies between 16.8 and 84.0 ‰ (Figs. 2 and 3; Table 1). It is noted that the averages of $\delta^{18}\text{O}(\text{NO}_3^-)$ for P4-P7 are comparable, while $\delta^{15}\text{N}(\text{NO}_3^-)$ means vary significantly, from 133.6 to 335.2‰. There is no obvious trend in the $\delta^{18}\text{O}(\text{NO}_3^-)$ profiles with depth in P1-P3, but this is not the case for the inland sites. $\delta^{18}\text{O}(\text{NO}_3^-)$ decreases over the top 25 cm, but gradual and consistent increases are observed below 25 cm in P4, P5 and P7 which continue to the pit base (200-300 cm; Fig. 23). A similar decrease in $\delta^{18}\text{O}(\text{NO}_3^-)$ is observed in the top of P6, but it is not clear if an increasing trend exists in the profile below.

$\Delta^{17}\text{O}(\text{NO}_3^-)$ of P1 varies from 25.2 to 42.9‰, with an average of 32.8‰. In general, the variation trend of $\Delta^{17}\text{O}(\text{NO}_3^-)$ is similar to that of $\delta^{18}\text{O}(\text{NO}_3^-)$ (Figs. 3 and 7), and a close relationship was observed between the two ($r^2=0.77$, $p<0.001$).

The difference between the coastal and inland pits observed here is similar to that observed in the Erbland et al. (2013) study. A comparison between the two studies is presented in the supplementary materials as Fig. S1.

4 Discussion

After deposition, NO_3^- can be lost from snow by photolysis or volatilization as HNO_3 (sometimes referred to as evaporation or physical release in other studies), and the extent of loss via these post-depositional processes is expected to be accumulation dependent (Röthlisberger et al., 2002; Grannas et al., 2007). At lower accumulation sites, NO_3^- loss is relatively high, synchronous with a large degree of isotopic fractionation (Blunier et al., 2005; Frey et al., 2009; Erbland et al., 2013). In contrast, post-depositional alteration of snow NO_3^- in high accumulation regions can be minor, and seasonal and interannual cycles can be preserved in the snowpack (e.g., Wagenbach et al., 1994; Hastings et al., 2004).

Based on the site differences in annual snow accumulation rate and the profile trends of $w(\text{NO}_3^-)$, $\delta^{15}\text{N}(\text{NO}_3^-)$ and $\delta^{18}\text{O}(\text{NO}_3^-)$, the seven pits are divided into two groups within the following discussion: group I includes the coastal, medium-high accumulation sites P1-P3 ($>91 \text{ kg m}^{-2} \text{ a}^{-1}$) and group II are the low accumulation and further inland sites P4-P7 ($<55 \text{ kg m}^{-2} \text{ a}^{-1}$). Below we consider what processes (and fractionation constants) can explain observations from the group I and group II snowpits, and whether it is possible to predict values at depth based on the loss processes near the surface.

4.1 NO_3^- loss in inland upper snowpack: top 20 cm

If it is assumed that post-depositional loss of snow NO_3^- is accompanied by a Rayleigh-type fractionation, the observed changes in $\delta^{15}\text{N}$ and $\delta^{18}\text{O}$ in a snowpit profile can be described as a function of $w(\text{NO}_3^-)$ via

$$\ln(\delta_{\text{snow}}+1) = \varepsilon^* \ln(w_{\text{snow}}) + [\ln(\delta_{\text{snow},0}+1) - \varepsilon^* \ln(w_{\text{snow},0})] \quad (\text{Eq. 2}),$$

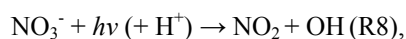
where $\delta_{\text{snow},0}$ and δ_{snow} denote isotopic ratios in the initial and remaining NO_3^- , respectively, and $w_{\text{snow},0}$ and w_{snow} are the initial and remaining NO_3^- mass fractions, respectively (e.g., Blunier et al., 2005). ϵ can be obtained from the slope of the linear regression for $\ln(w_{\text{snow}})$ vs. $\ln(\delta_{\text{snow}}+1)$, while $[\ln(\delta_{\text{snow},0}+1) - \epsilon \cdot \ln(w_{\text{snow},0})]$ would be the intercept. It is noted that ϵ is related to the fractionation factor α by $\epsilon = \alpha - 1$ (Criss, 1999).

Solar radiation decreases exponentially in the snowpack, with attenuation described in terms of an e -folding depth (z_e) where the actinic flux is reduced to $1/e$ (37%) of the surface value. Accordingly, roughly 95% of snowpack photochemistry should occur above the depth of three times z_e (Warren et al., 2006). For the individual pits here, we calculate apparent ϵ values (ϵ_{app}) from data in the upper ~~25 cm~~ 20 cm, 40 cm and 60 cm, to evaluate the impacts of post-depositional processes on snow NO_3^- (Table 2). ~~a depth that is close to the z_e calculated by~~ Zatko et al. (2013) calculated a z_e of about 20 cm for remote Antarctic sites, ~~to evaluate the impacts of post depositional processes on snow NO_3^- (Table 2).~~ For group II, relatively strong relationships are observed between $w(\text{NO}_3^-)$ and $\delta^{15}\text{N}(\text{NO}_3^-)$ or $\delta^{18}\text{O}(\text{NO}_3^-)$ in the top ~~25–60~~ 20 cm (as indicated by the statistically significant r^2 values for Eq. 2; Table 2). These pits are characterized by negative $\epsilon_{\text{app}}^{15, 45}$, with ~~the~~ values of ~~-78.177.8‰~~ (P4), ~~-84.493.1‰~~ (P5), ~~-60.650.2‰~~ (P6) and ~~-59.261.3‰~~ (P7) for the upper 20 cm snow layer (i.e., the 0–20 cm interval; Table 2); whereas $\epsilon_{\text{app}}^{18, 48}$ values are positive, indicating a depletion of $^{18}\text{O}(\text{NO}_3^-)$ with decreasing $w(\text{NO}_3^-)$. The observed fractionation constants ($\epsilon_{\text{app}}^{15, 45}$ and $\epsilon_{\text{app}}^{18, 48}$) for group II (P4–P7) are comparable to those from other snowpits on the East Antarctic plateau (Frey et al., 2009; Erbland et al., 2013; see also Fig. S1).

In the upper ~~25–20~~ 20 cm of the snowpack, a significant NO_3^- loss with increasing depth is seen in the group II pits and corresponds to ~~the a~~ a large enrichment of $^{15}\text{N}(\text{NO}_3^-)$. A large loss of NO_3^- leading to such high $\delta^{15}\text{N}(\text{NO}_3^-)$ values in the surface snow is consistent with the calculated low $\epsilon_{\text{app}}^{15, 45}$ in the upper snowpack and our expectations based on other findings in East Antarctica (e.g., Savarino et al., 2007; Erbland et al., 2013). Such strongly positive $\delta^{15}\text{N}$ values ($>100\%$) have not been observed in atmospheric NO_3^- .

4.1.1 Photolytic loss of NO_3^-

Photolysis of snow NO_3^- is thought to primarily occur within a disorder interface, sometimes referred to as a quasi-liquid layer, at the surface of the ice crystal via the reactions



with R8 exceeding R9 by a factor of 8–9 (Warneck and Wurzinger, 1988; Dubowski et al., 2001; Chu and Anastasio, 2003). Snow NO_3^- photolysis products are mainly NO_2 , greatly exceeding NO under most conditions (Dibb et al., 2002). Under acidic conditions ($\text{pH} < 5$), $\text{HONO}_{(\text{g})}$ formation from NO_2^- protonation is also important ~~can also be released~~ (Grannas et al., 2007 and references therein). Only NO_2 produced near the ice surface-air interface can be released to the firn air and subsequently escape from the snowpack to the overlying atmosphere (Boxe et al., 2005).

In order to identify the relative importance of photolysis and volatilization (section 4.1.23) on NO_3^- loss, the fractionation constant of each process should first be quantified. ~~Frey et al. (2009) proposed a theoretical model that has provided a useful approximation of photolytic fractionation.~~ The photolysis rate constant

$j_{\text{NO}_3^-}$ (s^{-1}) ~~can be~~ is expressed as

$$j_{\text{NO}_3^-} = \int \sigma_{\text{NO}_3^-}(\lambda, T) \times \phi_{\text{NO}_3^-}(\lambda, T, \text{pH}) \times I(\lambda) d\lambda \text{ (Eq. 3),}$$

where $\sigma_{\text{NO}_3^-}$ (cm^2) is the spectral ~~absorption cross section~~ absorptivity (Chu and Anastasio, 2003); $\phi_{\text{NO}_3^-}$ is the quantum yield (0-1), which was calculated to be 1.7×10^{-3} at 239K and pH=5 (Chu and Anastasio, 2003), and I is the spectral actinic flux ($\text{photons cm}^{-2} \text{ sec}^{-1} \text{ nm}^{-1}$). Frey et al. (2009) proposed a theoretical model for estimating nitrate photolytic isotopic fractionation constants, which is based on a framework originally developed by Yung and Miller (1997) for stratospheric N_2O . The framework exploits mass-dependent differences in the vibrational frequencies and ground-state energies for a given set of isotopologues. These differences result in a modeled spectral absorption cross section for the heavier isotopologue which is shifted to longer wavelengths, thus influencing the rate constant. ~~here taken from the Tropospheric Ultraviolet and Visible (TUV) radiation transfer model (Madronich and Flocke, 1998).~~ The isotopic fractionation constant can then be calculated by

$$\varepsilon = (j/j') - 1 \text{ (Eq. 4),}$$

where j corresponds to the heavy isotopologue (e.g., $^{15}\text{N}^{16}\text{O}_3^-$), and j' corresponds to the light isotopologue (e.g., $^{14}\text{N}^{16}\text{O}_3^-$). and it is assumed that the different isotopologues retain similar spectral absorption curves and equal quantum yields.

We calculate the photolytic $^{15}\varepsilon$ and $^{18}\varepsilon$ at sites P1 and P7 for peak summer radiation conditions (solstice solar noon on December 21, 2012) using actinic fluxes derived from the Tropospheric Ultraviolet and Visible (TUV5.0) radiation transfer model (Madronich and Flocke, 1998) assuming clear sky conditions and a total overhead ozone column of 300 DU for both sites. We use the nitrate absorption cross section from Chu and Anastasio (2003) and calculate quantum yields using the equation given in this same work for -10°C at P1 and -30°C at P7.

The resulting fractionation constants are $^{15}\varepsilon = -45.3\text{‰}$ (P1) and -48.0‰ (P7) and $^{18}\varepsilon = -32.5\text{‰}$ (P1) to -34.4‰ (P7), and the relatively small variability between the two sites indicates that the calculated values are representative for the two site groupings. Berhanu et al. (2014) have recently proposed absorption cross sections derived from the measurements of Chu and Anastasio (2003) but modeled directly for the $^{14}\text{N}^{16}\text{O}_3^-$ and $^{15}\text{N}^{16}\text{O}_3^-$ isotopologues at -30°C . When using these cross sections, $^{15}\varepsilon$ is calculated to be -48.9‰ at P1 and -52.8‰ at P7.

~~Under peak summer radiation conditions (solstice solar noon), $^{15}\varepsilon$ and $^{18}\varepsilon$ of photolysis are calculated to be between -45.3‰ (P1) and -48.0‰ (P7) and from -32.5‰ (P1) to -34.4‰ (P7), respectively.~~ The negative ε values suggest that photolysis will lead to a strong enrichment of both ^{15}N and ^{18}O in NO_3^- remaining in the snow. For $^{15}\varepsilon_{\text{app}}$ calculated from observations in the upper 25–60 cm of the group II pits (Table 2), the higher r^2 values imply that photolysis can largely explain enrichment of ^{15}N with the decrease of $w(\text{NO}_3^-)$. At Dome C, where snow accumulation is typically less than $50 \text{ kg m}^{-2} \text{ a}^{-1}$, close to the values of P4-P7 (Fig. 1), photolysis has also been reported as responsible for changes-large increases in $\delta^{15}\text{N}(\text{NO}_3^-)$ ~~in the upper snowpack with depth in the snow~~ (Frey et al., 2009; Erbland et al., 2013). The negative calculated $^{18}\varepsilon$, however, does not agree with the highly positive $^{18}\varepsilon_{\text{app}}$ values based on the observations.

4.1.2 Aqueous phase “secondary” NO_3^- formation

If the post-depositional loss of NO_3^- in the group II pits was driven solely by photolysis, ^{18}O should also be enriched in the remaining NO_3^- according to the modeled photolytic $^{18}\varepsilon$ values (-32.5 to -34.4‰). However, $\delta^{18}\text{O}$ decreases over the top 25–20 cm (Fig. 23) and the apparent $^{18}\varepsilon$ values ($^{18}\varepsilon_{\text{app}}$) $^{18}\varepsilon$ -values calculated from the observed data in the upper 25cm–20cm are instead positive, varying from 15.6–16.7 to

28.8±3.2‰ (Table 2). Furthermore, simple photolysis will lead to a linear relationship of $\delta^{18}\text{O}(\text{NO}_3^-)$ vs. $\delta^{15}\text{N}(\text{NO}_3^-)$ with a slope of roughly 0.7, i.e., equal to the ratio of the fractionation constants. However, there are negative relationships between $\delta^{18}\text{O}(\text{NO}_3^-)$ and $\delta^{15}\text{N}(\text{NO}_3^-)$ in the top 25–20 cm (Fig. 34), with slopes varying from -0.4 to -0.2.

Similar negative relationships have been observed in other East Antarctic snowpits (Frey et al., 2009; Erbland et al., 2013) and, following from experimental and theoretical work (McCabe et al., 2005; Jacobi and Hilker, 2007), were attributed to the aqueous-phase re-oxidation of the products of NO_3^- photolysis (e.g., NO_2) by OH and/or H_2O to form “secondary” NO_3^- .

In this way, the O atoms from OH/ H_2O provide a depleted ^{18}O source while $\delta^{15}\text{N}(\text{NO}_3^-)$ is seemingly not affected. For the group II pits, $\delta^{18}\text{O}(\text{H}_2\text{O})$ in surface snow falls roughly in the range of -45 to -60‰. These effects should be considered in explaining the observed positive $^{18}\epsilon_{\text{app}}$ values and negative relationships between $\delta^{18}\text{O}(\text{NO}_3^-)$ and $\delta^{15}\text{N}(\text{NO}_3^-)$ in the top 25–20 cm. (Direct exchange of O atoms between NO_3^- and H_2O is only thought to be important at NO_3^- concentrations that are orders of magnitude higher than those found in snow (Bunton et al., 1952)).

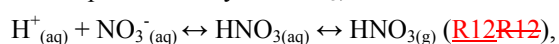
For the top 2.5 cm of snow in P7, $w(\text{NO}_3^-)$ and $\delta^{18}\text{O}(\text{NO}_3^-)$ is 374 ng g⁻¹ and 74.9‰ respectively, while $w(\text{NO}_3^-)$ decreases to 37.6 ng g⁻¹ at a depth of 20cm. Based on the modeled effect of photolysis, $\delta^{18}\text{O}$ in the remaining NO_3^- at 20 cm could be predicted by

$$\delta^{18}\text{O}_{\text{remaining}} = (1 + \delta^{18}\text{O}_0) * f^{(1/\epsilon)} - 1 \text{ (Eq. 5),}$$

where $\delta^{18}\text{O}_{\text{remaining}}$ represents $\delta^{18}\text{O}$ in the remaining NO_3^- ; $\delta^{18}\text{O}_0$ is that of initial NO_3^- ; f is the fraction of NO_3^- remaining in the snow; and $^{18}\epsilon$ is the photolysis fractionation constant (-34.4‰). If photolysis alone is responsible for the NO_3^- loss, $\delta^{18}\text{O}(\text{NO}_3^-)$ is expected to be 161‰ at 20cm and thus the observed $\delta^{18}\text{O}$ of 42.6‰ requires a cumulative 54% exchange of O atoms in the remaining NO_3^- assuming a $\delta^{18}\text{O}(\text{H}_2\text{O})$ of -60‰. For P4, P5 and P6, this exchange is estimated to be 48%, 40% and 11%, respectively. (It is noted that the exchange percent in P6 is relatively small, associated with the small difference in mass fractions and $\delta^{18}\text{O}$ of NO_3^- between the surface snow sample ($w(\text{NO}_3^-)=203$ ng g⁻¹, $\delta^{18}\text{O}(\text{NO}_3^-)=70$ ‰) and the snow at a depth of 20cm ($w(\text{NO}_3^-)=125$ ng g⁻¹, $\delta^{18}\text{O}(\text{NO}_3^-)=72$ ‰)). This simple mass balance approach, overall, indicates that re-oxidation plays a very significant role in determining how the $\delta^{18}\text{O}$ of NO_3^- evolves in the snow column during burial. This is a substantial exchange of O atoms, indicating that re-oxidation plays a major role in determining the $\delta^{18}\text{O}$ of NO_3^- in the upper snowpack.

4.1.3 Volatile loss of NO_3^-

Volatilization, or physical release, of HNO_3 may also be a pathway for post-depositional loss of NO_3^- in snow (Röthlisberger et al., 2000; Erbland et al., 2013). The importance of this process is unclear, however, as loss proceeds only as HNO_3 ,



and thus requires highly acidic conditions given the very high dissociation constant for HNO_3 (Sato et al., 2008). Volatilization may also be inhibited at low temperatures as suggested by laboratory and field observations (Erbland et al., 2013; Berhanu et al., 2014).

The current understanding of the isotopic impact of volatilization is somewhat limited also uncertain. An experiment conducted by Erbland et al. (2013) at Dome C suggested that the $^{15}\epsilon$ (mean±1σ) for volatilization varied from 0.9±3.5‰ (-30 °C) to -3.6±1.1‰ (-10 °C) (i.e., close to non-fractionating). However, the loss of nitrate in these experiments may have been driven by the large losses of snow via sublimation. No observational or experimental data for $^{18}\epsilon$ are available. Theoretical model estimates of

volatile fractionation, assuming that the aqueous-phase equilibrium in ~~R40-R12~~ is the controlling step in the overall fractionation (Frey et al., 2009), predict values of $^{15}\epsilon$ and $^{18}\epsilon$ to be from 12.6‰ (0 °C) to 16.8‰ (-73 °C) and between 1.1‰ (0 °C) and 0.6‰ (-73 °C), respectively (Table S3).

For the summertime temperatures at the P4-P7 sites (<30 °C), physical release should deplete both ^{15}N and ^{18}O in the remaining snow NO_3^- according to the modeled ϵ values, whereas the field experiment observations would suggest negligible change in $\delta^{15}\text{N}$ with decreasing $w(\text{NO}_3^-)$ in the snow. The observations for P4-P7 show increasing $\delta^{15}\text{N}(\text{NO}_3^-)$ with decreasing $w(\text{NO}_3^-)$, and that $\delta^{15}\text{N}(\text{NO}_3^-)$ is negatively correlated with $\delta^{18}\text{O}(\text{NO}_3^-)$ (Fig. 4), disagreeing with both expectations (i.e., field experiment observations and modeled results; Table S3). The current understanding of volatile fractionation, however, is very limited and experimental data for $^{18}\epsilon$ are not available to date. Nevertheless, little evidence is found to support a significant influence of volatilization at our sites given the existing state of knowledge.

4.2 Isotopic ~~variability with depth at inland sites (group II snowpits)~~ fractionation in deeper snow at inland sites

~~Fractionation constants and the isotopic relationships with $w(\text{NO}_3^-)$ were also examined in two deeper layers (25–100cm and 100cm–pit base) to assess possible variability with depth.~~ As shown in Table 2, the logarithmic relationships between $\delta^{15}\text{N}$ or $\delta^{18}\text{O}$ and mass fraction of NO_3^- are strongest in the upper ~~25–60~~ cm, as seen in the r^2 values, ~~but are~~ While generally weaker in the layers below, the r^2 values remain significant even when the entire snowpit is considered. For instance, for $^{15}\epsilon_{app}$, P4, P5, and P6 all have r^2 above 0.5 (with a $p < 0.05$) when observations from the entire snowpit are considered. ~~Interestingly, this loss of a relationship is more noticeable in $\delta^{18}\text{O}(\text{NO}_3^-)$ than $\delta^{15}\text{N}(\text{NO}_3^-)$.~~ Interestingly, while $\delta^{15}\text{N}(\text{NO}_3^-)$ maintains a negative relationship with $w(\text{NO}_3^-)$ at all depths, the relationships between $\delta^{18}\text{O}(\text{NO}_3^-)$ and $w(\text{NO}_3^-)$ shift from being positive in the upper ~~25–20~~ cm to generally negative in the deeper snow (Fig. 45). This leads to there generally being no association between $w(\text{NO}_3^-)$ and $\delta^{18}\text{O}(\text{NO}_3^-)$ when the entire snowpit depth interval is considered (Table 2).

It is also useful to discuss this variability with depth in terms of the isotopic fractionation constants. If there was only a single isotopically fractionating process driving the observed changes in the snow, such as photolysis, the apparent fractionation constants for $\delta^{15}\text{N}(\text{NO}_3^-)$ and $\delta^{18}\text{O}(\text{NO}_3^-)$ would be similar throughout the snow column. This expectation relies on two important assumptions. First, the boundary conditions that influence the fractionation constants remain similar over time. This is to say that factors such as the contribution of different NO_3^- sources, accumulation rate, the influence of total overhead ozone on the spectral actinic flux and photolysis rate, and the influence of snow chemistry on photolability of NO_3^- (e.g., Davis et al., 2008; Meusinger et al., 2014), remain similar over time. Second, the isotopic imprint of photolysis is set in the upper snowpack and then preserved below. This requires the assumption that once NO_3^- is moved below the photic zone, no additional in situ modifications take place. Stemming from these expectations, the isotopic composition of buried NO_3^- could be back-calculated to that originally at the surface if the isotopic imprint of alteration at the surface could be quantified in terms of a fractionation constant.

Based on the observations with depth, it is clear that the ϵ_{app} values are dependent on the depth range chosen (Table 2). Both $^{15}\epsilon_{app}$ and $^{18}\epsilon_{app}$ vary but with distinct differences. The $^{15}\epsilon_{app}$ tends to become more positive with depth, while $^{18}\epsilon_{app}$ decreases and even switches from positive to negative values. When taken together with variability in the strength of the isotopic relationships with $w(\text{NO}_3^-)$ and the observation that isotopic composition continues to change below the expected photic zone depths, especially for $\delta^{18}\text{O}(\text{NO}_3^-)$

(Fig. 3), it would seem that the assumptions above do not all apply. Either the fractionation constants change over time because of a change in boundary conditions and/or the isotopic imprint of photolysis is not preserved below the photic zone. The former hypothesis is much more likely as, thus far, there is little other evidence of processes well below the photic zone modifying buried NO_3^- .

If it is expected that only one isotopically fractionating process in the snow, such as photolysis, was responsible for post-depositional changes in $\delta^{15}\text{N}(\text{NO}_3^-)$ and $\delta^{18}\text{O}(\text{NO}_3^-)$, their respective fractionation constants should be similar at all depths. This is to say that the isotopic imprint of photolysis should be set in the upper snowpack and then preserved below. Also, $\delta^{15}\text{N}(\text{NO}_3^-)$ and $\delta^{18}\text{O}(\text{NO}_3^-)$ should not change once NO_3^- is moved below the photic zone. (Stemming from these expectations, the isotopic composition of buried NO_3^- could be back-calculated to that originally at the surface if the isotopic imprint of alteration at the surface could be quantified in terms of a fractionation constant.)

In contrast to this expectation, the calculated ϵ value is largely dependent on the depth range chosen. Figure 4 illustrates changes in the observed fractionation constants with depth in the group II snowpits. Both $^{15}\epsilon$ and $^{18}\epsilon$ vary but with distinct differences. The $^{15}\epsilon$ tends to become more positive with depth, while $^{18}\epsilon$ decreases and even switches from positive to negative values. When taken together with variability in the strength of the relationships with $w(\text{NO}_3^-)$ (Table 2) and the observation that isotopic composition continues to change below the expected photic zone depths, especially for $\delta^{18}\text{O}(\text{NO}_3^-)$ (2), it seems that a single process does not adequately explain post-depositional alteration at these inland sites. Instead, it appears that the effects on $w(\text{NO}_3^-)$, $\delta^{15}\text{N}(\text{NO}_3^-)$ and $\delta^{18}\text{O}(\text{NO}_3^-)$ vary with depth.

How could this occur? The lifetime of NO_x in snow should be determined by escape to the overlying atmosphere (wind pumping, convection and diffusion) and also by chemical conversion back to NO_3^- in the firn air, which may then be re-deposited (Zatko et al., 2013). Based on the discussion in section 4.1, the positive $^{18}\epsilon$ values for the upper 25 cm of snow can be explained by secondary NO_3^- formation in the condensed phase (some products are lost to the gas phase while those remaining are involved in re-oxidation reactions where O atoms from OH and/or H_2O are incorporated into this secondary NO_3^-). This can explain the positive relationship between $\delta^{18}\text{O}(\text{NO}_3^-)$ and $w(\text{NO}_3^-)$ in the upper snow. Deeper in the snow, however, it is possible that this relationship is lost because NO_x does not escape the snowpack but is instead converted back to NO_3^- in the interstitial firn air and then re-deposited. In this case, the increase in $\delta^{18}\text{O}(\text{NO}_3^-)$ with depth in the group II pits could potentially be explained by oxidation of NO_x by O_3 in the firn air. O_3 imparts a high positive $\delta^{18}\text{O}$ signature (on the order of 130‰, Vicars and Savarino, 2014), while other possible sources of O such as H_2O , OH or O_2 are considerably lower in $\delta^{18}\text{O}$ (e.g., >60‰ to 24‰).

Such changes with depth have not previously been observed in inland East Antarctica. In the work of Erbland et al. (2013), 10 of 11 snowpits from the plateau were not sampled below 50 cm depth, while the group II pits in this work were continuously sampled down to 200–300 cm. It is possible that sampling did not extend deep enough in the Erbland et al. (2013) study to capture this change in $\delta^{18}\text{O}(\text{NO}_3^-)$. However, the expectation would be that 50 cm should well cover the extinction of light into the snowpack (e.g., 50 cm is a greater than 3 times the ϵ -folding depth at Dome C), and therefore below this depth the isotopes should no longer be influenced by photolytic conversion of NO_3^- to NO_x . Another possible explanation could be that the ventilation depths (where NO_x is predominantly lost from the firn to the overlying atmosphere) are shallower and/or that light penetration is deeper at Dome A and the group II sites compared to previously sampled inland East Antarctic sites. Ventilated depths are dependent on a variety of firn properties that affect densification, porosity and air exchange (e.g., Zatko et al., 2013). If gas phase re-oxidation of NO_x in the deeper snowpack of only some inland Antarctic sites is substantial, this would add additional complexity to the interpretation of ice core NO_3^- records from sites with extensive photolytic influence.

~~So far, the direct observations of nitrogen compounds and oxidants in interstitial air are very limited. Concentrations of NO_x , HONO , HNO_3 , H_2O_2 , etc., have been measured in the upper snowpack (e.g., the top 10 cm) in Antarctica (Hutterli, et al., 2004; Frey et al., 2013; Legrand, et al., 2014), however, interstitial air in the deeper snowpack (e.g., >100cm in depth) has never been measured for mixing ratios of O_3 , OH , NO_x and HNO_3 . Such measurements in deeper snow would be helpful in answering whether or not $\text{NO}_x/\text{NO}_3^-$ undergoes other reactions at these deeper depths.~~

~~–~~

4.3 Predicting $w(\text{NO}_3^-)$, $\delta^{15}\text{N}(\text{NO}_3^-)$ and $\delta^{18}\text{O}(\text{NO}_3^-)$ values in buried snow

Erbland et al. (2013) proposed that snow $w(\text{NO}_3^-)$ and isotopic compositions may approach constant values, called “asymptotic” values, below the photic zone (or zone of active NO_3^- loss). By means of an exponential decrease regression, asymptotic values are calculated by

$$M(x) = M_{(as.)} + [M_{(0)} - M_{(as.)}] \times \exp(-c \times x) \quad (\text{Eq. 6}),$$

where $M_{(x)}$ is the $w(\text{NO}_3^-)$, $\delta^{15}\text{N}(\text{NO}_3^-)$ or $\delta^{18}\text{O}(\text{NO}_3^-)$ at depth x (cm); $M_{(as.)}$ is the asymptotic value for these parameters; $M_{(0)}$ is the value at the surface of the snowpit; and c is a constant. Asymptotic values for each snowpit are calculated from the best fit (minimizing the sum of squared residuals) of $M_{(x)}$ vs. depth.

Based on observations from only the top 20 cm of snow in different snowpits on the EAIS, the Erbland et al. (2013) study predicted values below the photic zone based on an exponential decrease regression. Because our snowpits extend deeper along the entire traverse, and as seen in Fig. 3 the snowpits did not typically follow a simple exponential decrease, we explored whether the asymptotic values change when derived from different depth ranges in the snowpit. In order to compare the asymptotic values derived from different snow depth ranges, observations from four intervals (0-20cm, 0-40cm, 0-60cm, and 0-100cm) were selected to make this calculation and the results are listed in Table 3. Several interesting results emerge. For asymptotic calculations of $w(\text{NO}_3^-)$, $\delta^{15}\text{N}(\text{NO}_3^-)$ and $\delta^{18}\text{O}(\text{NO}_3^-)$, all show important variations depending on the depth interval over which they are calculated. The variance, described in Table 3 by the standard error, is relatively large for the asymptotic values, but generally decreases the more observations that are included. In concert with this, the greater amount of observations included in the calculation the better the fit of the predicted values with the observed values as evidenced by the changing r^2 with calculations over different depth intervals. The sensitivity of the calculation of asymptotic values for different depth intervals in each of the group II snowpits is shown in Fig. 6.

What is the depth interval over which it is necessary to calibrate the asymptotic calculation? In other words, how much information must we know about surface conditions to make the asymptotic relationship useful for predicting isotope values at depth? Fig. 6 clearly shows that the more observations that are included the better the fit to the data will be, which is logical. But the range of profiles predicted by the asymptotic regressions also make it clear that much more information exists in the observations than can be explained by the simple assumption that photolytic loss, particularly in the top 20cm, is the overwhelming signal captured at this low accumulation sites. Overall, the $\delta^{18}\text{O}(\text{NO}_3^-)$ in deeper snow is more difficult to predict compared to $w(\text{NO}_3^-)$ and $\delta^{15}\text{N}(\text{NO}_3^-)$. This conclusion is consistent with the changes in $\delta^{18}\text{O}$ at deeper depths (Fig. 3) and the changes in ε_{app} with depth (Table 2).

~~As seen in and discussed above, $w(\text{NO}_3^-)$, $\delta^{15}\text{N}(\text{NO}_3^-)$ and $\delta^{18}\text{O}(\text{NO}_3^-)$ do not achieve constant values in the deeper snow layers of group I pits. As a result, it would be unreasonable to calculate asymptotic values for these pits based on an exponential decrease regression. On the contrary, variance in $w(\text{NO}_3^-)$, $\delta^{15}\text{N}(\text{NO}_3^-)$ and $\delta^{18}\text{O}(\text{NO}_3^-)$ in the deeper snowpack of the group II pits is relatively small. In order to compare the asymptotic values derived from different snow depth ranges, observations from five intervals (0-25cm,~~

0–60 cm, 0–80 cm, 0–100 cm, and the entire pit) were selected to make this calculation and the results are listed in Table 3. An illustration of the sensitivity of the calculation of asymptotic values for different depth intervals in a single snowpit is shown in the supporting information S2).

For a clear comparison across the snowpits, the five asymptotic values for each snowpit are displayed in 6. The averages of observed data in the bottom 20 cm of each pit (denoted as $w(\text{NO}_3^-)_{(\text{av.})}$, $\delta^{15}\text{N}_{(\text{av.})}$ and $\delta^{18}\text{O}_{(\text{av.})}$ in the following context) are also shown to check the agreement with the predicted asymptotic values. With regards to $w(\text{NO}_3^-)_{(\text{as.})}$, the values calculated using the 0–25 cm layer are typically higher than those using the deeper depth intervals, which is expected since $w(\text{NO}_3^-)$ continues to decrease below 25 cm (Fig. 23). Fig. 3 The values of $w(\text{NO}_3^-)_{(\text{as.})}$ calculated from the 0–100 cm interval and those using the entire snowpit are close to $w(\text{NO}_3^-)_{(\text{av.})}$ on the whole, indicating a better prediction. The values of $\delta^{15}\text{N}_{(\text{as.})}$ obtained from the 0–25 cm interval are generally lower than those calculated using the entire pit and 0–100 cm. $\delta^{15}\text{N}_{(\text{av.})}$ is roughly close to the $\delta^{15}\text{N}_{(\text{as.})}$ values calculated from 0–100 cm and from the entire pit, similar to the pattern for $w(\text{NO}_3^-)$. In contrast, $\delta^{18}\text{O}_{(\text{av.})}$ is generally higher than the values of $\delta^{18}\text{O}_{(\text{as.})}$, implying that $\delta^{18}\text{O}(\text{NO}_3^-)$ in deeper snow is more difficult to predict compared to $w(\text{NO}_3^-)$ and $\delta^{15}\text{N}(\text{NO}_3^-)$. This conclusion is consistent with the changes in $\delta^{18}\text{O}$ at deeper depths as discussed in section 4.2.

In cases where there is significant post-depositional loss and/or processing of NO_3^- , the $\delta_{(\text{as.})}$ in theory, could help account for the impact of post-depositional processing compared to preservation in reconstructing a primary atmospheric signal. Our results clearly show that $\delta_{(\text{as.})}$ (and ϵ_{app}) is sensitive to the depth interval over which exponential decrease is assumed. As suggested above, changes in factors such as the contribution of different NO_3^- sources, accumulation rate, total overhead ozone, and the influence of snow chemistry on photolability of NO_3^- may not remain similar over the time period covered by the snowpits. There do not appear to be significant trends in the annual accumulation rates based on data from Dome Argus. Wang et al. (2013) have compiled existing stake and snowpit accumulation measurements from Dome A and show 1) little spatial variability (surrounding 50 km) and 2) stable accumulation rates over recent decades and since 1260 AD (1965–2009 = 21 kg m⁻² a⁻¹; 2005–2008 = 18 kg m⁻² a⁻¹; 2005–2009 = 19 kg m⁻² a⁻¹; 2008–2009 = 21 kg m⁻² a⁻¹; and 1260–2005 = 21.6 to 23 kg m⁻² a⁻¹). Automatic weather station measurements presented in the same work show somewhat higher accumulation in the spring and summer (roughly 6–7 mm per month) vs. fall and winter (roughly 3–6 mm per month) with fairly stable values in the warmer months. Based on the Dome A studies, it is unlikely that significant changes in accumulation have occurred in the area of the group II snowpits. Therefore, this cannot explain the difference between what is predicted based upon the $\delta_{(\text{as.})}$ and what is observed (Fig. 6). Nor does it seem likely that changes in ϵ_{app} can be explained by accumulation rate. If it is assumed that snow accumulation has been constant for the group II snowpits, then the snowpits can be roughly dated based on measured accumulation and snow density (Fig. S2). This approximate dating suggests that the bottom of the P4 snowpit is about the year 2000; P5 dates from ~1994; P6 from 1985; and P7 from 1970. All four snowpits show a change in the relationship between $\delta^{18}\text{O}(\text{NO}_3^-)$ with $w(\text{NO}_3^-)$ and with $\delta^{15}\text{N}(\text{NO}_3^-)$ between near surface snow (<20 cm) and deeper snow (Fig. 5). Based on the approximate dating, the timing of this change is very different in the different snowpits. For example, for a depth of 100 cm, snow in P4 is dated to ~2007, P5 to ~2004, and P6 and P7 to ~2000. (Even given the imprecision of the dating method it is unlikely that more accurate dating would conclude that changes in the snowpits occur exactly together.)

Can changes in stratospheric ozone concentration help to explain this change? Both the photolytic rate constant and fractionation constants would be sensitive to significant changes in overhead ozone concentration (i.e. less stratospheric ozone leads to more penetration of light at wavelengths that can photolyze nitrate). Based on the approximate dating of the pits, P7 overlaps with the pre-ozone hole era

(generally considered prior to 1980), but there is no obvious change in the isotope observations (1980 occurs at a depth of about 250 cm; Fig. 3 and Fig. S2). Moreover, both ground-based observations at South Pole and satellite-based observations (TOMS/OMI) do not show any significant trend in total overhead ozone during spring and early summer over the time period 2000-2010 (<http://www.antarctica.ac.uk/met/jds/ozone/graphs.html>; http://www.cpc.noaa.gov/products/stratosphere/winter_bulletins/sh_09/http://ozonewatch.gsfc.nasa.gov/statistics/annual_data.html). This does not prove that there is not a link between the observed changes in the isotopic composition of snow nitrate and overhead ozone concentration, but this link over time is not obvious in this region. Finally, it is notable that the DC07 and DC04 pits (about 70 cm) from Frey et al. (2009) cover 8-10 years and thus overlap some with data from P4-P7. Neither of the DC pits show increasing $\delta^{18}\text{O}$ with depth (or decreasing $\delta^{15}\text{N}$ such as that in P7). Given the large spatial influence of stratospheric ozone on surface irradiance in Antarctica, it seems unlikely that Dome A and its surrounding region would be affected by this process and not Dome C. This suggests that something more localized, such as a change in the photolability of nitrate due to changes in snow chemistry, may have an important influence in recent decades.

~~As seen in Fig. 3 and discussed in the next section, pit profiles from the high accumulation sites in group I do not fit an exponential decrease function, but instead show periodic variability in mass fraction and isotopic composition of NO_3^- .~~

4.4 Seasonal shifts in NO_3^- sources to coastal snow (group I snowpits)

Pit profiles from the higher accumulation sites (group I) do not fit an exponential decrease function but instead show periodic variability in mass fraction and isotopic composition of NO_3^- (Fig. 3).

As discussed above, sharp decreases in $w(\text{NO}_3^-)$ in the top few centimeters of inland East Antarctic snowpits are interpreted as evidence of severe photolytic NO_3^- loss. $w(\text{NO}_3^-)$ in the top 10 cm of the coastal P1 snowpit also decreases from the surface (Fig. 3) and, if viewed in isolation, could also be taken as evidence for post-depositional loss. However, annual average snow accumulation at P1 is approximately 50 cm snow a^{-1} , and the full profile clearly shows that similarly high $w(\text{NO}_3^-)$ values are observed below 10 cm, as would be expected from seasonal cycles. We expect that if the coastal sites studied by Erbland et al. (2013) had been continuously sampled below 20 cm, similar features would have been observed. This should serve as caution in interpreting the behavior of NO_3^- at high accumulation sites based on observations that do not cover a full annual cycle of snowfall.

Profiles of the group I pits (P1-P3) show large variations in $w(\text{NO}_3^-)$ and isotopic composition throughout the snowpack, with some correspondence to $\delta^{18}\text{O}(\text{H}_2\text{O})$ which is a proxy for temperature (Fig. 7). The seasonality is most apparent at site P1 due to the highest sampling resolution (3.0 cm per sample compared to 5.0 cm per sample for pits P2 and P3) and highest snow accumulation rate (172 $\text{kg m}^{-2} \text{a}^{-1}$), though all group I sites feature high accumulation rates above 91 $\text{kg m}^{-2} \text{a}^{-1}$ (Table 1).

It is difficult to assign samples to four distinct seasons based on $\delta^{18}\text{O}(\text{H}_2\text{O})$ alone, so we choose a conservative classification of two periods: a warm season corresponding to higher $\delta^{18}\text{O}(\text{H}_2\text{O})$ and a cold season characterized by lower $\delta^{18}\text{O}(\text{H}_2\text{O})$ (Fig. 7). These assignments are also consistent with other established seasonal tracers measured in P1 in that the $\delta^{18}\text{O}(\text{H}_2\text{O})$ peaks (warm season) correspond to spikes in MSA and low Na^+ , while the opposite pattern is present during the identified cold seasons (C-J. Li, personal communication, 2014). The snow accumulation rate of 172 $\text{kg m}^{-2} \text{a}^{-1}$ at P1 site, which corresponds to 43-57 cm snow a^{-1} assuming a typical snow density of 0.3-0.4 g cm^{-3} , also fits with the thickness of the designated seasonal layers. Although coarse, this conservative dating of the snowpit is sufficient to make

broad comparisons throughout the year. This is aided by the high accumulation rate and the large amplitude variability in the data.

The samples and data assigned to warm and cold seasons for P1 are shown in Figs. 7 and 8. If the $\delta^{18}\text{O}(\text{H}_2\text{O})$ peaks are taken to roughly correspond with the middle of the warm season, this results in 61% of samples falling into the cold season compared with the warm season, which agrees well with the seasonal precipitation climatology where conditions slightly favor cold season accumulation (e.g., about 60% of snow occurs in the cold season on the coast; Laepple et al., 2011).

As illustrated in Fig. 7, snow $w(\text{NO}_3^-)$ spikes are present during the warm periods, while $w(\text{NO}_3^-)$ in the cold season is lower. The averages of $w(\text{NO}_3^-)$ in warm and cold seasons are 62.0 and 36.6 ng g⁻¹, respectively (Fig. 8a). ~~These seasonal cycles in mass fraction are consistent with previous observations at other Antarctic coastal sites suggested that NO_3^- mass fractions were generally higher in summer and lower in winter (Mulvaney et al., 1998; Wagenbach et al., 1998; Wolff et al., 2008). (Mulvaney et al., 1998; Wagenbach et al., 1998; Wolff et al., 2008), which is consistent with our findings.~~ In contrast, values of $\delta^{15}\text{N}$, $\delta^{18}\text{O}$ and $\Delta^{17}\text{O}$ of NO_3^- are all higher in cold seasons (with means of 31.0, 86.3 and 34.4‰, respectively); while the averages in warm seasons are 15.1, 77.4 and 30.4‰, respectively (Fig. 8a).

Photolytic loss of NO_3^- at high accumulation sites such as Summit, Greenland (where the 200 kg m⁻² a⁻¹ accumulation rate is comparable to P1) appears to be negligible (Hastings et al., 2004; Fibiger et al., 2013). In addition, the expected negative relationship between $w(\text{NO}_3^-)$ and $\delta^{15}\text{N}(\text{NO}_3^-)$ based upon the negative photolytic $^{15}\epsilon$ (-45.3‰) is not observed nor does $\delta^{15}\text{N}(\text{NO}_3^-)$ show a sharp increase with the decreasing $w(\text{NO}_3^-)$ in the upper 10 cm. Furthermore, given the results from the inland pits, a higher degree of photolytic NO_3^- loss (i.e., the extent of photolysis) could be expected to be accompanied by more secondary oxidation in the condensed phase (e.g., Jacobi and Hilker, 2007), leading to a decrease of $\delta^{18}\text{O}(\text{NO}_3^-)$ in the upper snowpack. But there is a significant increasing trend of $\delta^{18}\text{O}(\text{NO}_3^-)$ in the upper 30 cm of snow (Fig. 7) and there is no relationship between $\delta^{15}\text{N}(\text{NO}_3^-)$ and $\delta^{18}\text{O}(\text{NO}_3^-)$ in the dataset as a whole or when divided by season. Thus, it is concluded that photolytic loss of NO_3^- at P1 is likely not influential.

If volatilization was driving the variability of $w(\text{NO}_3^-)$, a relationship between $w(\text{NO}_3^-)$ and $\delta^{15}\text{N}(\text{NO}_3^-)$ could be expected based on the theoretically calculated value for $^{15}\epsilon$ (Table S3), but none is observed (Table 2). On the other hand, the $^{15}\epsilon$ value at -20 °C reported from the Dome C experiment ($^{15}\epsilon=-0.3\text{‰}$) is effectively non-fractionating (Erland et al., 2013). Based on this, it is difficult to attribute the isotopic variability in P1 to volatilization.

In summary, the observed variability in $w(\text{NO}_3^-)$ and isotopic composition cannot be explained by post-depositional processes in snow, given our current knowledge of isotopic fractionations of the processes discussed above. The observed large variations in the P1 isotopic and mass fraction data are more plausibly explained as presenting a seasonal NO_3^- source shift over different periods (see below), which may be further corroborated by the changing relationship of $w(\text{NO}_3^-)$ vs. $\delta^{18}\text{O}(\text{NO}_3^-)$ between cold and warm seasons (Fig. 8b).

A number of studies have suggested that the stratosphere is the primary source of NO_3^- to the Antarctic ice sheet (Mulvaney and Wolff, 1993; Wagenbach et al., 1998; Savarino et al., 2007), with an estimated annual flux of $6.3\pm 2.7\times 10^7$ kg N a⁻¹ (Muscari et al., 2003). As discussed by Savarino et al. (2007), interactions between NO_x and stratosphere-stratospheric ozone lead to some of the highest $\Delta^{17}\text{O}$ (and $\delta^{18}\text{O}$) of NO_3^- values, which have been thus far only been observed in polar regions. It is notable that $\delta^{18}\text{O}(\text{NO}_3^-)$ values above 90‰ are all present in cold season snow, and $\delta^{18}\text{O}(\text{NO}_3^-)$ and $\Delta^{17}\text{O}(\text{NO}_3^-)$ (ranging from 69.5 to 105.3‰ and 25.2 to 42.9‰, respectively) in this period are comparable to the data of atmospheric NO_3^- (inorganic NO_3^- aerosol) in winter at the coastal East Antarctic Dumont d'Urville station (DDU; 66°40'S,

140°01'E). At DDU, where the higher $\delta^{18}\text{O}(\text{NO}_3^-)$ and $\Delta^{17}\text{O}(\text{NO}_3^-)$ in winter is thought to be linked with stratospheric NO_3^- deposition (Savarino et al., 2007). The great enrichment of ^{18}O and ^{17}O in the cold season NO_3^- in P1 suggests that O atoms from stratospheric O_3 have been incorporated into NO_x and NO_3^- (R4-R6) that was subsequently deposited in snow as NO_3^- .

Interestingly, the highest $\delta^{18}\text{O}(\text{NO}_3^-)$ and $\Delta^{17}\text{O}(\text{NO}_3^-)$ values are all found in the most recent winter/spring in P1, namely 2012. This season was marked by much less stratospheric O_3 loss and a smaller O_3 hole extent than in previous seasons covered by the P1 snowpit; the mean 2012 O_3 hole area was 19% smaller than the prior 3 year average, and the minimum O_3 concentration of 139.1DU detected by satellite was the highest on record since 1988 (based on data from the NASA Goddard Space Flight Center: http://ozonewatch.gsfc.nasa.gov/meteorology/annual_data.txt). This might support that, where atmospheric NO_3^- is preserved in Antarctic snow, the O isotopes of NO_3^- could track stratospheric O_3 changes over time (McCabe et al., 2007).

At South Pole, McCabe et al. (2007) suggested that the $\Delta^{17}\text{O}(\text{NO}_3^-)$ may track changes in stratospheric ozone. However, McCabe et al. (2007) found an anti-correlation between $\Delta^{17}\text{O}(\text{NO}_3^-)$ with October-December column ozone concentrations. Two hypotheses were proposed in this work: 1) the nitrate oxygen isotopes are being primarily affected by increases in tropospheric ozone levels because of increased UV from decreased springtime column ozone levels, or 2) the oxygen isotopes are recording increases in the stratospheric nitrate flux during years of reduced column ozone. At South Pole, nitrate in snow is expected to preserve only 25% of the original stratospheric isotopic composition, whereas 75% reflects the tropospheric isotopic composition, due to nitrate produced locally from the snow-sourced, gas-phase recycled NO_x on the polar plateau (McCabe et al., 2007). The situation is really different at coastal site P1, where the photolysis imprint is rather minor. For snow nitrate in the cold season at P1, higher $\delta^{18}\text{O}(\text{NO}_3^-)$ and $\Delta^{17}\text{O}(\text{NO}_3^-)$ correspond to a smaller ozone hole (i.e., column ozone is higher) and this is most dramatic in 2012.

The $\delta^{15}\text{N}(\text{NO}_3^-)$ in P1 cold season snow has a mean of $31.0 \pm 14.5\text{‰}$, which is much higher than that found in atmospheric NO_3^- at DDU (maximum of 10.8‰). Savarino et al. (2007) calculated that the isotopic signature of NO formed in the stratosphere would be $19 \pm 3\text{‰}$ based upon the estimated fractionation of N_2O upon decomposition. Based on the expectation that more than 90% of stratospheric NO_y (sum of reactive nitrogen oxide compounds) is removed during denitrification, Savarino et al. (2007) further predicted that the $\delta^{15}\text{N}$ of NO is close to the $\delta^{15}\text{N}(\text{NO}_3^-)$. The much higher values found in coastal snow must then represent either a higher stratospheric $\delta^{15}\text{N}$ source value than predicted, or fractionation associated with chemistry, transport or deposition. The annual weighted average $\delta^{15}\text{N}(\text{NO}_3^-)$ in a skin layer of snow at the air-snow interface was found to be 24.7‰ higher than that in atmospheric nitrate and it was suggested that this was due to a fractionation associated with deposition (Erbland et al., 2013). A striking difference between $\delta^{18}\text{O}(\text{NO}_3^-)$ and $\Delta^{17}\text{O}(\text{NO}_3^-)$ in atmospheric nitrate and that in the skin layer was not found, and instead the oxygen isotopes were suggested to be in equilibrium. The $\delta^{18}\text{O}(\text{NO}_3^-)$ in P1 and the correlation of $\delta^{18}\text{O}(\text{NO}_3^-)$ and $\Delta^{17}\text{O}(\text{NO}_3^-)$ ($R^2=0.77$, $p<0.01$) fit well within the range expected for primary atmospheric nitrate, and it is unlikely that significant fractionation associated with ~~chemistry/transport/deposition~~ (or chemistry or transport) would affect only $\delta^{15}\text{N}(\text{NO}_3^-)$ and not $\delta^{18}\text{O}(\text{NO}_3^-)$. Thus, a higher $\delta^{15}\text{N}(\text{NO}_3^-)$ value (or range) than 19‰ from stratospheric denitrification is needed to explain the P1 cold season data.

The warm season snow in P1 exhibits lower mean $\delta^{15}\text{N}$, $\delta^{18}\text{O}$ and $\Delta^{17}\text{O}$ of NO_3^- (15.1, 77.4 and 30.4‰, respectively). These lower values, and the occurrence of $\delta^{15}\text{N}(\text{NO}_3^-) < 0\text{‰}$ in warm seasons, are also consistent with the DDU atmospheric data (Savarino et al., 2007). The very low and negative $\delta^{15}\text{N}(\text{NO}_3^-)$ values found between October-December at DDU were interpreted as resulting from HNO_3 formed in the

atmosphere from snow sourced NO_x emissions transported from the plateau. Namely, the release of NO_x from photolysis of surface snow NO_3^- can explain these values because of the very large and negative $^{15}\epsilon$ (see section 4.1.1 above). The seasonally lowered O isotopic composition can then be explained as arising from the gas-phase oxidation of snow-sourced NO_x to HNO_3 predominantly by OH (R3), which would be expected to be the predominant pathway of HNO_3 formation during the warm season (Alexander et al., 2009).

While the mean values shown in Fig. 8a are representative of the seasonal shifts in the isotopic composition of NO_3^- , it is also clear from Fig. 7 that there is significant interannual variability. A recent adjoint modeling study suggested that $w(\text{NO}_3^-)$ in Antarctic snow was most sensitive to tropospheric sources of NO_x , primarily fossil fuel combustion, biogenic soil emissions and lightning, though snow emissions were not considered in the model (Lee et al., 2014). The isotopic signatures of NO_x sources and their relationship with the $\delta^{15}\text{N}$ of NO_3^- are poorly constrained (e.g., Fibiger et al., 2014), particularly in the Southern Hemisphere. For example, the $\delta^{15}\text{N}$ of NO_x from vehicle emissions in South Africa were consistently negative (Heaton, 1990) while that found in Switzerland was mostly positive (Ammann et al., 1999) and a recent study in the U.S. suggests very positive values associated with vehicle emissions (Felix and Elliott, 2014). Natural, biogenic soil emissions have not been directly quantified, but—F fertilized soils in a laboratory study emitted NO_x with very low $\delta^{15}\text{N}$ (from -48.9 to -19.9 ‰) (Li and Wang, 2008), and lightning-sourced NO_x is expected to be near 0‰. Additionally, peroxyacetyl nitrate (PAN) is suggested as an important source of NO_x to the Antarctic atmosphere during the warm season (Lee et al., 2014). While no direct information is available in terms of the $\delta^{15}\text{N}$ of NO_x (or NO_3^-) produced from PAN decomposition, it has been suggested that this could explain sporadic high $\delta^{15}\text{N}$ of NO_3^- in the northern subtropical marine system (Altieri et al., 2013). Thus, it is not possible at this time to link the observed changes in isotopic composition directly to NO_x emission sources. Still, qualitatively, and based on the combination of isotopes, the P1 snowpit data would agree with a varying relative contribution of tropospheric NO_x sources from year-to-year in the warm season. In the cold season, the data suggest that there is still an important degree of stratospheric influence on NO_3^- loading in Antarctic snow, particularly in 2012 when the O_3 hole was unusually small.

5 Conclusion

The purpose of this study was to investigate the effects of post-depositional processes on isotopic fractionation of NO_3^- at different depths in the snowpack, and to understand variation of NO_3^- isotopic composition in different environments on the EAIS. In the EAIS interior, where accumulation rates are very low (group II snowpits; $<55 \text{ kg m}^{-2} \text{ a}^{-1}$), a higher degree of NO_3^- loss is found. The high values of $\delta^{15}\text{N}(\text{NO}_3^-)$ found in near-surface snow (i.e., top 25–20 cm) and the relationship between $w(\text{NO}_3^-)$ and $\delta^{15}\text{N}(\text{NO}_3^-)$ are consistent with a Rayleigh-type process and theoretically predicted $^{15}\epsilon$ values for NO_3^- photolysis. The concurrent decreases in $\delta^{18}\text{O}(\text{NO}_3^-)$, however, are best explained as resulting from condensed-phase re-oxidation forming secondary NO_3^- that contains oxygen atoms derived from in situ H_2O (e.g., $\delta^{18}\text{O}(\text{H}_2\text{O})$ of -50‰). This significantly decreases the $\delta^{18}\text{O}(\text{NO}_3^-)$ overall from what was originally deposited, and explains the positive relationship between $w(\text{NO}_3^-)$ and the $\delta^{18}\text{O}$ of NO_3^- (and therefore the positive observed $^{18}\epsilon_{\text{app}}$ values). Interestingly, below 25–20 cm in the group II snowpits, a change in the relationship between $w(\text{NO}_3^-)$ and $\delta^{18}\text{O}(\text{NO}_3^-)$ is observed. These findings highlight the utility of the combined use of $\delta^{15}\text{N}(\text{NO}_3^-)$ and $\delta^{18}\text{O}(\text{NO}_3^-)$ for detecting post-depositional processing of NO_3^- and the difficulty in predicting the isotopic composition of NO_3^- at depth based on the fractionation of near-surface

NO₃⁻ alone. We find that in both group II and group I snowpits (accumulation >91 kg m⁻² a⁻¹), $w(\text{NO}_3^-)$, $\delta^{15}\text{N}(\text{NO}_3^-)$, and $\delta^{18}\text{O}(\text{NO}_3^-)$ cannot be fit by a simple exponential decrease model, implying that photolytic loss cannot be assumed to operate consistently over time. In the case of the group II snowpits, a significant negative relationship is observed between $w(\text{NO}_3^-)$ and $\delta^{18}\text{O}(\text{NO}_3^-)$ at depths between 100-200 cm. We suggest that the change over time in the behavior of the isotopes is best explained as being driven by changes in the photolability of nitrate and thus, chemistry of the snow. In the case of the group I snowpits, seasonal variability is found in $w(\text{NO}_3^-)$, $\delta^{15}\text{N}$, $\delta^{18}\text{O}$, and $\Delta^{17}\text{O}$ of NO₃⁻ throughout the profiles. We suggest that the seasonality observed in higher accumulation, more coastal EAIS sites is driven by the influence of seasonal changes in NO₃⁻ sources. The best explanation for the range of values seen, given current knowledge, is the importance of stratospheric production of atmospheric NO₃⁻ in the cold season compared to more tropospheric NO_x source influence in the warm season.

Supplementary material related to this article is attached.

Acknowledgements. This research was supported by the National Science Foundation of China (Grant Nos. 41206188 to GS, 41476169 to SJ), the U.S. National Science Foundation Antarctic Glaciology Program (Grant No. 1246223 to MGH) and Chinese Polar Environment Comprehensive Investigation and Assessment Programmes (Grant Nos. CHINARE 2014-02-02 to BS, 2014-04-01 to GS). We are also grateful to Ruby Ho at Brown University and the 29th CHINARE inland members for technical support and assistance, and Dr. Erbland and two anonymous reviewers for their helpful comments.

References

- Alexander, B., Savarino, J., Kreutz, K. J., and Thieme, M.: Impact of preindustrial biomass-burning emissions on the oxidation pathways of tropospheric sulfur and nitrogen, *J. Geophys. Res.*, 109, D08303, doi:10.1029/2003JD004218, 2004.
- Alexander, B., Hastings, M., Allman, D., Dachs, J., Thornton, J., and Kunasek, S.: Quantifying atmospheric nitrate formation pathways based on a global model of the oxygen isotopic composition ($\Delta^{17}\text{O}$) of atmospheric nitrate, *Atmos. Chem. Phys.*, 9, 5043-5056, 2009.
- Altieri, K., Hastings, M., Gobel, A., Peters, A., and Sigman, D.: Isotopic composition of rainwater nitrate at Bermuda: The influence of air mass source and chemistry in the marine boundary layer, *J. Geophys. Res.*, 118, 11304-11316, 2013.
- Ammann, M., Siegwolf, R., Pichlmayer, F., Suter, M., Saurer, M., and Brunold, C.: Estimating the uptake of traffic-derived NO₂ from ¹⁵N abundance in Norway spruce needles, *Oecologia*, 118, 124-131, 1999.
- Böhlke, J., Mroczkowski, S., and Coplen, T.: Oxygen isotopes in nitrate: New reference materials for ¹⁸O: ¹⁷O: ¹⁶O measurements and observations on nitrate-water equilibration, *Rapid Commun. Mass Spectrom.*, 17, 1835-1846, 2003.
- Berhanu, T. A., Meusinger, C., Erbland, J., Jost, R., Bhattacharya, S., Johnson, M. S., and Savarino, J.: Laboratory study of nitrate photolysis in Antarctic snow. II. Isotopic effects and wavelength dependence, *J. Chem. Phys.*, 140, 244306, doi:10.1063/1.4882899, 2014.
- Blunier, T., Floch, G., Jacobi, H.-W., and Quansah, E.: Isotopic view on nitrate loss in Antarctic surface snow, *Geophys. Res. Lett.*, 32, L13501, doi:10.1029/2005GL023011, 2005.
- Boxe, C., Colussi, A., Hoffmann, M., Murphy, J., Wooldridge, P., Bertram, T., and Cohen, R.: Photochemical production and release of gaseous NO₂ from nitrate-doped water ice, *J. Phys. Chem.*, 109,

8520-8525, 2005.

Buffen, A. M., Hastings, M. G., Thompson, L. G., and Mosley-Thompson, E.: Investigating the preservation of nitrate isotopic composition in a tropical ice core from the Quelccaya Ice Cap, Peru, *J. Geophys. Res.*, 119, 2674-2697, doi: 10.1002/2013JD020715, 2014.

Bunton, C., Halevi, E., and Llewellyn, D.: Oxygen exchange between nitric acid and water. Part I, *J. Chem. Soc.*, 4913-4916, doi:10.1039/jr9520004913, 1952.

Casciotti, K., Sigman, D., Hastings, M. G., Böhlke, J., and Hilkert, A.: Measurement of the oxygen isotopic composition of nitrate in seawater and freshwater using the denitrifier method, *Anal. Chem.*, 74, 4905-4912, 2002.

Chu, L., and Anastasio, C.: Quantum yields of hydroxyl radical and nitrogen dioxide from the photolysis of nitrate on ice, *J. Phys. Chem.*, 107, 9594-9602, 2003.

Criss, R. E.: Principles of stable isotope distribution, Oxford University Press, New York, 254 pp., 1999.

[Davis, D. D., Seelig, J., Huey, G., Crawford, J., Chen, G., Wang, Y., Buhr, M., Helmig, D., Neff, W., Blake, D., Arimot, R., and Eisele, F.: A reassessment of Antarctic plateau reactive nitrogen based on ANTCI 2003 airborne and ground based measurements, *Atmos. Environ.*, 42, 2831-2848, 2008.](#)

Delmas, R., Serca, D., and Jambert, C.: Global inventory of NO_x sources, *Nutr. Cycl. Agroecosys*, 48, 51-60, 1997.

Dibb, J. E., Arsenault, M., Peterson, M. C., and Honrath, R. E.: Fast nitrogen oxide photochemistry in Summit, Greenland snow, *Atmos. Environ.*, 36, 2501-2511, 2002.

Dibb, J. E., and Fehsenfeld, M.: Snow accumulation, surface height change, and firn densification at Summit, Greenland: Insights from 2 years of in situ observation, *J. Geophys. Res.*, 109, D24113, doi: 10.1029/2003JD004300, 2004.

Ding, M., Xiao, C., Jin, B., Ren, J., Qin, D., and Sun, W.: Distribution of $\delta^{18}\text{O}$ in surface snow along a transect from Zhongshan Station to Dome A, East Antarctica, *Chin. Sci. Bull.*, 55, 2709-2714, 2010.

Ding, M., Xiao, C., Li, Y., Ren, J., Hou, S., Jin, B., and Sun, B.: Spatial variability of surface mass balance along a traverse route from Zhongshan station to Dome A, Antarctica, *J. Glaciol.*, 57, 658-666, 2011.

Dubowski, Y., Colussi, A., and Hoffmann, M.: Nitrogen dioxide release in the 302 nm band photolysis of spray-frozen aqueous nitrate solutions. Atmospheric implications, *J. Phys. Chem.*, 105, 4928-4932, 2001.

Elliott, E. M., Kendall, C., Wankel, S. D., Burns, D. A., Boyer, E. W., Harlin, K., Bain, D. J., and Butler, T. J.: Nitrogen isotopes as indicators of NO_x source contributions to atmospheric nitrate deposition across the midwestern and northeastern United States, *Environ. Sci. Technol.*, 41, 7661-7667, doi: 10.1021/es070898t, 2007.

Erbland, J., Vicars, W., Savarino, J., Morin, S., Frey, M., Frosini, D., Vince, E., and Martins, J.: Air-snow transfer of nitrate on the East Antarctic Plateau - Part 1: Isotopic evidence for a photolytically driven dynamic equilibrium in summer, *Atmos. Chem. Phys.*, 13, 6403-6419, 2013.

[Felix, J. D., and Elliott, E. M.: Isotopic composition of passively collected nitrogen dioxide emissions: Vehicle, soil and livestock source signatures, *Atmos. Environ.*, 92, 359-366, 2014.](#)

Fibiger, D. L., Hastings, M. G., Dibb, J. E., and Huey, L. G.: The preservation of atmospheric nitrate in snow at Summit, Greenland, *Geophys. Res. Lett.*, 40, 3484-3489, 2013.

Frey, M. M., Brough, N., France, J. L., Anderson, P. S., Traulle, O., King, M. D., Jones, A. E., Wolff, E. W., and Savarino, J.: The diurnal variability of atmospheric nitrogen oxides (NO and NO₂) above the Antarctic Plateau driven by atmospheric stability and snow emissions, *Atmos. Chem. Phys.*, 13, 3045-3062, 2013.

853 Frey, M. M., Savarino, J., Morin, S., Erbland, J., and Martins, J.: Photolysis imprint in the nitrate stable
854 isotope signal in snow and atmosphere of East Antarctica and implications for reactive nitrogen cycling,
855 Atmos. Chem. Phys., 9, 8681-8696, 2009.

856 Grannas, A., Jones, A. E., Dibb, J., Ammann, M., Anastasio, C., Beine, H., Bergin, M., Bottenheim, J., Boxe,
857 C., and Carver, G.: An overview of snow photochemistry: evidence, mechanisms and impacts, Atmos.
858 Chem. Phys., 7, 4329-4373, 2007.

859 Hastings, M. G., Sigman, D. M., and Lipschultz, F.: Isotopic evidence for source changes of nitrate in rain at
860 Bermuda, J. Geophys. Res., 108, 4790, doi:10.1029/2003JD003789, 2003.

861 Hastings, M. G., Steig, E., and Sigman, D.: Seasonal variations in N and O isotopes of nitrate in snow at
862 Summit, Greenland: Implications for the study of nitrate in snow and ice cores, J. Geophys. Res., 109,
863 D20306, doi:10.1029/2004JD004991, 2004.

864 Hastings, M. G., Jarvis, J. C., and Steig, E. J.: Anthropogenic impacts on nitrogen isotopes of ice-core
865 nitrate, Science, 324, 1288-1288, 2009.

866 Hastings, M. G.: Evaluating source, chemistry and climate change based upon the isotopic composition of
867 nitrate in ice cores, IOP Conference Series: Earth and Environmental Science,
868 9, 012002, doi:10.1088/1755-1315/9/1/012002, 2010.

869 Heaton, T. H. E.: $^{15}\text{N}/^{14}\text{N}$ ratios of NO_x from vehicle engines and coal-fired power stations, Tellus. B, 42,
870 304-307, 1990.

871 ~~Hutterli, M. A., McConnell, J. R., Chen, G., Bales, R. C., Davis, D. D., and Lenschow, D. H.: Formaldehyde~~
872 ~~and hydrogen peroxide in air, snow and interstitial air at South Pole, Atmos. Environ., 38, 5439-5450,~~
873 ~~2004.~~

874 Jacobi, H.-W., and Hilker, B.: A mechanism for the photochemical transformation of nitrate in snow, J.
875 Photochem. Photobiol. A, 185, 371-382, 2007.

876 Johnsen, S. J., Clausen, H. B., Dansgaard, W., Gundestrup, N. S., Hammer, C. U., Andersen, U., Andersen,
877 K. K., Hvidberg, C. S., Dahl-Jensen, D., and Steffensen, J. P.: The $\delta^{18}\text{O}$ record along the Greenland Ice
878 Core Project deep ice core and the problem of possible Eemian climatic instability, J. Geophys. Res.,
879 102, 26397-26410, 1997.

880 Kaiser, J., Hastings, M. G., Houlton, B. Z., Röckmann, T., and Sigman, D. M.: Triple oxygen isotope
881 analysis of nitrate using the denitrifier method and thermal decomposition of N_2O , Anal. Chem., 79,
882 599-607, 2007.

883 Laepple, T., Werner, M., and Lohmann, G.: Synchronicity of Antarctic temperatures and local solar
884 insolation on orbital timescales, Nature, 471, 91-94, 2011.

885 Lee, D., Köhler, I., Grobler, E., Rohrer, F., Sausen, R., Gallardo-Klenner, L., Olivier, J., Dentener, F., and
886 Bouwman, A.: Estimations of global NO_x emissions and their uncertainties, Atmos. Environ., 31,
887 1735-1749, 1997.

888 Lee, H.-M., Henze, D. K., Alexander, B., and Murray, L. T.: Investigating the sensitivity of surface-level
889 nitrate seasonality in Antarctica to primary sources using a global model, Atmos. Environ., 89, 757-767,
890 2014.

891 ~~Legrand, M., Preunkert, S., Frey, M., Bartels-Rausch, T., Kukui, A., King, M. D., Savarino, J., Kerbrat, M.,~~
892 ~~and Jourdain, B.: Large mixing ratios of atmospheric nitrous acid (HONO) at Concordia (East Antarctic~~
893 ~~Plateau) in summer: a strong source from surface snow?, Atmos. Chem. Phys., 14, 9963-9976, 2014.~~

894 Li, D., and Wang, X.: Nitrogen isotopic signature of soil-released nitric oxide (NO) after fertilizer
895 application, Atmos. Environ., 42, 4747-4754, 2008.

896 Madronich, S., and Flocke, S.: The role of solar radiation in atmospheric chemistry, in: Handbook of

- Environmental Chemistry, edited by: Boule, P., Springer Verlag, Heidelberg, 1-26, 1998.
- Mayewski, P. A., and Legrand, M. R.: Recent increase in nitrate concentration of Antarctic snow, *Nature*, 346, 258-260, 1990.
- McCabe, J., Boxe, C., Colussi, A., Hoffmann, M., and Thiemens, M.: Oxygen isotopic fractionation in the photochemistry of nitrate in water and ice, *J. Geophys. Res.*, 110, D15310, doi:10.1029/2004JD005484, 2005.
- McCabe, J. R., Thiemens, M. H., and Savarino, J.: A record of ozone variability in South Pole Antarctic snow: Role of nitrate oxygen isotopes, *J. Geophys. Res.*, 112, D12303, doi:10.1029/2006JD007822, 2007.
- Meusinger, C., Berhanu, T. A., Erbland, J., Savarino, J., and Johnson, M. S.: Laboratory study of nitrate photolysis in Antarctic snow. I. Observed quantum yield, domain of photolysis, and secondary chemistry, *J. Chem. Phys.*, 140, 244305, doi: 10.1063/1.4882898, 2014.
- Michalski, G., Savarino, J., Böhlke, J., and Thiemens, M.: Determination of the total oxygen isotopic composition of nitrate and the calibration of a $\Delta^{17}\text{O}$ nitrate reference material, *Anal. Chem.*, 74, 4989-4993, 2002.
- Michalski, G., Scott, Z., Kabiling, M., and Thiemens, M. H.: First measurements and modeling of $\Delta^{17}\text{O}$ in atmospheric nitrate, *Geophys. Res. Lett.*, 30, 1870, doi: 10.1029/2003GL017015, 2003.
- Morin, S., Savarino, J., Frey, M. M., Yan, N., Bekki, S., Bottenheim, J. W., and Martins, J. M.: Tracing the origin and fate of NO_x in the Arctic atmosphere using stable isotopes in nitrate, *Science*, 322, 730-732, 2008.
- Mulvaney, R., and Wolff, E.: Evidence for winter/spring denitrification of the stratosphere in the nitrate record of Antarctic firn cores, *J. Geophys. Res.*, 98, 5213-5220, 1993.
- Mulvaney, R., Wagenbach, D., and Wolff, E. W.: Postdepositional change in snowpack nitrate from observation of year-round near-surface snow in coastal Antarctica, *J. Geophys. Res.*, 103, 11021-11031, 1998.
- Muscari, G., de Zafra, R. L., and Smyshlyaev, S.: Evolution of the $\text{NO}_y\text{-N}_2\text{O}$ correlation in the Antarctic stratosphere during 1993 and 1995, *J. Geophys. Res.*, 108, 4428, doi:10.1029/2002JD002871, 2003.
- Röthlisberger, R., Hutterli, M. A., Sommer, S., Wolff, E. W., and Mulvaney, R.: Factors controlling nitrate in ice cores: Evidence from the Dome C deep ice core, *J. Geophys. Res.*, 105, 20565-20572, 2000.
- Röthlisberger, R., Hutterli, M. A., Wolff, E. W., Mulvaney, R., Fischer, H., Bigler, M., Goto-Azuma, K., Hansson, M. E., Ruth, U., and Siggaard-Andersen, M.-L.: Nitrate in Greenland and Antarctic ice cores: A detailed description of post-depositional processes, *Ann. Glaciol.*, 35, 209-216, 2002.
- Sato, K., Takenaka, N., Bandow, H., and Maeda, Y.: Evaporation loss of dissolved volatile substances from ice surfaces, *J. Phys. Chem.*, 112, 7600-7607, 2008.
- Savarino, J., Kaiser, J., Morin, S., Sigman, D. M., and Thiemens, M. H.: Nitrogen and oxygen isotopic constraints on the origin of atmospheric nitrate in coastal Antarctica, *Atmos. Chem. Phys.*, 7, 1925-1945, 2007.
- Sigman, D. M., Casciotti, K. L., Andreani, M., Barford, C., Galanter, M., and Böhlke, J. K.: A bacterial method for the nitrogen isotopic analysis of nitrate in seawater and freshwater, *Anal. Chem.*, 73, 4145-4153, 2001.
- Traversi, R., Becagli, S., Castellano, E., Cerri, O., Morganti, A., Severi, M., and Udisti, R.: Study of Dome C site (East Antarctica) variability by comparing chemical stratigraphies, *Microchem. J.*, 92, 7-14, 2009.
- ~~Vicars, W. C., and Savarino, J.: Quantitative constraints on the ^{17}O excess ($\Delta^{17}\text{O}$) signature of surface ozone: Ambient measurements from 50°N to 50°S using the nitrite-coated filter technique, *Geochim.*~~

- [Cosmochim. Acta, 135, 270-287, 2014.](#)
- [Wang, Y., Sodemann, H., Hou, S., Masson-Delmotte, V., Jouzel, J., and Pang, H.: Snow accumulation and its moisture origin over Dome Argus, Antarctica, Clim. Dynam., 40, 731-742, doi: 10.1007/s00382-012-1398-9, 2013.](#)
- Wagenbach, D., Graf, V., Minikin, A., Trefzer, U., Kipfstuhl, J., Oerter, H., and Blindow, N.: Reconnaissance of chemical and isotopic firn properties on top of Berkner Island, Antarctica, Ann. Glaciol., 20, 307-312, 1994.
- Wagenbach, D., Legrand, M., Fischer, H., Pichlmayer, F., and Wolff, E. W.: Atmospheric near-surface nitrate at coastal Antarctic sites, J. Geophys. Res., 103, 11007-11020, 1998.
- Warneck, P., and Wurzinger, C.: Product quantum yields for the 305-nm photodecomposition of nitrate in aqueous solution, J. Phys. Chem., 92, 6278-6283, 1988.
- Warren, S. G., Brandt, R. E., and Grenfell, T. C.: Visible and near-ultraviolet absorption spectrum of ice from transmission of solar radiation into snow, Appl. Optics, 45, 5320-5334, 2006.
- Wolff, E. W.: Nitrate in polar ice, in: in Ice core studies of global biogeochemical cycles, edited by: Delmas, R. J., Springer, New York, 195-224, 1995.
- Wolff, E. W., Jones, A. E., Bauguitte, S.-B., and Salmon, R. A.: The interpretation of spikes and trends in concentration of nitrate in polar ice cores, based on evidence from snow and atmospheric measurements, Atmos. Chem. Phys., 8, 5627-5634, 2008.
- Wolff, E. W., Bigler, M., Curran, M., Dibb, J., Frey, M., Legrand, M., and McConnell, J.: The Carrington event not observed in most ice core nitrate records, Geophys. Res. Lett., 39, L08503, doi:10.1029/2012GL051603, 2012.
- [Xiao, C., Ding, M., Masson-Delmotte, V., Zhang, R., Jin, B., Ren, J., Li, C., Werner, M., Wang, Y., and Cui, X.: Stable isotopes in surface snow along a traverse route from Zhongshan station to Dome A, East Antarctica, Clim. Dynam., 41, 2427-2438, 2013.](#)
- [Yung, Y. L., and Miller, C. E.: Isotopic fractionation of stratospheric nitrous oxide, Science, 278, 1778-1780, doi:10.1126/science.278.5344.1778., 1997.](#)
- Zatko, M., Grenfell, T., Alexander, B., Doherty, S., Thomas, J., and Yang, X.: The influence of snow grain size and impurities on the vertical profiles of actinic flux and associated NO_x emissions on the Antarctic and Greenland ice sheets, Atmos. Chem. Phys., 13, 3547-3567, 2013.

973

Table 1. Summary information for the seven snowpits presented in this study.

<u>Snowpit</u>	<u>Location</u>	<u>Elevation,</u> <u>m</u>	<u>Distance</u> <u>from</u> <u>coast, km</u>	<u>Mean annual</u> <u>accumulation,</u> <u>kg m⁻² a⁻¹ 1)</u>	<u>Mean annual</u> <u>Temperature,</u> <u>°C 2)</u>	<u>Depth,</u> <u>cm</u>	<u>Sampling</u> <u>resolution,</u> <u>cm</u>	<u>Sampling date,</u> <u>DD.MM.YYYY</u>
<u>P1</u>	<u>71.13°S,</u> <u>77.31°E</u>	<u>2037</u>	<u>200</u>	<u>172.0</u>	<u>-29.12</u>	<u>150</u>	<u>3.0</u>	<u>18.12.2012</u>
<u>P2</u>	<u>71.81°S,</u> <u>77.89°E</u>	<u>2295</u>	<u>283</u>	<u>99.4</u>	<u>-32.87</u>	<u>200</u>	<u>5.0</u>	<u>20.12.2012</u>
<u>P3</u>	<u>73.40°S,</u> <u>77.00°E</u>	<u>2545</u>	<u>462</u>	<u>90.7</u>	<u>-35.72</u>	<u>200</u>	<u>5.0</u>	<u>22.12.2012</u>
<u>P4</u>	<u>76.29°S,</u> <u>77.03°E</u>	<u>2843</u>	<u>787</u>	<u>54.8</u>	<u>-41.28</u>	<u>200</u>	<u>2.0</u>	<u>28.12.2012</u>
<u>P5</u>	<u>77.91°S,</u> <u>77.13°E</u>	<u>3154</u>	<u>968</u>	<u>33.3</u>	<u>-46.37</u>	<u>200</u>	<u>2.0</u>	<u>30.12.2012</u>
<u>P6</u>	<u>79.02°S,</u> <u>76.98°E</u>	<u>3738</u>	<u>1092</u>	<u>25.4</u>	<u>-53.13</u>	<u>200</u>	<u>2.5</u>	<u>02.01.2013</u>
<u>P7</u>	<u>80.42°S,</u> <u>77.12°E</u>	<u>4093</u>	<u>1256</u>	<u>23.5</u>	<u>-58.50</u>	<u>300</u>	<u>2.5</u>	<u>06.01.2013</u>

974

1) Mean annual snow accumulation rates are obtained from bamboo stick field measurements, updated to 2013 from Ding et al. (2011).

975

976

2) Mean annual temperatures are derived from 10m borehole temperatures and automatic weather station observations (Ding et al., 2010; Xiao et al., 2013).

977

978

Table 1. Statistics of snow $w(\text{NO}_3^-)$, $\delta^{15}\text{N}$ and $\delta^{18}\text{O}$ of NO_3^- in the seven snowpits collected from East Antarctica.

Parameter	Snowpit	P1	P2	P3	P4	P5	P6	P7
$w(\text{NO}_3^-)$, ng g^{-1}	Mean	46.6	79.1	91.6	56.5	42.6	83.7	23.8
	Min	26.7	38.5	59.5	24.1	14.6	35.4	7.9
	Max	97.1	173.0	266.3	151.3	175.1	202.6	373.8
	SD	17.6	25.4	35.3	21.4	31.1	39.9	46.4
$\delta^{15}\text{N}$, ‰	Mean	24.7	23.0	21.3	133.6	196.3	160.9	335.2
	Min	-14.8	-12.1	-2.2	15.5	48.0	50.8	111.0
	Max	59.4	70.8	39.9	184.2	280.4	236.8	460.8
	SD	17.5	17.9	9.0	31.7	48.2	47.7	52.5
$\delta^{18}\text{O}$, ‰	Mean	82.5	81.1	85.1	59.9	54.4	52.5	48.9
	Min	66.7	69.9	52.5	45.8	42.7	36.2	16.8
	Max	105.3	96.8	111.2	75.6	82.2	81.9	84.0
	SD	11.0	7.7	16.2	7.0	9.0	10.1	12.1

Table 2. Observed fractionation constants for ^{15}N and ^{18}O of NO_3^- ($^{15}\epsilon_{\text{app}}$ and $^{18}\epsilon_{\text{app}}$) calculated for different snow layer depths from the linear regression of $\ln(\delta_{\text{snow}}+1)$ vs. $\ln(w_{\text{snow}})$ in Eq. (2). Four different depth intervals were selected for calculating ϵ_{app} : 0-20cm, 0-40cm, 0-60cm, 100-bottom and the entire pit. Also given are the standard error (1σ), r^2 values and the significance level, p , where bolded values represent $p < 0.05$.

Snow pit	Depth	^{15}N			^{18}O		
		$^{15}\epsilon_{\text{app}} \pm 1\sigma, \text{‰}$	p	r^2	$^{18}\epsilon_{\text{app}} \pm 1\sigma, \text{‰}$	p	r^2
P1	0-20cm	<u>2.4±2.0</u>	<u>0.379</u>	<u>0.157</u>	-15.3±6.0	0.044	0.588
	0-40cm	<u>-0.4±5.0</u>	<u>0.943</u>	<u>0.000</u>	<u>-8.7±7.0</u>	<u>0.248</u>	<u>0.109</u>
	0-60cm	<u>-3.9±14.0</u>	<u>0.785</u>	<u>0.004</u>	<u>-9.4±10.0</u>	<u>0.368</u>	<u>0.043</u>
	100-Bottom	<u>17.2±14.0</u>	<u>0.248</u>	<u>0.094</u>	<u>-6.5±5.0</u>	<u>0.175</u>	<u>0.127</u>
	Entire	<u>-11.8±7.0</u>	<u>0.098</u>	<u>0.056</u>	<u>-3.7±4.0</u>	<u>0.390</u>	<u>0.015</u>
P2	0-20cm	<u>-45.5±26.0</u>	<u>0.184</u>	<u>0.497</u>	4.0±1.0	0.017	0.887
	0-40cm	<u>0.8±10.0</u>	<u>0.936</u>	<u>0.001</u>	<u>-4.2±4.0</u>	<u>0.274</u>	<u>0.167</u>
	0-60cm	<u>4.1±15.0</u>	<u>0.789</u>	<u>0.007</u>	<u>-2.1±4.0</u>	<u>0.647</u>	<u>0.020</u>
	100-Bottom	<u>21.5±16.0</u>	<u>0.197</u>	<u>0.091</u>	11.2±4.2	0.015	0.287
	Entire	<u>11.9±9.1</u>	<u>0.198</u>	<u>0.043</u>	<u>7.0±3.6</u>	<u>0.060</u>	<u>0.090</u>
P3	0-20cm	-36.8±6.7	0.012	0.909	<u>-19.8±13.5</u>	<u>0.237</u>	<u>0.420</u>
	0-40cm	-27.5±11.0	0.036	0.488	<u>-15.4±11.0</u>	<u>0.188</u>	<u>0.233</u>
	0-60cm	-28.8±9.1	0.009	0.476	<u>-14.0±8.7</u>	<u>0.135</u>	<u>0.192</u>
	100-Bottom	<u>12.3±12.0</u>	<u>0.318</u>	<u>0.059</u>	<u>13.5±18.6</u>	<u>0.478</u>	<u>0.030</u>
	Entire	<u>-1.2±4.9</u>	<u>0.811</u>	<u>0.002</u>	<u>15.4±8.0</u>	<u>0.061</u>	<u>0.092</u>
P4	0-20cm	-77.8±9.2	0.000	0.888	17.1±3.1	0.000	0.778
	0-40cm	-81.6±7.5	0.000	0.868	14.0±2.1	0.000	0.706
	0-60cm	-73.3±9.8	0.000	0.665	11.4±2.5	0.000	0.419
	100-Bottom	-56.0±5.3	0.000	0.703	-3.4±1.3	0.011	0.126
	Entire	-58.7±5.0	0.000	0.584	<u>1.4±1.8</u>	<u>0.433</u>	<u>0.006</u>
P5	0-20cm	-93.1±23.6	0.003	0.633	30.2±12.3	0.036	0.401
	0-40cm	-92.1±10.8	0.000	0.791	24.9±5.5	0.000	0.522
	0-60cm	-92.5±8.1	0.000	0.820	16.0±3.6	0.000	0.412
	100-Bottom	<u>27.3±13.7</u>	<u>0.053</u>	<u>0.083</u>	-9.6±4.0	0.022	0.114
	Entire	-56.9±5.0	0.000	0.577	<u>0.0±1.6</u>	<u>0.985</u>	<u>0.000</u>
P6	0-20cm	-50.2±7.3	0.000	0.889	16.7±5.1	0.017	0.638
	0-40cm	-63.0±21.0	0.010	0.390	<u>16.2±12.1</u>	<u>0.201</u>	<u>0.114</u>
	0-60cm	-70.8±25.1	0.010	0.265	<u>17.9±9.3</u>	<u>0.066</u>	<u>0.145</u>
	100-Bottom	-61.3±8.0	0.000	0.605	-7.8±2.4	0.003	0.216
	Entire	-76.8±5.8	0.000	0.694	11.3±2.1	0.000	0.265
P7	0-20cm	-61.3±9.8	0.000	0.849	18.4±4.1	0.003	0.738
	0-40cm	-73.9±8.5	0.000	0.834	16.4±2.4	0.000	0.753
	0-60cm	-81.0±8.7	0.000	0.789	15.2±1.9	0.000	0.728
	100-Bottom	<u>20.7±14.4</u>	<u>0.154</u>	<u>0.026</u>	<u>10.0±4.5</u>	<u>0.051</u>	<u>0.060</u>
	Entire	-31.5±5.0	0.000	0.251	<u>-0.7±1.7</u>	<u>0.690</u>	<u>0.001</u>

Table 2 Observed fractionation constants for ^{15}N and ^{18}O of NO_3^- calculated for different snow layer depths from the linear regression of $\ln(\delta_{\text{snow}}+1)$ vs. $\ln(w_{\text{snow}})$ in Eq. (2). Four different depth intervals were selected for calculating ϵ : 0-25cm, 25-100cm, 100 cm to the pit base and the entire pit. Also given are the r^2 values and the significance level, p , where bolded values represent $p < 0.05$.

Snow-pit	Depth	^{15}N			^{18}O		
		$^{15}\epsilon, \text{‰}$	p	r^2	$^{18}\epsilon, \text{‰}$	p	r^2
P1	0-25cm	2.5	0.29	0.16	-13.7	0.11	0.33
	25-100cm	-61.7	0.00	0.44	32.3	0.00	0.39
	100-bottom	18.7	0.14	0.15	-8.2	0.08	0.21
	Entire	-14.0	0.05	0.08	-1.8	0.38	0.00
P2	0-25cm	-16.3	0.50	0.12	-0.4	0.87	0.01
	25-100cm	25.0	0.09	0.20	7.3	0.19	0.12
	100-bottom	21.5	0.20	0.09	11.2	0.02	0.29
	Entire	11.9	0.20	0.04	6.9	0.06	0.09
P3	0-25cm	-35.7	0.01	0.88	-22.0	0.17	0.41
	25-100cm	8.3	0.37	0.06	-7.2	0.58	0.02
	100-bottom	12.3	0.32	0.06	13.5	0.48	0.03
	Entire	-1.2	0.81	0.00	15.4	0.06	0.09
P4	0-25cm	-78.1	0.00	0.91	15.9	0.00	0.78
	25-100cm	-50.1	0.00	0.34	6.2	0.05	0.11
	100-bottom	-56.0	0.00	0.70	-3.4	0.01	0.13
	Entire	-58.7	0.00	0.58	1.7	0.43	0.01
P5	0-25cm	-84.4	0.00	0.63	28.8	0.01	0.44
	25-100cm	-52.5	0.00	0.60	-2.5	0.03	0.12
	100-bottom	27.3	0.05	0.08	-9.6	0.02	0.11
	Entire	-56.9	0.00	0.58	0.4	0.99	0.00
P6	0-25cm	-54.0	0.00	0.82	18.0	0.00	0.64
	25-100cm	-46.4	0.03	0.16	7.9	0.15	0.07
	100-bottom	-61.3	0.00	0.61	-7.8	0.00	0.22
	Entire	-76.8	0.00	0.69	11.3	0.00	0.27
P7	0-25cm	-59.2	0.00	0.86	17.8	0.00	0.74
	25-100cm	34.4	0.01	0.24	-9.4	0.00	0.36
	100-bottom	20.7	0.15	0.03	10.0	0.05	0.06
	Entire	-31.5	0.00	0.25	-0.7	0.69	0.00

Table 3. Asymptotic values of $w(\text{NO}_3^-)$, $\delta^{15}\text{N}$ and $\delta^{18}\text{O}$ of NO_3^- calculated based on four different snow depth intervals (0-20cm, 0-40cm, 0-60cm and 0-100cm) of each snowpit. p is the significance level of observed data fitted using the exponential decrease regression Eq. (6), and r^2 denotes squared correlation coefficient of observed data compared to the regression model predicted values. Also given is the standard error (1σ) of asymptotic values.

Snowpit	Depth	$w(\text{NO}_3^-)_{(\text{as.})}, \text{ng g}^{-1}$			$\delta^{15}\text{N}_{(\text{as.})}, \text{‰}$			$\delta^{18}\text{O}_{(\text{as.})}, \text{‰}$		
		$w(\text{NO}_3^-) \pm 1\sigma$	p	r^2	$\delta^{15}\text{N} \pm 1\sigma$	p	r^2	$\delta^{18}\text{O} \pm 1\sigma$	p	r^2
P4	0-20cm	26.9±15.7	0.00	0.92	165.4±18.3	0.00	0.94	41.2±7.4	0.00	0.88
	0-40cm	38.1±3.5	0.00	0.92	173.2±5.4	0.00	0.95	49.2±1.3	0.00	0.80
	0-60cm	45.3±2.7	0.00	0.83	158.4±4.3	0.00	0.82	51.6±1.1	0.00	0.58
	0-100cm	54.5±2.5	0.00	0.58	144.3±3.9	0.00	0.51	54.5±0.9	0.00	0.29
P5	0-20cm	50.0±4.3	0.00	0.82	166.2±6.5	0.00	0.74	41.6±3.1	0.00	0.63
	0-40cm	39.6±13.5	0.00	0.91	216.6±58.7	0.00	0.95	43.5±4.1	0.00	0.80
	0-60cm	39.9±6.1	0.00	0.92	277.9±51.2	0.00	0.89	46.0±1.8	0.00	0.71
	0-100cm	25.8±3.3	0.00	0.93	254.6±10.6	0.00	0.92	48.2±1.0	0.00	0.65
P6	0-20cm	101.3±32.9	0.00	0.73	106.4±11.1	0.09	0.43	63.4±38.4	0.20	0.26
	0-40cm	131.1±7.7	0.01	0.45	95.2±7.4	0.45	0.04	48.3±105.6	0.03	0.29
	0-60cm	121.4±6.7	0.00	0.39	160.1±196.8	0.00	0.42	22.7±15.0	0.00	0.54
	0-100cm	40.4±3.6	0.00	0.65	179.7±54.5	0.00	0.43	39.9±7.4	0.00	0.61
P7	0-20cm	15.7±26.9	0.00	0.96	298.7±40.5	0.00	0.85	29.2±18.5	0.00	0.73
	0-40cm	22.3±6.9	0.00	0.97	490.0±23.0	0.00	0.90	23.2±7.0	0.00	0.78
	0-60cm	23.3±3.9	0.00	0.97	448.7±33.1	0.00	0.86	29.7±2.5	0.00	0.75
	0-100cm	17.9±2.3	0.00	0.97	383.8±9.4	0.00	0.75	33.9±1.4	0.00	0.64

Table 3. Asymptotic values of $w(\text{NO}_3^-)$, $\delta^{15}\text{N}$ and $\delta^{18}\text{O}$ of NO_3^- calculated based on five different snow depth intervals (0-25cm, 0-60cm, 0-80cm, 0-100cm and entire depth) of each snowpit. p is the significance level of observed data fitted using the exponential decrease regression Eq. (6), and r^2 denotes squared correlation coefficient of observed data compared to the regression model predicted values.

Snowpit	Depth	$w(\text{NO}_3^-)_{(\text{as.})}, \text{ng g}^{-1}$			$\delta^{15}\text{N}_{(\text{as.})}, \text{‰}$			$\delta^{18}\text{O}_{(\text{as.})}, \text{‰}$		
		$w(\text{NO}_3^-)$	p	r^2	$\delta^{15}\text{N}$	p	r^2	$\delta^{18}\text{O}$	p	r^2
P4	Entire	53.6	0.00	0.41	137.2	0.00	0.27	46.8	0.00	0.45
	0-100cm	54.5	0.00	0.58	144.3	0.00	0.51	54.5	0.00	0.29
	0-80cm	55.3	0.00	0.57	146.3	0.00	0.55	53.6	0.00	0.34
	0-60cm	45.3	0.00	0.83	158.4	0.00	0.82	51.6	0.00	0.58
	0-25cm	27.2	0.00	0.93	180.5	0.00	0.95	44.5	0.00	0.89
P5	Entire	25.7	0.00	0.93	220.3	0.00	0.75	53.3	0.00	0.24
	0-100cm	25.8	0.00	0.93	254.6	0.00	0.92	48.2	0.00	0.65
	0-80cm	19.7	0.00	0.92	282.0	0.00	0.91	46.9	0.00	0.69
	0-60cm	39.9	0.00	0.92	277.9	0.00	0.89	46.0	0.00	0.71
	0-25cm	40.8	0.00	0.88	176.5	0.00	0.72	35.4	0.00	0.65
P6	Entire	34.1	0.00	0.80	256.4	0.00	0.72	47.6	0.00	0.59
	0-100cm	40.4	0.00	0.65	179.7	0.00	0.43	39.9	0.00	0.61
	0-80cm	55.0	0.00	0.52	196.0	0.00	0.37	20.9	0.00	0.59

		0-60cm	121.4	0.00	0.39	160.1	0.00	0.42	22.7	0.00	0.54
		0-25cm	123.4	0.01	0.53	96.5	0.31	0.11	69.9	0.27	0.14
	P7	Entire	14.1	0.00	0.97	344.5	0.00	0.47	48.3	0.00	0.10
		0-100cm	17.9	0.00	0.97	383.8	0.00	0.75	33.9	0.00	0.64
		0-80cm	20.9	0.00	0.97	406.2	0.00	0.83	31.5	0.00	0.73
		0-60cm	23.3	0.00	0.97	448.7	0.00	0.86	29.7	0.00	0.75
		0-25cm	26.1	0.00	0.97	287.7	0.00	0.86	34.2	0.00	0.73
1007											
1008											
1009											
1010											

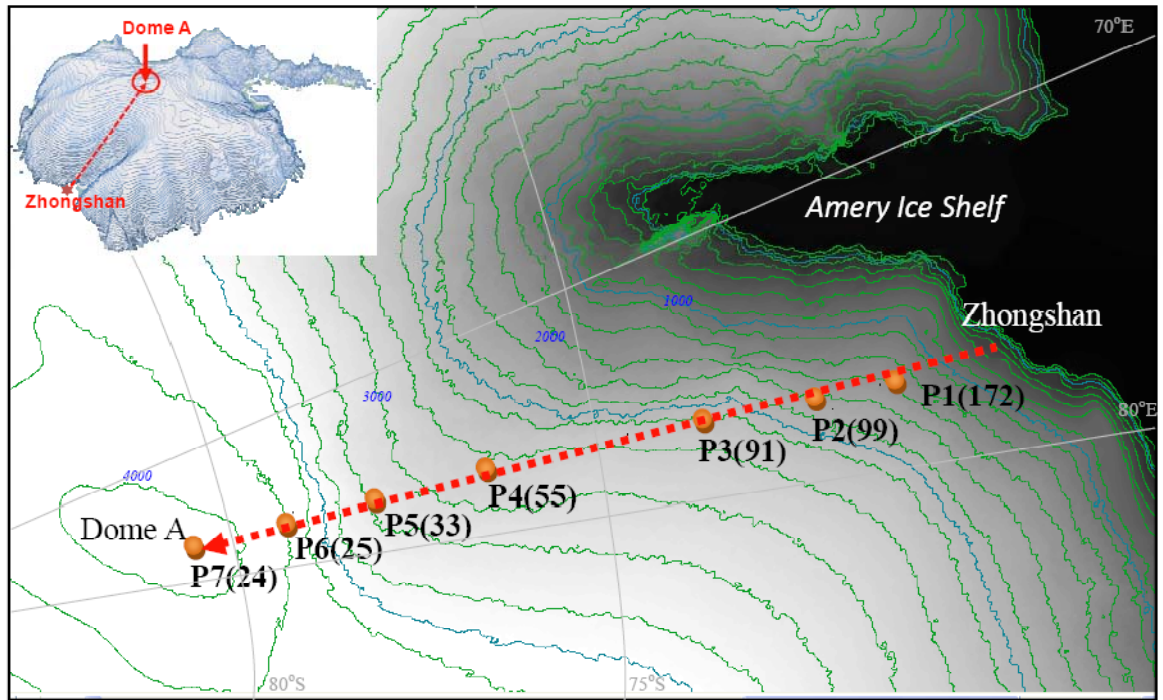


Fig. 1. Snowpit locations sampled during the 2012/2013 Chinese National Antarctic Research Expedition (CHINARE) inland traverse. The numbers in parentheses denote the annual snow accumulation rates ($\text{kg m}^{-2} \text{a}^{-1}$) which are extended to 2013 from bamboo stick field measurements (Ding et al., 2011).

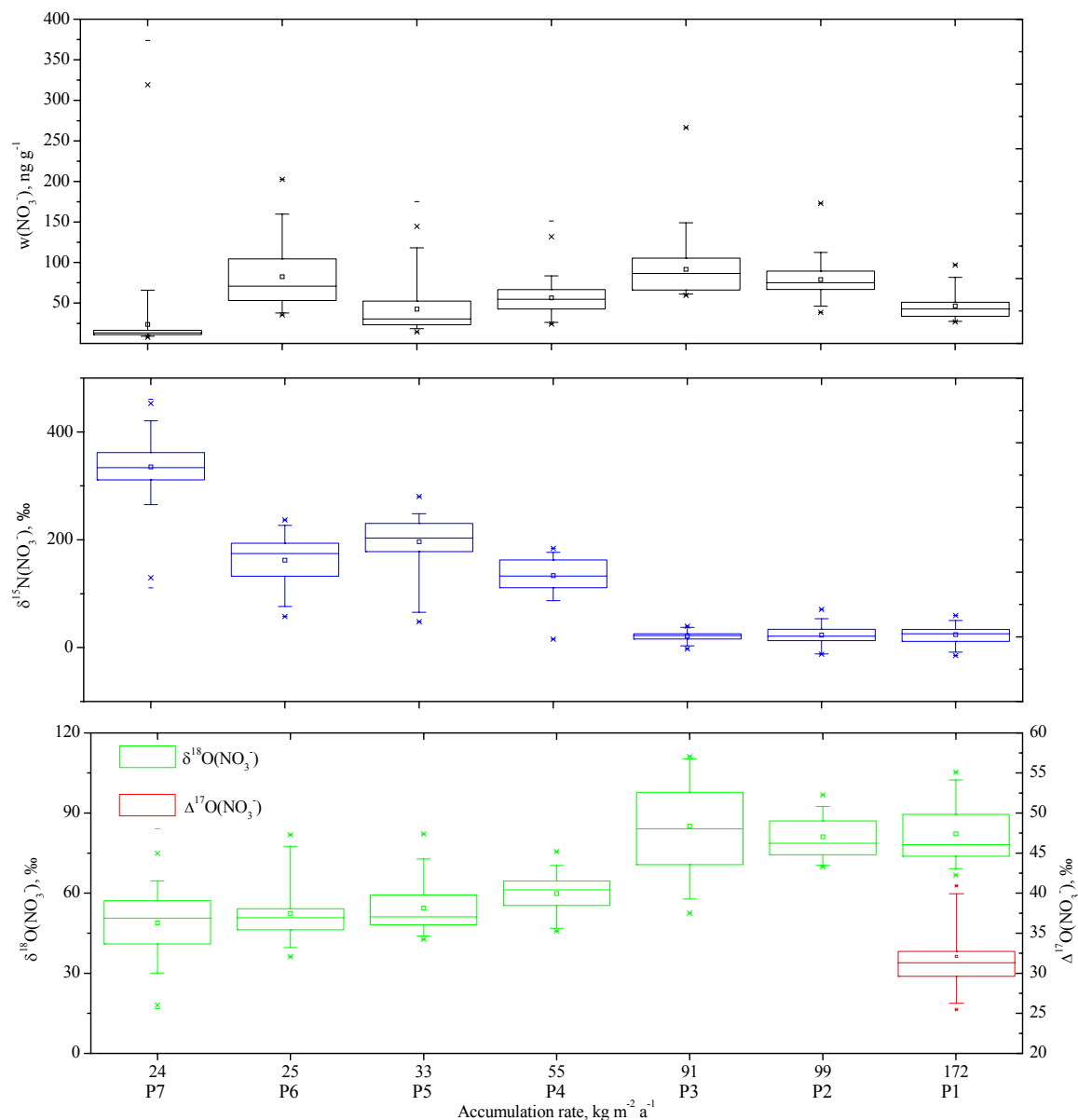


Fig. 2. Statistics of mass fraction and isotopic compositions of NO_3^- for each snowpit (P1-P7), plotted as a function of snow accumulation rate. Box and whisker plots represent maximum (top x symbol for each box), minimum (bottom x symbol for each box), percentiles (5th, 25th, 75th, and 95th), and median (50th, solid line) and mean (open square near center of each box). It is noted that the data of $\Delta^{17}\text{O}(\text{NO}_3^-)$ are only available for P1 pit.

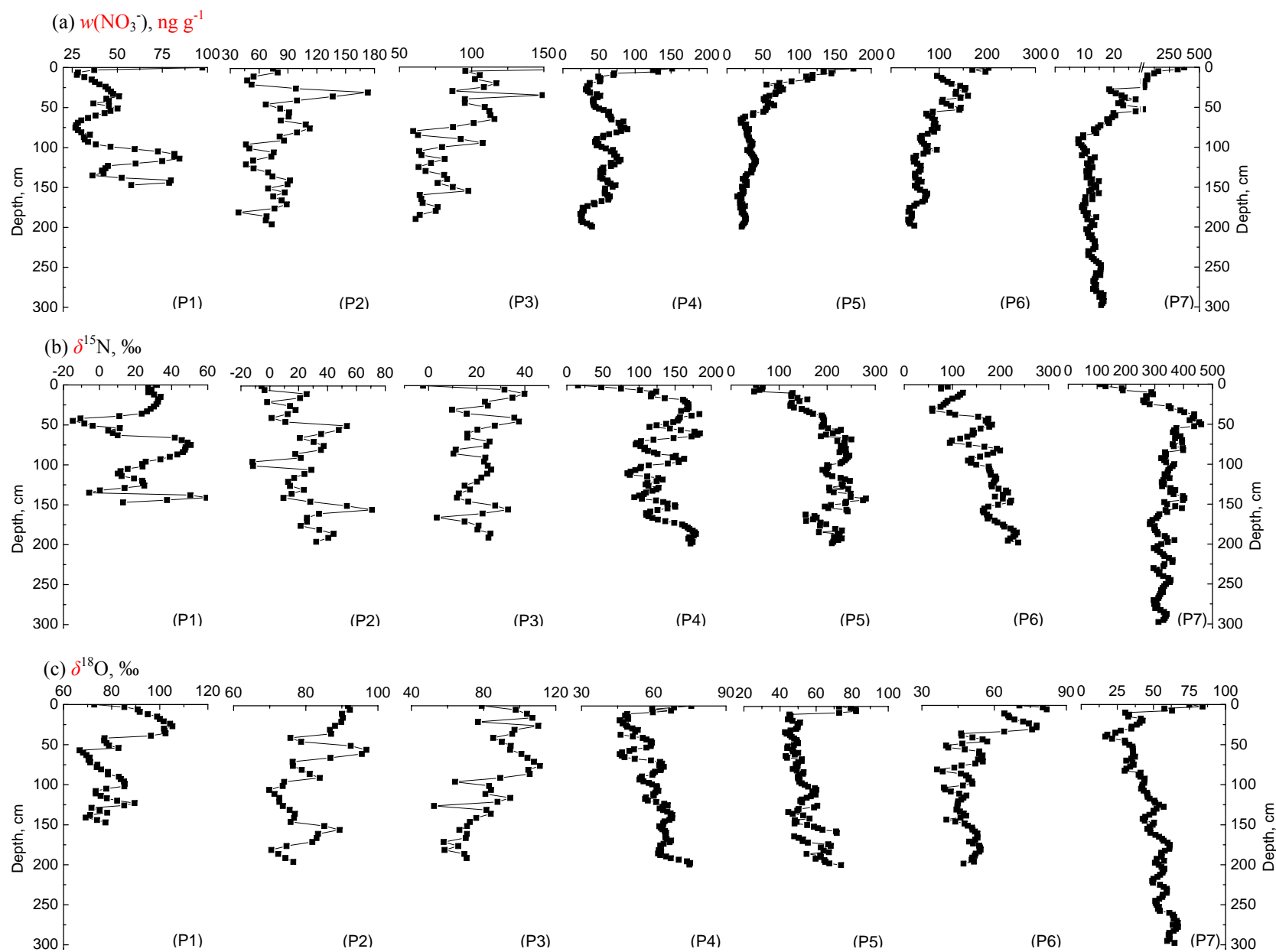


Fig. 23. Detailed profiles of $w(\text{NO}_3^-)$ (a) and isotopic composition $\delta^{15}\text{N}$ (b) and $\delta^{18}\text{O}$ of NO_3^- (c) in the P1-P7 snowpits. It is noted that the x-axis of $w(\text{NO}_3^-)$ in P6 was broken to show the trend clearly in deeper snowpack.

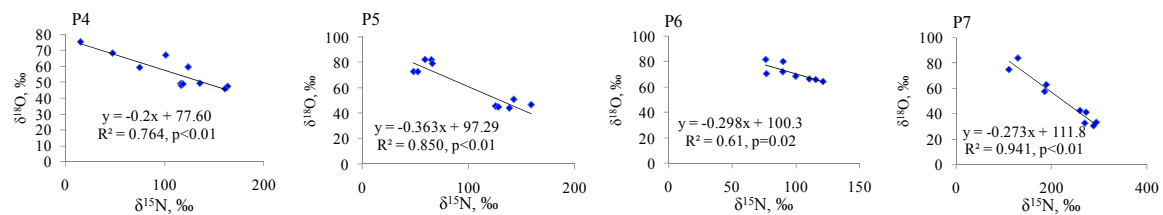


Fig. 34. Linear relationships between $\delta^{18}\text{O}$ (top row) and $\delta^{15}\text{N}$ (bottom row) of NO_3^- with $w(\text{NO}_3^-)$ in the topmost 20 cm of the snowpits. Least squares regressions are shown and are all significant at $p < 0.05$.

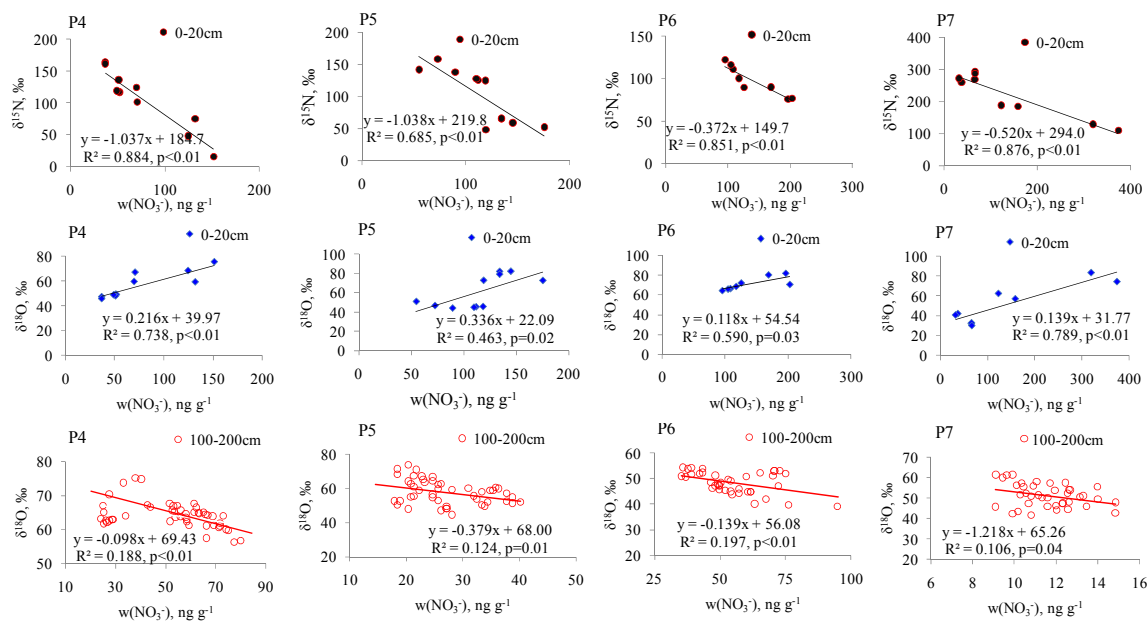


Fig. 5. Linear relationships between $w(\text{NO}_3^-)$ and $\delta^{18}\text{O}$ and $\delta^{15}\text{N}$ of NO_3^- in the near surface (top and middle rows) and at depth (bottom row) snow ranges. Least squares regressions are shown and are all significant at $p < 0.05$.

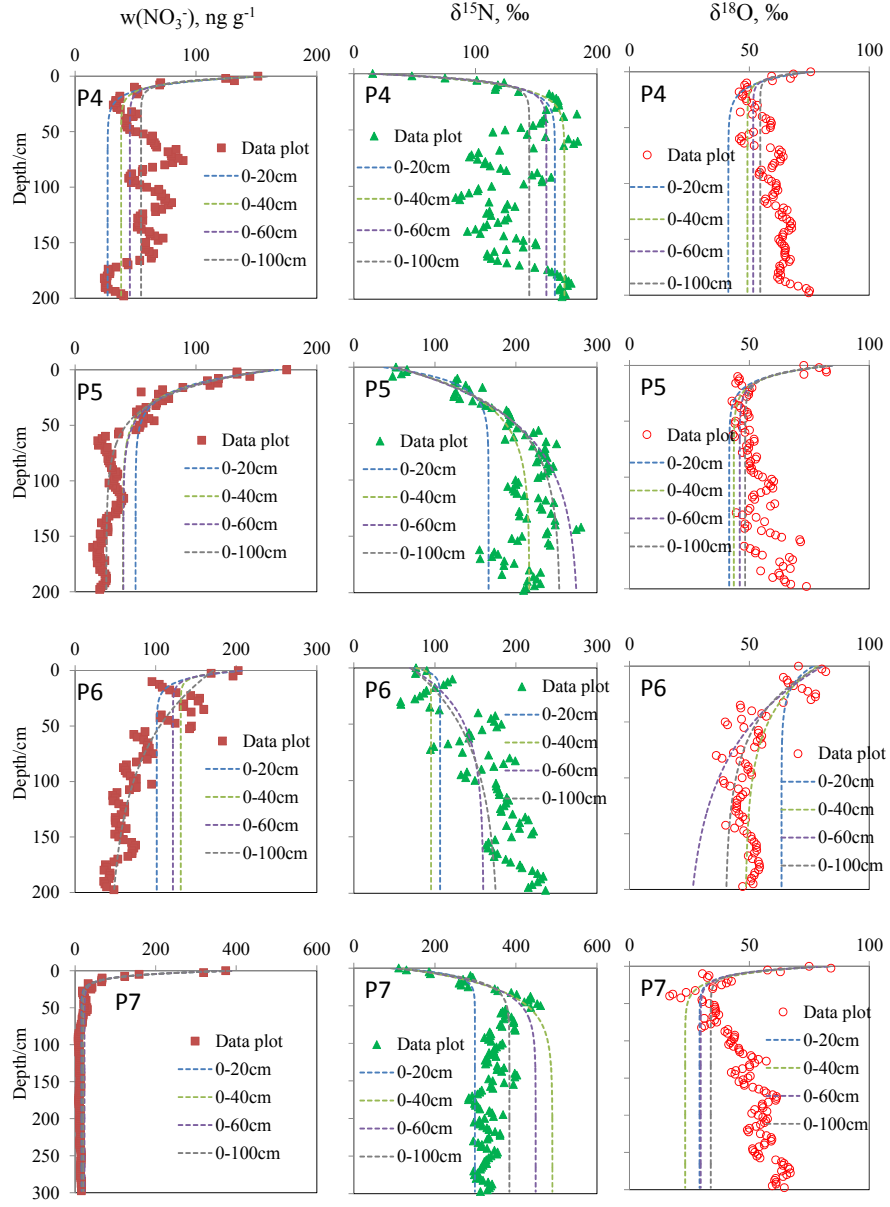


Fig. 6. Detailed profiles of $w(\text{NO}_3^-)$, $\delta^{15}\text{N}$ and $\delta^{18}\text{O}$ in different snow depth intervals (0-20cm, 0-40cm, 0-60cm, and 0-100cm) for the snowpits P4-P7. The dashed lines are the best fit regressions for the observed data, and asymptotic values are calculated for $w(\text{NO}_3^-)$, $\delta^{15}\text{N}$ and $\delta^{18}\text{O}$ by Eq. (6).

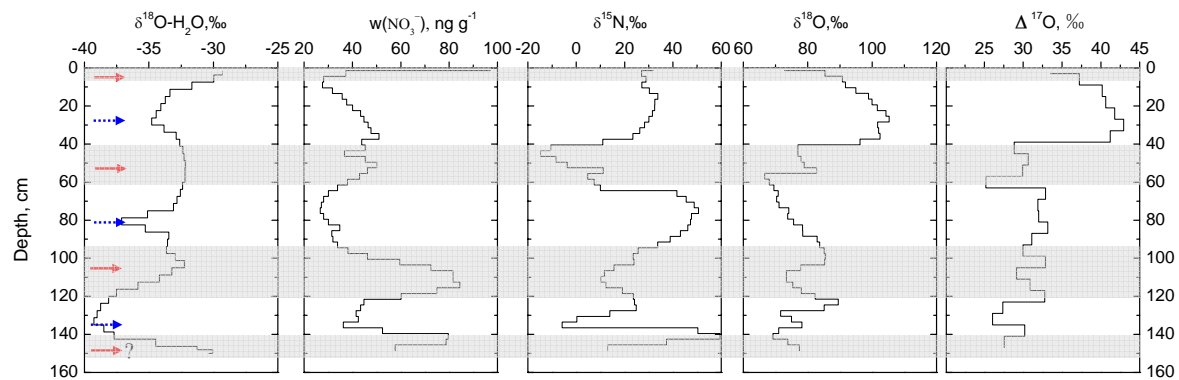


Fig. 77. Seasonality in $w(\text{NO}_3^-)$, $\delta^{15}\text{N}$, $\delta^{18}\text{O}$ and $\Delta^{17}\text{O}$ of NO_3^- in the P1 snowpit. Red solid arrows and blue dashed arrows represent the middle of the identified warm and cold seasons, respectively, and shaded areas denote warm seasons (see text). One seasonal cycle represents one $\delta^{18}\text{O}(\text{H}_2\text{O})$ peak to the next. Seasonal assignment of snow near the pit base is subject to uncertainty due to the limited coverage and absent comparison with a preceding cold season.

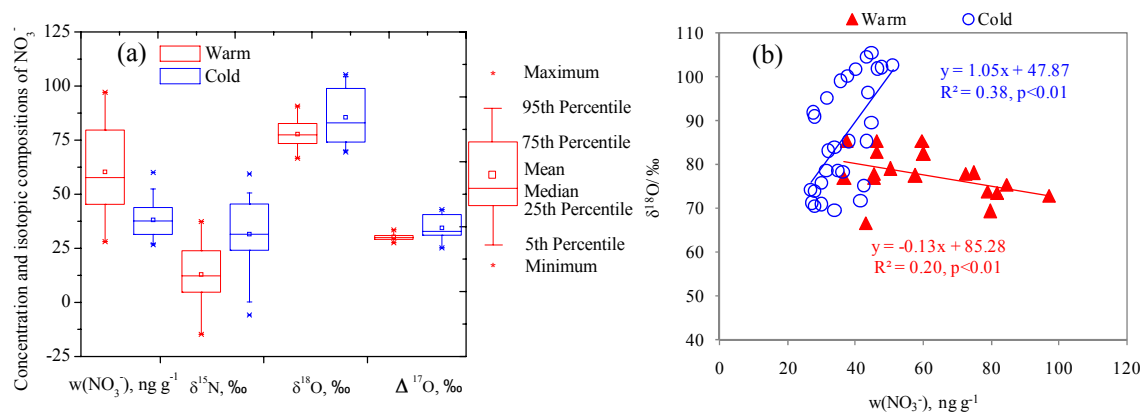


Fig. 88. $w(\text{NO}_3^-)$, $\delta^{15}\text{N}$, $\delta^{18}\text{O}$ and $\Delta^{17}\text{O}$ of NO_3^- in warm and cold season samples from snowpit P1. Summary statistics by season are shown in (a), and the seasonal relationships between $w(\text{NO}_3^-)$ and $\delta^{18}\text{O}$ of NO_3^- are shown in (b).